

Sensor Technology for Unobtrusive Athlete Monitoring

Steijlen, A.S.M.

DOI

[10.4233/uuid:8eee4c39-3a63-41b3-86fa-d83724f90eff](https://doi.org/10.4233/uuid:8eee4c39-3a63-41b3-86fa-d83724f90eff)

Publication date

2022

Document Version

Final published version

Citation (APA)

Steijlen, A. S. M. (2022). *Sensor Technology for Unobtrusive Athlete Monitoring*. [Dissertation (TU Delft), Delft University of Technology]. <https://doi.org/10.4233/uuid:8eee4c39-3a63-41b3-86fa-d83724f90eff>

Important note

To cite this publication, please use the final published version (if applicable).
Please check the document version above.

Copyright

Other than for strictly personal use, it is not permitted to download, forward or distribute the text or part of it, without the consent of the author(s) and/or copyright holder(s), unless the work is under an open content license such as Creative Commons.

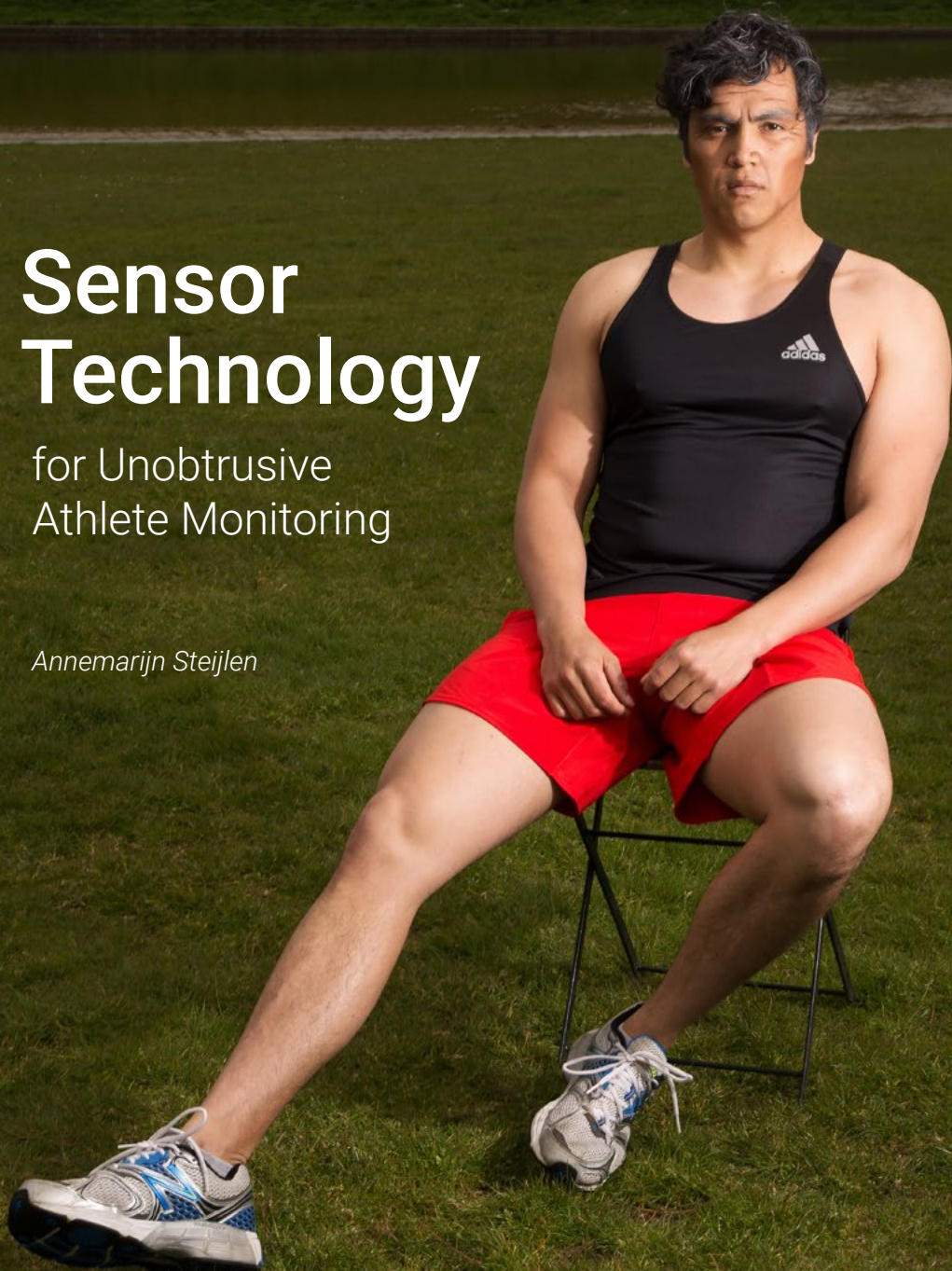
Takedown policy

Please contact us and provide details if you believe this document breaches copyrights.
We will remove access to the work immediately and investigate your claim.

Sensor Technology

for Unobtrusive
Athlete Monitoring

Annemarijn Steijlen



Sensor Technology for Unobtrusive Athlete Monitoring

Proefschrift

ter verkrijging van de graad van doctor aan de Technische
Universiteit Delft,
op gezag van de Rector Magnificus, Prof.dr.ir. T.H.J.J. van der Hagen,
voorzitter van het College voor Promoties,
in het openbaar te verdedigen op
Vrijdag, 30 september, 2022 om 10 uur
door

Annemarijn Sebastinie Marie STEIJLEN

Master of Science in Integrated Product Design,
Technische Universiteit Delft, Nederland
geboren te Nijmegen, Nederland

Dit proefschrift is goedgekeurd door de promotoren.

Samenstelling promotiecommissie bestaat uit:

Rector magnificus, voorzitter

Prof.dr. P.J. French, Technische Universiteit Delft, promotor

Prof.dr.ir. K.M.B. Jansen, Technische Universiteit Delft, promotor

Dr.ir. A. Bossche, Technische Universiteit Delft, copromotor

Onafhankelijke leden:

Prof.dr.ir. J.M.J. den Toonder, Technische Universiteit Eindhoven

Prof.dr. H.A.M. Daanen, Vrije Universiteit Amsterdam

Prof.dr. S. Carrara, École Polytechnique Fédérale de Lausanne, Zwitserland

Prof.dr.ir. J. Harlaar, Technische Universiteit Delft

Prof.dr.ir. W.A. Serdijn, Technische Universiteit Delft (reservelid)

Het onderzoek in dit proefschrift werd financieel gesteund door de Nederlandse Organisatie voor Wetenschappelijk Onderzoek (NWO) in het kader van het Citius, Altius, Sanius programma met projectnummer P16-28.

Copyright © 2022 by Annemarijn Steijlen

printed by Ridderprint

Cover photo: Tasha Arlova

model: Julian Roza

makeup: Doris Broers

graphic design: Jeanne Frints

ISBN 978-94-6458-478-3

An electronic version of this dissertation is available at:

<http://repository.tudelft.nl/>



*Het snoer
leek op een navelstreng,
en werd verbonden
in de knop
van de computer.
O moederband,
weer aangehecht,
waar wetenschap
een netwerk vlecht.
Funiculus,
het was een klus,
een werk van jaren.
Maar nu, dan ook
kan je de band bewaren.*

J.M. Steijlen-Smits

Contents

Summary	8
Samenvatting	10

I. Overview & Research Approach

1. Introduction	16
1.1. Research vision	16
1.2. The Citius Altius Sanius programme	17
1.3. Thesis outline	18
2. Physiological parameters of interest	19
2.1. Physiological response to exercise	19
2.2. Biomechanics	24
2.3. Overview of important physiological parameters	25
3. Wearable sensor system design approach	30
3.1. Design framework	30
3.2. Design cases	32
3.3. Conclusions	34

6

II. Sweat Sensing during Exercise

Motivation	38
Research Approach	40
4. Wearable fluidic collection patch for sweat monitoring during exercise	42
4.1. Method	42
4.2. Results & discussion	47
4.3. Conclusions	51
5. Sweat patch for continuous analyte monitoring and offline analysis	52
5.1. Materials & methods	52
5.2. Results & discussion	56
5.3. Conclusions	63
6. Continuous sweat NH₃, Na⁺ and Cl⁻ monitoring	64
6.1. NH ₃ capsule	64
6.2. Potentiometric sensor patch	68
6.3. Conclusions	72
Summarizing conclusions for sweat sensing	73

.....

III. Movement Tracking in Field Sports

Motivation	76
Research approach	78
7. Smart sensor tights 1.0: a proof of concept	81
7.1. Interconnects	81
7.2. Proof of concept	82
7.3. Sensor locations	83
7.4. Conclusions	85
8. Smart sensor tights 2.0: a validation study in a football context	86
8.1. Materials & methods	86
8.2. Results & discussion	92
8.3. Conclusions	98
9. Smart sensor tights 3.0: wireless data transmission	99
9.1. Wireless communication protocol	99
9.2. Hardware selection	100
9.3. Dashboard	102
9.4. Conclusions	103
10. Smart sensor tights 4.0: washable integrated sensor modules	104
10.1. Encapsulation tests	105
10.2. Future improvements	107
Summarizing conclusions for movement tracking	109

IV. Discussion & Conclusions

11. General discussion	114
11.1. The design process	114
11.2. Scientific impact	115
11.3. Societal & environmental impact	116
12. Conclusions & outlook	118
12.1. Sweat sensing during exercise	118
12.2. Movement tracking in field sports	120
Bibliography	122
Appendices: Chapter 4	134
Appendices: Chapter 5	137
Appendices: Chapter 9	146
Acknowledgements	149
List of publications	152
About the author	153

Summary

Our sedentary lifestyle leads to a significant risk of chronic diseases and an increased burden on our healthcare system. Sports participation can reduce the prevalence of chronic diseases but introduces a new risk of injuries related to exercise. In this research, we developed novel wearable sensor systems that empower physiologists and movement scientists to identify injury risk factors and develop injury prevention programmes. The new wearable sensor systems can continuously measure physiological and biomechanical data of athletes in an unobtrusive way.

The first part of this research focuses on developing sweat sensor systems to identify new biomarkers for injury prevention. The second part focuses on movement tracking of the lower limbs in field sports. During the development of these new sensor systems, an application-oriented design approach was followed. Sensor systems were tested in an early phase in physiological experiments. The outcomes of these tests were used as a starting point for the next design iteration.

Sweat sensing during exercise

8

Advances in microelectronics and material science opened up opportunities for designing wearable sensor patches that can measure real-time sweat composition unobtrusively. However, from a physiological perspective, little is known about the physiological mechanisms of sweating and how sweat composition relates to an athlete's health status. To find new sweat biomarkers, reliable real-time sweat measurement systems are required that are validated in a physiological setting. Current validation studies are limited since standardised validation strategies for novel sweat sensors do not yet exist. Therefore, we designed a new sweat collection patch that enables chronological sweat sampling in a sequence of reservoirs for offline analysis. The functioning of this collection patch was validated in a physiological setting. Second, a redesign of the patch was made which enabled continuous measurement of ionic content using a conductivity sensor. In an elaborate physiological experiment, real-time sweat conductivity measurements were compared against offline ion chromatography results (Na^+ , Cl^- , K^+) from the collected samples. A linear relationship was found between sweat conductivity and $[\text{Na}^+]$ and $[\text{Cl}^-]$ ($R^2=0.97$). Furthermore, patch filling rate and real-time conductivity measurements were compared against a ventilated capsule sweat rate measurement. Ventilated capsule measurements were linearly related to sweat conductivity as well. From these results, it was concluded that the collection patch can be used for real-time sweat measurement and chronological sampling for offline analysis of sweat composition afterwards.

The sweat conductivity sensors in the collection patch provide information about the total ionic content in sweat. The final part of the sweat sensing research focuses on developing sensors to monitor specific analytes continuously. Two systems are presented here. The first system is an NH_3 sensor integrated into a ventilated capsule, which measures the NH_3 levels in the air evaporated from sweat. The second system is a potentiometric sensor patch

.....

with Na⁺ and Cl⁻ selective electrodes. Initial sensor characterisation experiments with these new systems were performed. Further development is required to use these systems in a physiological setting.

Movement tracking in field sports

Real-time monitoring of the load on the hip-related muscles can contribute to the prevention of hamstring or groin injuries in field sports. To derive limb kinematics related to the load of the lower limbs in the field, movement scientists commonly use inertial measurement units (IMUs) that are taped to the skin. This measurement method is labour-intensive and is not suitable for day-to-day use. Therefore, the aim of this research project was to create smart sensor tights with integrated inertial measurement units that can be used during everyday training activities and matches. An iterative design approach was followed to develop the smart sensor tights. During a four-year research project, a new, improved prototype was developed and tested in the field in collaboration with human movement science researchers every year.

The smart sensor tights enclose an IMU at each limb segment and the pelvis. The IMUs measure linear accelerations, angular velocities and the earth magnetic field. The first prototype with commonly used sensors was created as a proof of concept to identify challenges for future product development. For the second prototype, larger range sensors (30g, 4000°/s) were implemented, and high sample rates (250 Hz) were achieved. Furthermore, the integration of electronics was improved. In a lab validation study, kinematics derived from the smart sensor tights were compared to measurements with an optoelectronic system, and good validity was shown. Field tests proved that participants found the tights comfortable to wear. The data from the tights need to be sent wirelessly to the side of the football field for fast interpretation by football coaches and medical personnel. While prototype 2 saved data locally on an SD card, prototype 3 was able to wireless transmit the sensor data to a user dashboard. Lastly, in the final prototype, the integration of the electronics was improved. The prototype contained encapsulated sensor modules that are ultra-light and thin and can be washed together with the textile.

In short, the sensor systems in this thesis provide researchers with new physiological and biomechanical data during exercise. The new sweat patch was designed for chronological collection of sweat samples and continuous measurement of sweat composition to research the change in sweat content during exercise. The patch can be used in physiological validation studies of novel sweat sensors that continuously measure sweat composition. These sensors can be employed to identify new sweat biomarkers related to an athlete's health status. In the second project of this thesis, easy-to-use smart sensor tights were developed that can be worn during day-to-day training activities to monitor lower limb kinematics. The sensor tights facilitate large scale longitudinal movement science studies that aim to identify injury risk factors related to the load around the hip-related muscles. The outcomes of this research can be used to develop new load parameters that predict hamstring and groin injury risk in football and field hockey.

Samenvatting

Onze zittende levensstijl leidt tot een significant risico op chronische ziektes en tot overbelasting van de gezondheidszorg. Sportparticipatie kan de prevalentie van chronische ziektes verminderen, maar introduceert een nieuw risico op sportblessures. In dit onderzoek ontwikkelden we nieuwe draagbare sensorsystemen, die fysiologen en bewegingswetenschappers in staat stellen om blessurerisicofactoren te onderzoeken en om nieuwe preventieprogramma's te ontwikkelen. De nieuwe draagbare sensorsystemen kunnen continu fysiologische en biomechanische informatie verzamelen zonder de atleet te hinderen tijdens het sporten.

Het eerste deel van dit onderzoek focust op de ontwikkeling van zweet sensorsystemen. Het tweede deel gaat over het monitoren van beweging tijdens veldsporten. Tijdens de ontwikkeling van deze nieuwe sensorsystemen werd een toepassingsgerichte ontwerpaanpak gevolgd. Sensorsystemen werden in een vroeg stadium van ontwikkeling getest in fysiologische experimenten. De uitkomsten van deze testen werden gebruikt als startpunt van de volgende ontwerpiteratie.

Zweet meten tijdens het sporten

10

De technische vooruitgang binnen de micro-elektronica en de materiaalwetenschappen zorgde voor nieuwe kansen om op een onmerkbare manier de samenstelling van zweet te monitoren met behulp van slimme zweetpleisters. Als men echter naar de fysiologische literatuur kijkt, dan is er nog weinig bekend over de fysiologische mechanismen van het zweten en hoe zweetsamenstelling gerelateerd is aan de gezondheidsstatus van de atleet. Om nieuwe zweetbiomarkers te ontdekken, is het een vereiste dat er nieuwe betrouwbare zweetmonitoringsystemen ontwikkeld worden die gevalideerd zijn in fysiologische experimenten. De uitvoering van fysiologische validatiestudies in de huidige literatuur is beperkt, omdat gestandaardiseerde validatieprotocollen voor nieuwe zweetsensoren nog niet bestaan. Daarom ontwikkelden wij een nieuw zweetopvangsysteem dat het mogelijk maakt om zweetmonsters over tijd te verzamelen en op te slaan in een reeks van reservoirtjes. Naderhand kunnen deze zweetmonsters geanalyseerd worden in het laboratorium. Het naar behoren functioneren van de zweet opvangpleister werd getest in een fysiologisch experiment. In een daaropvolgend onderzoek werd er een herontwerp van de pleister gemaakt. Dit herontwerp maakte het mogelijk om continu de ionische inhoud in zweet te meten met een conductiviteitsensor. In een uitgebreider fysiologisch experiment werden de conductiviteitsmetingen vergeleken met de analyse van de zweetmonsters met ionenuitwisselingschromatografie (Na^+ , Cl^- , K^+) in het laboratorium. Er werd een lineair verband gevonden tussen zweetconductiviteit en $[\text{Na}^+]$ en $[\text{Cl}^-]$ ($R^2=0.97$). Daarnaast werden de vulgraad, die ook werd gemeten in de pleister, en de conductiviteitsmetingen vergeleken met zweetsnelheid, die werd gemeten met de geventileerde capsule techniek. De zweetsnelheidsmetingen gemeten met de geventileerde capsule bleken lineair gerelateerd aan de zweetconductiviteit. Hieruit kan geconcludeerd worden dat de nieuwe

zweetpleister gebruikt kan worden voor het continu meten van zweetsamenstelling en voor het chronologisch verzamelen van zweet voor laboratoriumanalyse naderhand.

De conductiviteitssensoren in het zweetverzamelstelsel verstrekken informatie over de totale ionische inhoud van zweet. In het laatste deel van het zweetonderzoek wordt er gefocust op de ontwikkeling van sensoren om specifieke analyten te meten. Twee systemen worden hier gepresenteerd. Het eerste systeem is een NH_3 sensor die geïntegreerd is in een geventileerde capsule. De sensor meet de NH_3 in de lucht die is verdampt uit het zweet. Het tweede systeem is een potentiometrische sensorpleister die Na^+ - en Cl^- -selectieve elektrodes bevat. Initiële sensor karakteriseringsexperimenten werden al uitgevoerd met deze nieuwe systemen. Voordat deze systemen in fysiologische experimenten gebruikt kunnen worden, is verdere sensorontwikkeling vereist.

Bewegingsregistratie in veldsporten

Het continu meten van de belasting op de spieren rondom het heupgewricht kan een bijdrage leveren aan de preventie van hamstring- en liesblessures in veldsporten. Doorgaans worden in de bewegingswetenschappen zogenaamde 'Inertial Measurement Units' (IMU's) op de huid geplakt om de kinematica tijdens het sporten te verkrijgen, die gerelateerd zijn aan de belasting op de onderste ledematen. Deze meetmethode is arbeidsintensief en niet geschikt voor dagelijks gebruik. In dit onderzoeksproject ontwikkelden wij een slimme sensorbroek met geïntegreerde IMU's die gebruikt kan worden tijdens dagelijkse trainingen en wedstrijden. Om deze slimme sensorbroek te ontwikkelen werd er een iteratieve ontwerpaanpak gevolgd. Tijdens het project van vier jaar, werd er elk jaar een nieuw verbeterd prototype ontwikkeld en getest in samenwerking met bewegingswetenschappers. De slimme sensorbroek omvat een IMU op elk segment van de benen en op de pelvis. De IMU's meten lineaire versnellingen, hoeksnelheden en het aardmagnetisch veld. Het eerste prototype werd gemaakt als een proefversie met laagdrempelige sensoren om de uitdagingen voor verdere productontwikkeling in kaart te brengen. Voor het tweede prototype werden sensoren met een groter meetbereik geïmplementeerd (30g, 4000°/s) en werd de samplefrequentie verhoogd tot 250 Hz. Tevens werd de integratie van de elektronica verbeterd. In een validatiestudie in het lab werden de kinematica die werden verkregen met de slimme sensorbroek vergeleken met gelijktijdige metingen met een opto-elektronisch systeem. De resultaten kwamen goed overeen. Gebruikers vonden de broek comfortabel om te dragen in veldtesten. Voor snelle interpretatie van de data door coaches en medisch personeel, moeten de data draadloos naar de zijlijn verzonden kunnen worden. Waar prototype 2 de data nog enkel opsloeg op een SD kaart, kon prototype 3 de data draadloos versturen naar een dashboard. Ten slotte werd in prototype 4 de integratie van de elektronica verbeterd. Het prototype omvatte ultralichte en dunne ingekapselde sensormodules die samen met het textiel gewassen kunnen worden.

Samenvatting

Kortom, de sensorsystemen in deze dissertatie verschaffen onderzoekers nieuwe fysiologische en biomechanische gegevens tijdens beweging. De nieuwe zweetpleister werd ontworpen voor het chronologisch verzamelen van zweetmonsters en het continu meten van zweetsamenstelling om de verandering in zweetcompositie te monitoren tijdens het sporten. De pleister kan gebruikt worden in validatiestudies van nieuwe zweetsensoren die zweetcompositie monitoren over tijd. Daarna kunnen deze sensoren ingezet worden om nieuwe zweetbiomarkers te identificeren, die gerelateerd zijn aan de gezondheidsstatus van de atleet. In het tweede project van deze dissertatie, werd een slimme sensorbroek ontwikkeld die gemakkelijk te gebruiken is en die gedragen kan worden tijdens dagelijkse trainingen om de kinematica van de benen te monitoren. De sensorbroek faciliteert longitudinale bewegingsstudies op grotere schaal voor de identificatie van blessurerisicofactoren met betrekking tot de belasting rondom het heupgewricht. De uitkomsten van dit onderzoek kunnen gebruikt worden om nieuwe belastingsparameters te ontwikkelen die in voetbal en hockey het risico op hamstring- en liesblessures kunnen voorspellen.

.....

I

Overview & Research Approach

1

Introduction

16

Living in a wealthy first-world country with an abundance of automated technology, we lead a sedentary life. In higher income western countries, 36,8 % of the population performs less than 150 minutes of moderate-intensity exercise per week (Guthold et al., 2018). This includes activities that cause a mild increase in heart rate, such as walking and bicycling (Bull et al., 2020). Our sedentary lifestyle, in combination with the ageing population, leads to a tremendously increased prevalence of chronic diseases. If historical trends continue, 5.5 million people in the Netherlands will suffer from multiple chronic conditions in 2040 (National Institute for Public Health and the Environment, 2018). The COVID-crisis showed that with large amounts of new patients, the burden on the healthcare system becomes untenable (Dinmohamed et al., 2020; Miller et al., 2020). To prevent that future doctors spend all their time prescribing anticoagulants and bronchodilators and to make people more resilient to new viruses, we have to stimulate people to become active. The World Health Organization advises all adults to undertake 150–300 min of moderate-intensity, or 75–150 min of vigorous-intensity physical activity or a combination of the two. This reduces the risk of hypertension, cardiovascular disease mortality, type 2 diabetes, mental health problems, site-specific cancers and improves cognitive health, sleep and measures of adiposity (Bull et al., 2020; World Health Organization, 2020).

However, sports participation increases the risk of injuries. For example, in recreational running which is one of the most popular sports worldwide, injury rates of 20.8 injuries per 100 female runners and 20.4 injuries per 100 male runners were reported (Hollander et al., 2021). Furthermore, in football, which is the most popular sport in the world, Ekstrand et al. (2017) reported that a professional football team can expect 1.8 injuries per player per season. Injury prevention programs can help to significantly decrease injury occurrence, which is a relatively new field of research (Pless, 2006).

1.1. Research vision

This research is part of a nationwide multidisciplinary research consortium, in which movement scientists, data scientists and sensor developers joined forces with the ultimate aim to make injury-free exercise available for everyone. Within this consortium, our role

was to develop wearable sensor systems to support movement science research on injury prevention. Wearable sensor systems can provide researchers with new physiological data, to identify injury risk factors that can be used to develop injury prevention programmes. Moreover, these sensors can be used to create awareness about sedentary behaviour and to stimulate physical activity. In this thesis, a wearable sensor system is defined as:

“An on-body technological device that measures physiological signals (semi-) continuously to unobtrusively monitor a subject’s health status.”

A well-known example of a wearable sensor system is the heart rate belt (e.g. Polar H10, Finland), which is commonly used by professional athletes as well as recreational athletes to improve their cardio-respiratory fitness. In this research project we aim to develop novel wearable sensor systems that acquire physiological information of athletes in action, that can support in making injury-free exercise available for everyone.

1.2. The Citius Altius Sanius programme

Figure 1.1 shows the structure of the consortium. The program is divided in nine projects. Three fundamental research projects focus on sensor technology, data science and feedback. Six applied projects apply the knowledge from the three fundamental projects to research the most prevalent injuries in the Netherlands in a specific sports domain. In each project, two or three researchers specialized in movement science or engineering were appointed. Within this consortium, our role was to develop wearable sensor technology (P1) to acquire real-time physiological information for injury prevention and performance optimization. Furthermore, to stimulate interaction with the applied projects, a link was made with project P6. For project P6, we were asked to create a smart sensor garment for movement tracking of the lower limbs in football and field hockey.

P1. Sensor technology	P2. Data science	P2. Feed-back
P4.	Fitness	Over use
P5.	Running	Over use
P6.	Football/hockey	Hamstring/groin
P7.	Tennis/baseball	Shoulder/elbow
P8.	Paralympic	Thermal
P9.	Cycling	Falling

Figure 1.1. Overview of the Citius Altius Sanius programme

1.3. Thesis outline

To identify potential parameters of interest to unobtrusively monitor athletes for the prevention of injuries, physiological literature was studied and experts in physiology were consulted. An overview of potential physiological parameters was created based on the reviewed literature. At the same time, technological opportunities in wearable sensors research were assessed too and by combining the opportunities in both fields, the research directions were identified. The overview of physiological parameters of interest and the selected research directions are presented in **chapter 2**. **Chapter 3** explains the design framework that was used for wearable sensor system development. This design framework describes the different stages in wearable sensor system development. All sub-projects in this thesis make use of this framework. After presentation of the framework, a summary of the two research projects is given. The first research project in this thesis focusses on sweat sensor systems for continuous analyte monitoring and offline analysis. First, a novel sweat collection system focusing on reliable collection of sweat and on the methodology for offline chemical analysis, is presented in **chapter 4**. A new improved version of the sweat patch includes real-time conductivity sensors and filling rate sensors. Validation experiments in a physiological setting prove that the system works well. The design and physiological validation of the second design are presented in **chapter 5**. **Chapter 6** describes two sweat sensor system concepts for continuous monitoring of specific analytes: NH_3 , Na^+ and Cl^- . The second research project focuses on the design of a sensor garment (tights or shorts) with integrated inertial measurement units for movement tracking in football and hockey. In **chapter 7 till chapter 10**, the development of four prototypes of the sensor tights are presented, including a technical validation study and user experience evaluation of prototype 2 in **chapter 8**. In **chapter 11** of this thesis, the most important findings of the research are discussed. **Chapter 12** comprises the main conclusions of this thesis and research outlook.

2

Physiological parameters of interest

Advances in microelectronics, printed electronics and sensors created a tremendous number of different technological opportunities to develop wearable sensors for monitoring an athlete's health and performance status. Many wearable sensor projects for unobtrusive athlete monitoring start from a technological premise. However, to develop sensor systems that will make a difference in supporting healthy sports participation, the following questions must be addressed first: I. Which physiological information provides insight in a subjects health status? II. What are the parameters of interest from a physiological perspective? These questions are answered in this chapter.

19

2.1. Physiological response to exercise

Intensity, duration and frequency of exercise together with the environmental conditions influence the physiological response to exercise. This response is reflected by a change in a large range of physiological parameters. These parameters are divided in 4 groups:

1. Respiratory parameters
2. Cardiovascular parameters and blood assays
3. Sweat analytes and sweat rate
4. (Saliva and urine markers)

In this chapter, the first three categories are addressed to identify parameters of interest for unobtrusive athlete monitoring. Saliva and urine markers are not addressed in this overview, because they are either not commonly used in exercise physiology or do not enable real-time monitoring.

2.1.1. Respiratory parameters

During physical exercise, there is an increased need of oxygen and substrate (like glucose) in the skeletal muscle to form ATP (Adenosine triphosphate), which is the principal energy molecule that enables muscle contraction. In the beginning of exercise, lung ventilation increases abruptly and later, this increase becomes more gradual. The amount of air moving in and out of the lungs per minute is called minute ventilation (VE). VE is defined as the tidal

volume (VT) times the respiratory rate. For fit individuals, VE will increase from 8 to 12-150 L/min. The respiratory rate can remain elevated after exercise for up to 1–2 h (Astrand & Rodahl, 1970; O'Connor et al., 2009). The rate of oxygen demand is proportional to the rate of work. At the moment that a person starts exercising at a submaximal level, oxygen uptake increases asymptotically towards a steady state value. During severe exercise, oxygen uptake keeps rising slowly (Jones et al., 2011). Young men (20-30 years old) generally have a maximal oxygen uptake (VO_2 max) of around 2.5 L/min. For well-trained male athletes, this maximal oxygen uptake is typically twice as high. It needs to be kept in mind that there can be a large individual variation (Astrand & Rodahl, 1970). When the period of exercise ends, there remains an increased need for oxygen for some time. This is called the oxygen debt. The more a person got his energy from anaerobic processes during exercise, the greater the oxygen debt will be.

2.1.2. Cardiovascular parameters and blood assays

The cardiovascular system circulates 5 litres of blood per minute. However, during heavy exercise, this quantity can increase more than 4 to 8 times (~40 L/min), due to increased heart rate, stroke volume and peripheral resistance. The cardiovascular system also makes sure that more blood flows to the skeletal muscle and less blood is going to the non-exercising areas. During peak exercise, 85% of the total blood flow can be redirected to the skeletal muscle.

An athlete's heart rate can go from <40 bpm in resting state to >200 bpm during severe exercise (Baggish & Wood, 2011). There exists a linear relationship between heart rate and VO_2 . This is why heart rate is often used as a predictor of VO_2 . Figure 2.1 shows typical changes in blood and respiratory parameters from rest to maximum exercise. When there is not enough oxygen available, pyruvate will accept energy carriers and lactic acid starts to accumulate. This is called the anaerobic threshold (Wasserman et al., 1973). Although energy can be retrieved fast during the anaerobic process, in total, less energy is retrieved than during the aerobic process. From the aerobic process, 18 times more ATP/mole of glucose is generated (Burton et al., 2004; Johnson, 2007). Skinner and McLellan (1980) suggest a blood lactate level of 4 mmol/L as the quantitative definition of the anaerobic threshold. During incremental exercise, blood glucose levels tend to reduce until it reaches a breakpoint. Adrenaline produces an increase in blood glucose below a certain point, which is called the glycemic threshold (Sales et al., 2019; H. G. Simões et al., 2003).

Furthermore, arterial blood gas pressures provide information about the pulmonary response to exercise. The changes in partial pressure of arterial blood gases (pO_2 and pCO_2) and the pH of blood are usually small during moderate exercise. During intense exercise (above the anaerobic threshold), the pCO_2 level initially rises, however this is counteracted by increased ventilation which results in a decrease in CO_2 in the blood, and also compensates for further lactic acid production, preventing a decline in blood pH (Burton et al., 2004). Anaerobic exercise complicates maintaining a stable pH level (McArdle et al., 2010).

Additionally, concentration changes of oxyhemoglobin (O_2Hb) and deoxyhemoglobin (HHb) in tissue, measured close to the exercising muscle with near-infrared spectroscopy, relate

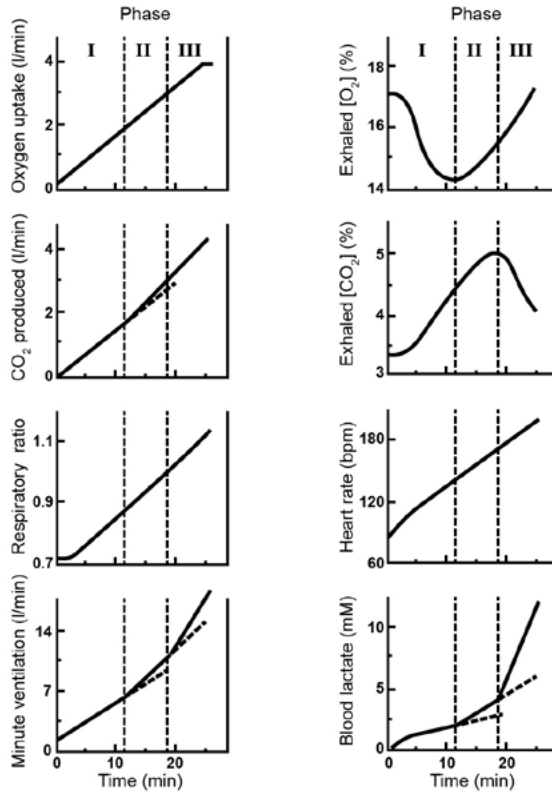


Figure 2.1. Typical changes in blood and respiratory parameters from rest to maximum exercise level. The aerobic threshold is defined as the shift from phase I to phase II. The shift from phase II to phase III is the anaerobic threshold. Adapted from (Skinner & McLellan, 1980).

to possible oxygen limitation in the muscle fibres. A breakpoint in Hb difference ($\Delta[\text{O}_2\text{Hb}-\text{HHb}]$) occurs during an incremental exercise test and shows high correlations with the lactate threshold (Grassi et al., 1999). However it needs to be mentioned that adipose tissue thickness can strongly affect the measurements (van der Zwaard et al., 2016).

Electrolytes

Electrolyte concentrations provide information about an athlete's physical status as well. Studies have shown that K^+ concentration in plasma rises significantly (typically rising from 4 mM to 6 mM) during exercise and is related to exercise intensity (Atanasovska et al., 2014) among others. Most cells possess an Na^+-K^+ -ATPase which pumps Na^+ out of the cell and K^+ into the cell. In this way, the potential difference across the membrane can be maintained, which is critical for proper cell functioning in the muscles and nerves for example (Palmer, 2015). Furthermore, Na^+ concentrations and osmolality of blood plasma increase with dehydration (Lee et al., 2017).

Hormones

Hormones are essential for the physiological adaptations to exercise. Mainly testosterone and cortisol can be interesting biomarkers. Testosterone stimulates protein synthesis and glycogen replenishment, while cortisol inhibits protein synthesis, which means that an increased cortisol level inhibits muscle growth and recovery. Therefore, it can be interesting to monitor the testosterone/cortisol ratio. (Lee et al., 2017).

Cytokines, urea nitrogen, creatine kinase

Lastly, several other blood constituents reflect the muscles health status. A few important examples are mentioned here. First, increases of cytokine levels (like IL-1 β and IL-6) can indicate inflammation. However, it needs to be kept in mind that, due to the numerous functions of cytokines, multiple cytokines and other variables related to physiological function need to be measured to detect chronic inflammation (Lee et al., 2017). Second, an elevation in blood urea nitrogen may indicate protein breakdown and third, chronically elevated creatine kinase level may indicate insufficient recovery of muscle damage (Lee et al., 2017).

2.1.3. Sweat analytes and sweat rate

The muscles convert the energy retrieved from ATP to work. The efficiency of this process is only 20-25%. This means that a lot of heat is produced during this process. To maintain a constant body core temperature, this heat needs to be dissipated and the blood flow to the skin and the production of sweat are increased. In the absence of these physiological mechanisms, body core temperature would rise sharply, which can lead to heat exhaustion or heat stroke (Baker, 2019). Next to thermoregulatory function, sweating also has other important homeostatic functions that may relate to the performance and health status of an athlete. Sweat is secreted from more than two million sweat glands and whole-body transepidermal water loss ranges from 0.6 to 2.3 L for a thermoneutral individual with a skin surface of 1.8 m² on a daily basis (Taylor & Machado-Moreira, 2013). This amount of sweat is easily accessible during moderate to heavy exercise, which makes it a very attractive body fluid for real-time health and performance monitoring.

Nevertheless, the knowledge about the physiological mechanisms behind sweating is limited. Literature about how sweat analytes relate to blood biomarkers is inconclusive, due to several challenges involved in sweat sampling. At first, the chosen sweat induction method (e.g. active heating, passive heating or pilocarpine iontophoresis (Hussain et al., 2017)) may influence the measured concentrations. Second, sweat collection methods are labour-intensive and prone to contamination. The most commonly used collection systems are the absorbent patch, the arm bag technique and Macroduct sweat collector (Hammond et al., 1994). Sweat can easily evaporate during sampling, sweat composition changes over time, and differences in skin preparation and hydration level can influence the measurements.

Although more physiological research is inevitable, sweat contains several constituents of potential interest for monitoring an athletes performance and health status. The most

abundant ions in sweat are sodium and chloride. For these electrolytes, the secretion mechanisms are known (Baker, 2019). $[\text{Na}^+]$ and $[\text{Cl}^-]$ are related to sweat rate (Baker et al.; Dobson & Sato, 1972; Sato et al., 1989) which can possibly be used to estimate an athlete's hydration status (Robinson et al., 1956). Furthermore, researchers suggested that $[\text{Na}^+]$ and $[\text{Cl}^-]$ may give an indication about electrolyte imbalance (Morgan et al., 2004). However, it needs to be mentioned that correlations between $[\text{Na}^+]$ and sweat rate in between-participant comparisons show mixed results (Baker & Wolfe, 2020).

To identify potential sweat biomarkers, a first step would be to find out which well-established blood biomarkers are represented in sweat (Klous et al., 2020). However, blood biomarkers do not necessarily relate to sweat constituents and, as explained before, research about how blood biomarkers translate to the same constituents in sweat is ambiguous and inconclusive. An example that illustrates the ambiguity around the use of sweat constituents as a biomarker for human health, is lactate. Plasma lactate levels can be used to monitor anaerobic metabolism during exercise. Hence, there is interest in using sweat lactate levels to monitor physiological stress in athletes. Multiple physiological articles state that sweat lactate levels do not correlate well with plasma lactate levels (Alvear-Ordenes et al., 2005; Baker & Wolfe, 2020). Lactate levels in blood are higher than in sweat, because it is produced as a by-product of sweat gland metabolism (Wolfe et al., 1970). Nevertheless, several lactate sensors were developed for this purpose (Anastasova et al., 2017; Promphet et al., 2019) and, for example Seki et al. recently reported a good correlation between sweat lactate threshold and blood lactate threshold (Seki et al., 2021). In short, there is no unequivocal answer to whether sweat lactate sensors can be used in sports physiology (Van Hoovels et al., 2021).

As an alternative for using sweat lactate as a biomarker, several researchers investigated the potential use of $[\text{NH}_4^+]$ as an alternative measure of muscle fatigue (Alvear-Ordenes et al., 2005; Guinovart et al., 2013). When ATP levels run very low during very intense exercise, IMP and ammonium are formed from AMP, which is part of the purine nucleotide cycle (Bhagavan & Ha, 2011). In the scenario that this NH_4^+ is excreted via the sweat, increased NH_4^+ could possibly indicate muscle fatigue (Alvear-Ordenes et al., 2005).

Blood glucose was mentioned as another parameter of interest during exercise. However, sweat glucose concentrations can be ~100 times lower than blood glucose concentrations (Klous et al., 2020). There is little evidence that sweat glucose levels relate to blood glucose levels and mixed results can be found (Baker & Wolfe, 2020).

Lastly, exercise causes a significant increase in blood $[\text{K}^+]$. It is known that sweat $[\text{K}^+]$ is often overestimated because of skin contamination. For $[\text{K}^+]$ part of the sweat gland secretion mechanisms is known. For the relation between blood and sweat $[\text{K}^+]$ contradictory results can be found as well (Holmes, 2016; Patterson et al., 2000). The ambiguous nature of the literature about the relation between blood and sweat analytes does not rule out the existence of any relationship between sweat and blood. The current methodologies for measuring sweat composition and sweat rate are underdeveloped and numerous different approaches are used in the research presented above. Furthermore, an important aspect that needs to be considered is the possibility that can take a reasonable amount

of time before a biomarker molecule in blood is secreted via the sweat. Novel real-time measurement systems and standardized protocols would empower physiologists to research the relations between sweat and blood markers in more detail and to identify the physiological mechanisms of sweating. For this reason, the sweat parameters are of interest for future applications of athlete monitoring.

2.2. Biomechanics

Biomechanics plays an important role in understanding the mechanisms of human movement. While the parameters mentioned in the previous paragraphs are related to internal load (Halson, 2014), biomechanical measurements are related to external load, which is defined as *'the work completed by the athlete, measured independently of his or her internal characteristics'* (Halson, 2014; Wallace et al., 2009). With biomechanics it is possible to estimate the muscle forces during physical activity and these muscle forces can tell something about the muscle tissue load, which is related to musculoskeletal injury. In several applied projects of the Citius Altius Sanius programme, the analysis of movement and the forces acting on the muscles is taken as a starting point to identify injury risk factors. In order to translate measurable data to actual muscle forces, neuromuscular modelling methods can be used. Inverse dynamics is most commonly used to determine the joint moments and forces based on data collected by three-dimensional motion analysis (Hong & Bartlett, 2008). In Figure 2.2, an overview of this model can be found. As can be seen in this overview, kinematic data are used to find the location, speed and accelerations of the body segments (Al-Amri et al., 2018). Force plate data quantify the externally applied loads (Payton & Bartlett, 2008). Electromyography (EMG) provides information about muscle activation (Hong & Bartlett, 2008; Kleissen et al., 1998) and lastly, anatomical information can be retrieved from anthropometric data or more specific MRI/CT data.

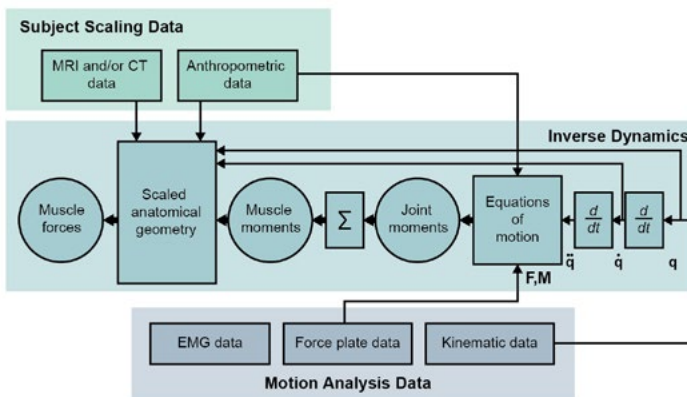


Figure 2.2. Schematic overview of an inverse dynamic model. Adapted from (Hong & Bartlett, 2008).

2.3. Overview of important physiological parameters

To summarize the physiological parameters of interest for injury prevention and monitoring athlete performance, an overview was made (Table 2.1). Please note that in particular for sweat and blood parameters a selection of important more commonly researched constituents is made. The parameters are categorized in parameters that measure internal load and parameters that measure external load (Halson, 2014; Wallace et al., 2009). Taylor et al. (2012) identified four main purposes for training monitoring. They reported injury prevention, monitoring effectiveness of the training program, maintaining performance and prevention of overtraining as the main reasons. We used their definition as a starting point to form two more specific purposes:

1. Injury prevention: these contain muscle injuries, thermal injuries, dehydration and nutrition and metabolic health issues.
2. Monitoring effectiveness of the training/match: including maintaining performance, and prevention of overtraining and overreaching.

Most of the parameters mentioned in the table show the potential to be used for both purposes.

Table 2.1: Selection of physiological parameters of interest

<u>Parameter</u>	<u>What to detect?/ Purpose</u>	<u>Possible Sensing Technique</u>	<u>Required Measurement Range*</u>
Oxygen uptake	Anaerobic Threshold/ VO_2 max/ Minute Ventilation ^{1,2}	Galvanic fuel cell	VO_2 : 0.5-3.0 l/min (Özyener et al., 2001)
Minute ventilation		Turbine flow meter	10-150 l/min (Chlif et al., 2018; Veicsteinas et al., 1985)
Exhaled CO_2 concentration		Non dispersive infrared sensor	0.3-5 l/min (Chlif et al., 2018; Wasserman et al., 1973)
Energy/ Water intake	Prevent dehydration/ energy shortage ^{1,2}	Manually	kilocalories/liters
Environmental data	Humidity, temperature, atmos- pheric pressure ^{1,2}	Capacitive humidity sensor/thermistor	-20 to 50 °C/ 0-100%/ 101-37 kPa

Heart Rate	Heart rate variability ^{1,2}	Electrocardiography / Optical sensor	4-250 bpm
Body core temperature	Hyper-/hypothermia ¹	Thermistor	30-45 °C
Electrical muscle activity	Muscle activity ^{1,2}	Electromyography	Freq. range: 5-450 Hz , Voltage (V _{pp}): 0 to 6mV
Blood [lactate]	Anaerobic threshold ^{1,2}	Laboratory testing/ hand held devices that use enzymatic amperometric detection (glucose & lactate)	1-4 mM (R. P. Simões et al., 2010)
Blood pH level	Decrease in pH value ^{1,2}		7.5-7.2 (H. G. Simões et al., 2003)
Blood [glucose]	Glycemic threshold ^{1,2}		4 mM -6 mM (H. G. Simões et al., 2003)
Blood [K ⁺]	Hyperkalemia ¹		3-7 mM (Atanasovska et al., 2014)
Blood osmolality	Prevent dehydration ^{1,2}		280-310 mM (Cheuvront et al., 2013)
Blood [Urea]	Elevated blood urea nitrogen ²		9-13 mM in serum (Lemon & Mullin, 1980)
Blood Proteins: Creatine kinase(CK), Cytokines like IL-6	Chronically elevated CK ² /Elevated Cytokine levels ¹		IL-6: 2.15*10 ⁻⁴ - 5.69 *10 ⁻⁴ nM (Sonner et al., 2015) CK: 100-400 UI/L (Alvear-Ordenes et al., 2005)
Blood Hormones: Cortisol/ Testosterone	Decrease in C/T ratio ²		Cortisol: 300-700 nM Testosterone: 10-30 nM (Tanskanen et al., 2011)
Arterial Blood Gases pO ₂ and pCO ₂ (partial pressure)	Increase in pCO ₂ and decrease pO ₂ , related to AT ^{1,2}	Laboratory testing	pO ₂ : 75-100 mmHg pCO ₂ : 30-45 mmHg (H. G. Simões et al., 2003)

2. Physiological parameters of interest

Oxygen saturation SpO ₂	Decrease in SpO ₂ ^{1,2}	Pulse Oximetry	100%-90% (Stewart & Pickering, 2007)
O ₂ and CO ₂ concentration in tissue	Δ [O ₂ Hb-HHb]/ oxygenation index ^{1,2}	Near Infrared spectroscopy	Δ [O ₂ Hb-HHb]: 0 till -0.8 A.U. (Grassi et al., 1999)
Sweat Volume	Sweat rate ^{1,2}	Impedance measurement/ scale/ humidity measurement	<1-20 nl/min/gland Gland density: 100-150 glands/cm ² (Sonner et al., 2015)
Sweat [Na ⁺] & [Cl ⁻]	Prevent dehydration/ measure exercise intensity ^{1,2}	Ion-selective electrodes	10-90 mM (Baker, 2019)
Sweat [Lactate]	Anaerobic threshold/ muscle fatigue ^{1,2}	Enzymatic/ amperometric detection	5-40 mM (Baker, 2019)
Sweat [NH ₄ ⁺]	Muscle fatigue ^{1,2}	ion-selective electrodes	0.5-8 mM (Sonner et al., 2015)
Sweat [K ⁺]	Hyperkalemia ¹	ion-selective electrodes	2-8 mM (Baker, 2019)
Sweat [glucose]	Anaerobic threshold ^{1,2}	enzymatic amperometric detection	0.01 mM - 0.20 mM (Baker, 2019)
Body kinematics	Limb segment orientation/joint angles/Segment strain	Video sensing, Inertial measurement units, strain sensors, goniometry	Depending on sensing method
Global body location	body location	GPS, RFID	e.g. 0-150 m to cover a football field
Angular Velocity	Angular velocity of body segments	Gyroscopes	e.g. elbow during baseball pitch: >2000 °/s (Dun et al., 2007)



Linear Acceleration	Acceleration of body segments	Accelerometer	e.g. foot peak acc. during kicking in football can be >50 g (Arpinar-Avsar & Soylu, 2010)
Reaction forces	Reaction forces of the environment	Force platforms	0-2500 N (Cross, 1999)
<p>*Values give an indication of the measurement range.¹ Injury prevention: these contain muscle injuries, thermal injuries, dehydration and nutrition and metabolic health issues. ² Monitoring effectiveness of the training/match: including maintaining performance, and prevention of overtraining and overreaching. ³hypothetical purposes</p>			

2.4. Research directions

From the overview presented in Table 2.1, four possible research directions were identified for unobtrusive athlete monitoring (Figure 2.3). By assessing scientific potential from physiological as well as technological perspective, while taking the research directions from the movement scientists within the consortium into account as well, two of these four research directions were selected. The chosen directions are highlighted.

1. **Measurement of internal load via sweat analytes.** The physiological mechanisms behind sweating and their relation to blood biomarkers is not yet fully understood. An important reason for this knowledge gap is the lack of standardized measurement techniques for sweat collection and analysis. Real-time sweat sensor patches can empower physiologists to unravel the relations between sweat and blood biomarkers for future athlete monitoring applications. Therefore, we will focus on the development of a sweat collection patch for continuous monitoring during exercise and offline laboratory analysis of electrolytes afterwards. Four types of analytes were selected based on their potential purposes for athlete monitoring: ammonia, potassium, sodium and chloride concentrations in sweat.
2. **Measure respiratory rate and heart rate to detect anaerobic threshold.** Respiratory rate sensors and heart rate sensors can be used to measure pulmonary and cardiovascular reaction to exercise. Optical as well as electrical heart rate sensors are already widely used in sports. Respiratory rate is relatively easy to detect with for example an accelerometer or strain sensor.
3. **Measurement of the EMG signal.** Electromyography is widely used among movement scientists to measure muscle activity. Wet Ag/AgCl electrodes are the standard electrodes used in such research. These electrodes cannot be used in day-to-day monitoring applications. A potential research direction would be to

identify ways of acquiring a reliable signal with wet or dry electrodes that are integrated in clothing for day-to-day use.

4. **Tracking local movement of body segments.** Measuring limb kinematics during trainings and matches would be of great value in determining external training load and the prevention of injuries. Currently, common practice is to tape inertial measurement units (IMUs) to the skin. However, this is labour-intensive, requires a lot of data processing steps and is not suitable for day-to-day use. Therefore, it would be desirable to develop an easy-to-use garment with integrated IMUs, which can monitor limb movements on the field and during daily training sessions. Such a garment should be co-developed with human movement scientists and would provide a highly practical tool for monitoring studies focusing on injury prevention.

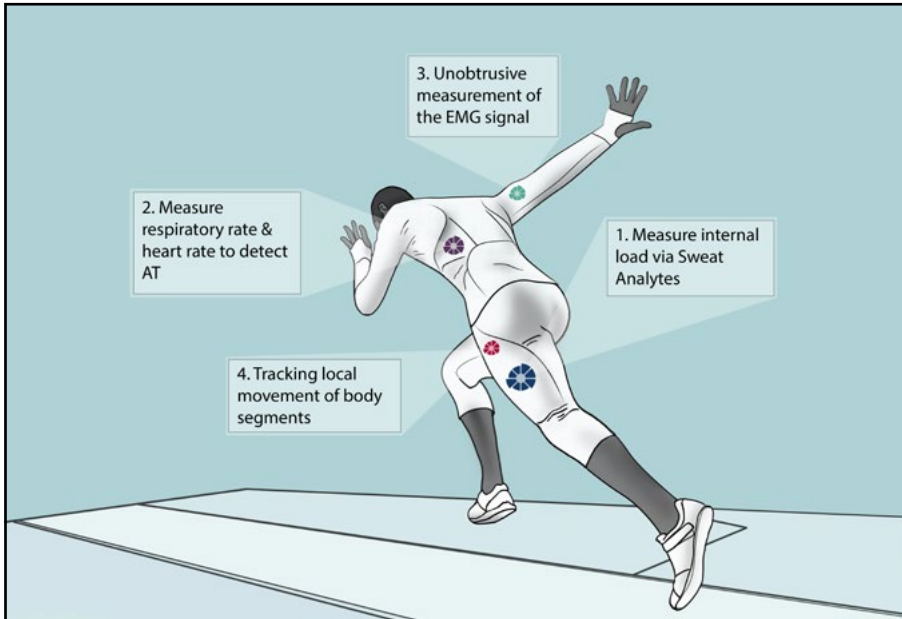


Figure 2.3. Potential research directions for unobtrusive athlete monitoring.

3

Wearable sensor system design approach

In this research, we used an application-oriented research and design approach towards the successful implementation of wearable sensor systems. This chapter describes our approach summarized in a framework that shows the different stages in wearable sensor system development. First, a general explanation of the framework is given. Afterwards, it is explained how the framework is applied to the two research projects presented in this thesis.

30

3.1. Design framework

As can be seen in Figure 3.1, the starting point for each project is a problem statement, research question, or need from a physiological or medical perspective. On the one hand, a problem statement can be based on a curiosity-driven research question. To give an example, a curiosity-driven research question from a physiological perspective can be: “Do sodium and chloride levels in sweat relate to hydration status during exercise?”. To find an answer to this research question, reliable sweat collection and analysis methods are required. For this research, the technological problem statement would therefore be: “There are no standardized methods to measure sodium and chloride levels in sweat real-time during exercise”

On the other hand, the problem statement can be application-driven. In this situation, the physiological parameter of interest has a clearly defined purpose, but the technological solution to measure this parameter does not yet exist or has major limitations. An application-driven research question would be “Can we measure body kinematics during day-to-day sports activities?”.

After identification of the physiological starting point. It needs to be decided, which sensors are required to measure the parameter of interest. In some cases, the required sensors that have the desired specifications are commercially available and the designer can move to the system development phase. In other cases, a new sensor needs to be developed. Selecting the sensing concept, sensor fabrication, microsystem integration, and sensor characterization are part of this phase. In the wearable sensor system development phase, the sensor is integrated in a wearable device. This phase includes designing read-out

3. Wearable sensor system design approach

electronics, software development, electronics integration, and lab validation.

After system development, validation studies are performed in the application environment. In this case, the sensor systems are tested during sports activities. The fourth phase comprises technical validation and user testing. During the technical validation studies, the new sensors are compared against reference systems to prove that the sensors are measuring the desired parameter reliably. In user tests, user experience is researched.

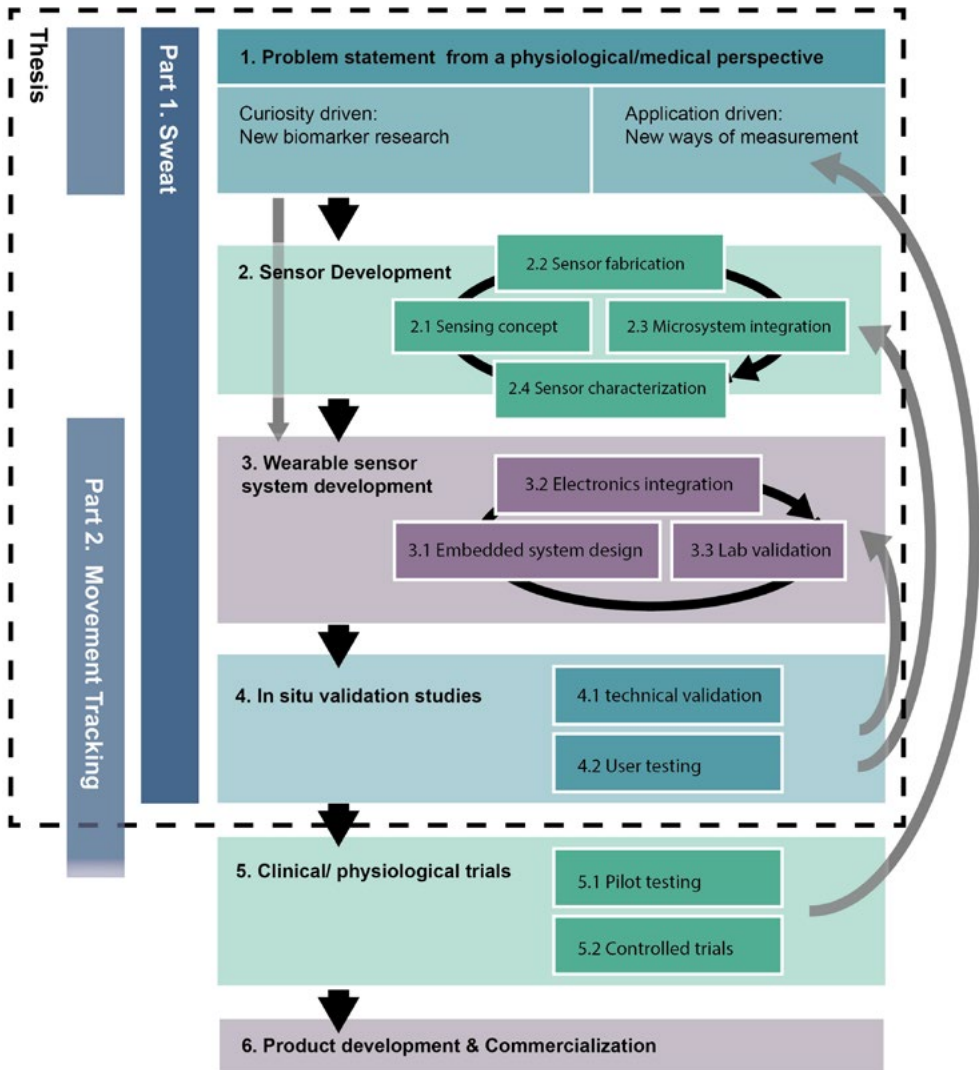


Figure 3.1. Design framework for wearable sensor systems (right) and research topics addressed in this thesis (left).

These *in situ* validation studies are not all-encompassing in the first place. Often, a certain part of the functioning is tested *in situ* and iterations are performed to improve the system. To emphasize that the development is not a linear process and that iterations are necessary to develop a successful wearable that supports in answering the initial research question, the arrows on the right side of Figure 3.1 are included.

This thesis is concluded with the results of successful in-situ validation studies of a selection of wearable devices. In a subsequent phase, the sensor systems are ready to be used by physiologists or clinicians to perform extensive physiological and clinical trials. When these trials have positive outcomes, a commercial product can be developed, which is the last phase of wearable sensor system development.

3.2. Design cases

This section describes how the framework was applied in the two research projects of this thesis. In the first project, three sweat sensor systems are developed starting from a curiosity-driven problem statement. In the second project, a clear application-driven motivation formed the start of the research project. A sensor garment with integrated inertial measurement units is developed to monitor lower limb kinematics in the sports field.

32

Sweat

Sweat sensing offers new opportunities for real-time unobtrusive monitoring of biomarkers. Although the sensor technology advances fast (Bariya et al., 2018), little is known about the mechanisms behind sweating and how sweat composition relates to blood composition. Therefore, scientifically validated applications of sweat sensors are still limited. An important reason for this limited physiological knowledge about sweating, is the absence of standardized methodology for collecting and analysing sweat during exercise. Current sweat collection methods include the absorbent patch technique (Morris et al., 2013), the armbag technique (Appenzeller et al., 2007) and sweat collection with the Macroduct sweat collector (Katchman et al., 2018) that is designed for the diagnostic process of cystic fibrosis (Doorn et al., 2015). These methods are labour-intensive and prone to contamination during exercise (Baker, 2017). Chemical analysis is performed offline.

To enable reliable sweat collection and analysis, a novel sweat patch was developed. This patch collects sweat in a sequence of reservoirs that fill chronologically. To validate the use of this patch *in situ*, a physiological experiment was performed. Sweat samples were collected with the new patch from the back of an athlete and analysed offline using ion chromatography. The design and development of the first patch is presented in chapter 4.

In the first part of this project, the fluidic patch was designed and developed and validated in a physiological setting. Chapter 5 presents the next steps in this project. Based on the first design, a new patch was developed that contains a filling rate sensor system and continuous sweat conductivity sensors. After benchtop characterization of this sensor system, the sweat patch 2.0 was validated in a more elaborate physiological experiment. Six participants performed an exercise in a climate chamber. The patch was placed at three locations at

the back and the continuous conductivity measurements from the patches were compared against other reference systems: a ventilated capsule measurement system and offline ion-chromatography.

With the sweat patch 2.0, total ionic content could be measured real-time. To measure specific analytes, other sensor principles need to be applied. In chapter 6, continuous measurement systems for specific analytes are presented. At first, we developed an electrochemical sensor that can measure $[\text{Na}^+]$ and $[\text{Cl}^-]$ in sweat. Second a sensor system was developed that can continuously measure NH_3 that is evaporated from the sweat underneath a ventilated capsule. The development of these last two systems is part of an ongoing development process. The sensors were characterized and tested in preliminary physiological tests. Further benchtop characterization is necessary to use these systems in a more elaborate physiological experiment.

Movement tracking

Football is played by more than 260 million people worldwide (Fédération Internationale de Football Association, 2007). During an elite football game, players run about 10 km at 80 to 90 percent of their maximal heart rate. Numerous explosive actions take place, including high intensity sprints (which are quick accelerations followed by deceleration), turning, tackles, jumping, kicking and sustaining forceful contractions to maintain balance of the body and to control the ball (Stølen et al., 2005). In elite European football, 6 to 7 hamstring muscle injuries occur per team per season, which results in an absence of 14 to 180 days (Ekstrand et al., 2017). These injuries occur typically in the last part of a training or match. This implies that the accumulation of demanding actions is an important factor for hamstring injury risk.

In current practice, physical player load is measured at the field by deriving the global location of the player with Global Positioning Systems (GPS) and Radio Frequency Identification (RFID) systems. However, these systems are not able to monitor leg movement and to distinguish demanding actions like kicking, cutting and jumping to monitor the load on the lower limbs. In order to monitor these actions in the field to quantify injury risk, a novel design of a smart garment is being developed. The smart garments are used by human movement scientists to research the aetiology of hamstring injuries.

During the design phase of the new sensor garment, a participatory design approach (Dell’Era & Landoni, 2014) was followed. The movement scientists are involved in every main decision in the design process. State-of-the-art movement tracking systems include optoelectronic systems (e.g. Vicon V5 cameras, Vicon Motion Systems Ltd., UK) and inertial measurement units (Al-Amri et al., 2018). Optoelectronic systems are restricted to a lab environment. But inertial measurement units (IMUs) are miniaturized sensor units that contain 3-axis accelerometer, gyroscope and magnetometer, which allows to bring them to the field. These sensors can be placed at lower limb segments and with sensor fusion algorithms, limb kinematics can be derived. In this project, IMUs were integrated in shorts or tights, to enable measurement during day-to-day trainings and matches.

Design challenges focused on identifying the right sensor locations, reliably reading out and storing data at a sample frequency of 250 Hz, washability and wireless data transfer.

The project had a time span of 4 years and every year a new, improved prototype was created. Each prototype represents a new iteration cycle in a new chapter (chapter 7 till chapter 10). The prototypes were used in two types of validation experiments. On the one hand, prototypes were technically validated with an optoelectronic system, which is the golden standard in movement tracking. Results of one of those studies can be found in chapter 8. On the other hand, field tests and user experience tests were performed. Athletes were asked to fill in a small questionnaire including questions about comfort and ease-of-use.

After the *in situ* validation tests new improved prototypes were developed. The function of wireless data transmission was integrated in a third prototype and in a fourth prototype robustness of the connections and washability was improved. At the current stage, the prototypes can be used in more extensive physiological tests, in which hamstring injury risk factors can be researched.

3.3. Conclusions

During the course of this research project, a design framework was developed that can support sensor researchers and system engineers in developing wearable sensor systems for scientifically validated applications. For successful implementation, it is of great importance to work closely together with physiologists and to test the wearable systems *in situ* at an early stage. Based on the findings of early physiological tests, design iterations can be performed and systems can be created that fit the user's needs. In the two research projects that were presented in this chapter, the framework was applied. All projects started with a problem statement from a physiological perspective. In this research project, we reached the stage of elaborate physiological testing in the movement tracking project as well as in the sweat patch project.

3. Wearable sensor system design approach

II

Sweat Sensing during Exercise

.....
*This section is based on the following publications:

Steijlen, A. S. M., Jansen, K. M. B., Bastemeijer, J., French, P. J., Bossche, A. (2022) A low-cost wearable fluidic sweat collection patch for continuous analyte monitoring and offline analysis. *Analytical Chemistry*. 94(18), 6893-6901. doi:10.1021/acs.analchem.2c01052

Steijlen, A. S. M., Bastemeijer, J., Groen, P., Jansen, K. M. B., French, P. J., & Bossche, A. (2020a). A wearable fluidic collection patch and ion chromatography method for sweat electrolyte monitoring during exercise. *Analytical Methods*. doi:10.1039/D0AY02014A

Steijlen, A. S. M., Bastemeijer, J., Jansen, K. M. B., French, P. J., & Bossche, A. (2020). A novel sweat rate and conductivity sensor patch made with low-cost fabrication techniques. Presented at IEEE SENSORS 2020.

Steijlen, A., Bastemeijer, J., Nederhoff, R., Jansen, K., French, P., & Bossche, A. (2021). A New Approach for Monitoring Sweat Ammonia Levels Using a Ventilated Capsule. *Engineering Proceedings*, 10(1), 38.

Motivation

Continuous health monitoring can contribute to the prevention of chronic diseases, by creating awareness about lifestyle and by stimulating physical activity (Girginov et al., 2020; Gualtieri et al., 2016). Furthermore, it may support in the prevention of injuries (Di Paolo et al., 2021; Yan et al., 2017) and it can contribute to effective and efficient treatment of diseases (Rodbard, 2017; Rosero et al., 2013). Common health monitoring devices include heart rate monitors and movement sensors. Recent advances in wearable sweat sensor systems show great potential to add new physical and chemical information about a person's health status. Sweat samples can be collected unobtrusively and continuously, which are main advantages compared to widely used blood tests. The unobtrusive nature of sweat sensing and its potential use in real-time health monitoring, motivated researchers to develop electrochemical sweat sensors to monitor sweat constituents. Literature reviews show a vast number of recently developed sweat sensors (Bariya et al., 2018; Ghaffari et al., 2021; Kaya et al., 2019; Mohan et al., 2020; Moonen et al., 2020).

Although, sweat provides ways to unobtrusively monitor biomarkers, measuring sweat constituents introduces new challenges, that are not present in blood sampling. Below, the most important challenges are reported, based on literature and our own experiments (Baker, 2017; Heikenfeld, 2016).

38

1. Sweat rates vary over time and influence sweat composition.
2. Sweat rate and composition differ per body location
3. Due to the low sweat rates per gland (nl /min/mm²), sample volumes are small.
4. Skin and sweat gland metabolism influence the concentration levels in sweat.
5. Contamination of new sweat with old sweat, or by skin contaminants can occur.
6. Sample collection is difficult due to evaporation from the highly distributed sweat glands, and the irregular skin surface.
7. Several sweat analytes, such as glucose and proteins, are present in very low concentrations.

Furthermore, scientific knowledge about the physiological mechanisms of sweating and how sweat analyte levels relate to blood levels, is limited (Klous et al., 2020). During strenuous exercise and/or exposure to hot environments, body core temperature rises. Evaporation of sweat from the skin plays a critical role in regulating body temperature (Baker, 2019). The thermoregulatory function of sweating is well-accepted, but the physiological knowledge about using sweat constituents, i.e. electrolytes and metabolites, as a biomarker is limited. For most constituents in sweat, correlations between concentrations in blood and concentrations in sweat are not known.

For sodium and chloride, with concentrations in sweat ranging from 10 mM till 100 mM, secretion mechanisms are known (Sonner et al., 2015). Na⁺ and Cl⁻ ions are secreted in the secretory coil of a sweat gland and partially reabsorbed in the duct. The number of reabsorbed ions has a direct relation to the sweat rate. When sweat rates increase, a lower percentage of ions is reabsorbed and the absolute concentration of these ions in sweat

increases (Baker, 2019; Buono et al., 2008). Several articles suggest that an increase in Na^+ or Cl^- levels can be used as a biomarker for dehydration (Gao et al., 2017; Rose et al., 2015). There are also researchers who state that $[\text{Na}^+]$ and $[\text{Cl}^-]$ loss can indicate electrolyte imbalance (Bandonkar et al., 2014). However, in physiological literature, even for these most available ions in sweat, equivocal and even contradictory results can be found (Baker & Wolfe, 2020). The main reason for these existing gaps in literature is the lack of standardized methods for chrono-sampling of sweat (Hussain et al., 2017). Sweat samples are mostly collected with simple devices, such as absorbent patches and the Macroduct sweat collector (Liu et al., 2020). Chrono-sampling with these devices requires a lot of repetitive work. This results in a limited number of samples.

To facilitate chronological sampling of sweat and to enable continuous sweat monitoring, many new sweat sensor systems have been developed recently. Most sensors focus on continuous measurement of a sweat constituent, such as electrolytes and metabolites, with a miniaturized wearable device. To give a few examples in the category of electrochemical sensing systems, Guinovart et al. (2013) created a potentiometric sensor integrated in a tattoo that can measure NH_4^+ in sweat. Gao et al. (2016) designed a sensor array that enables potentiometric measurement of electrolytes, like Na^+ and K^+ and amperometric measurement of metabolites such as lactate and glucose. Mugo and Alberkant (2020) developed a non-enzymatic cortisol sensor that makes use of molecular imprinted polymers for selectivity, and Yuan et al. (2019) created a sensor that can measure sweat rate, total ionic charge and sodium concentration. Some researchers focus on the microfluidic system that enables capture and transport of the sweat to the sensor (Koh et al., 2016; Ma et al., 2020; Nyein et al., 2018). While other researchers focus on the fabrication and improving the specifications of the sensor itself (Liu et al., 2016; Zoerner et al., 2018). In particular, a lot of research is being executed in optimizing the sensitivity, selectivity and durability of the electrode materials (Kinnamon et al., 2017; Lin et al., 2019; Liu et al., 2021). Additionally, significant progress has been achieved in design integration of the fluidic system and the sensors (Gao et al., 2016; Nyein et al., 2018).

These novel systems may support physiologists in their research to find sweat biomarkers, but there are two major limitations. First, the fabrication of the systems has high complexity and requires advanced equipment and expensive materials. Second, the new systems are validated in an exercise setting with a very limited number of participants. Interpretation of the data and comparing them against results from other articles is a challenge, because protocols are not standardized, and in most cases no sweat reference measurements are performed during the exercise.

Research Approach

The aim of this research was to develop novel sweat sensor systems that enable continuous *in situ* monitoring of sweat composition and controlled sampling of sweat for (offline) reference measurements. At first, a new sweat sensing concept was developed that facilitates novel sweat sensor validation and physiological research towards finding new sweat biomarkers. The concept is presented in Figure 4.1. Sweat is collected from an enclosed part of the skin surface. Afterwards, it flows into an analysis chamber that contains real-time sensors for measuring sweat composition. The inflow of sweat needs to be monitored, because the sweat composition depends on the sweat rate (Baker & Wolfe, 2020). The sweat passes the sensor electrodes and flows into a sequence of reservoirs. The chemical composition of the samples can be analysed after the physiological tests in a chemical laboratory.

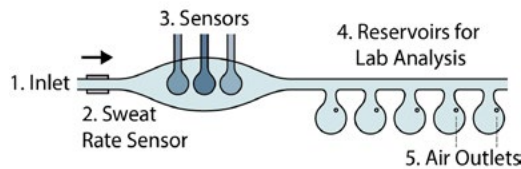


Figure 4.1. Schematic representation of the new sensor patch concept.

Several iterations were performed during the development of the sensor patch. First the sweat collection system was developed. CFD simulations were performed and lab experiments with a syringe pump were executed. After validation in the lab, a first physiological experiment was performed. The design and validation of the first patch are

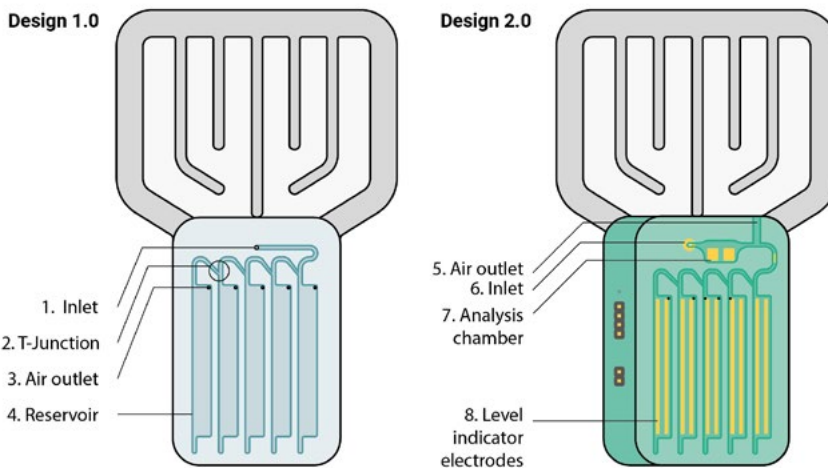


Figure 4.2. The two main designs of the sweat patch.

presented in chapter 4. Second, conductivity sensors were integrated in a new version of the sensor patch (Figure 4.2). These sensors measure the filling rate of the patch and also perform a continuous sweat conductivity measurement. The second sensor patch was validated in a larger physiological experiment. The design and *in situ* validation experiments are presented in chapter 5.

The sensor patch that is presented in chapter 5 measured total ionic content in sweat. A next step is the development of sensors for specific analytes. Continuous measurement of specific analytes can be of great value in research about physiological mechanisms behind sweating and identifying new sweat biomarkers. In chapter 6, two measurement systems for specific analytes are presented. The first system is an electrochemical sensor that can measure Na^+ and Cl^- concentrations in sweat and the second system measures sweat NH_3 levels in a ventilated capsule.

4

Wearable fluidic collection patch for sweat monitoring during exercise

42

Although a large quantity of compact and continuous sweat sensing systems are presented in recent literature, applications for monitoring an athlete's or patient's status are still limited. Physiologists are lacking proper collection and analysis systems for continuous monitoring to find useful sweat biomarkers and how they change over time. While in the technological literature, validation of novel sweat sensor systems in human trials appears difficult, because there are no standardized ways to perform reference measurements by chronosampling sweat and analysing it in the lab afterwards. To solve these problems, we propose a new sweat collection device that can automatically collect a sequence of sweat samples ($> 100 \mu\text{l}$). The system is easier to fabricate and the collection surface is larger than in previously presented solutions, which facilitates the use of the system by both engineers and physiologists and increases reliability of the measurements. Physiological experiments and chromatography measurements are executed to prove that this method can be used to analyse electrolyte variations over time. The sweat collector device can in principle be connected to an electrochemical sensing system for continuous measurements. The testing of our new sweat collectors with an in-situ analysis system will be discussed in a subsequent chapter.

4.1. Method

In order to allow for continuous uptake of sweat volumes and to simplify the collector placement process, it was decided to develop a simple disposable foil type sensor patch that can automatically collect a sequence of 5 samples. The design, simulations of the inflow of sweat and lab experiments are presented first. After demonstrating the working principle of the collector, the new system was tested in a physiological experiment. Sweat was collected with the new patch during exercise and analysed in the lab with ion chromatography.

Design & simulations

The fluidic system contains a sequence of reservoirs that are created from two layers of hydrophilic film (Visgard 275 (La Casse & Creasy, 1999), a PET film with a PU coating) with a double-sided adhesive (3M 1522 (3M, 2013), a PE tape with an acrylate adhesive) in between.

4. Wearable fluidic collection patch for sweat monitoring during exercise

Design

In Figure 4.3, an exploded view and a front view of the final design of the sweat collection system are presented. The sweat collection surface is 40 cm². The funnel-shaped 2D structure of the skin adhesive (Figure 4.3, nr. 1.) guides the sweat to the inlet. In combination with the grating structure, it serves as a spacer to the skin too, to make sure that the sweat drops down. Due to capillary forces, the sweat flows from the inlet (Figure 4.3, nr. 7.) to the reservoirs (Figure 4.3, nr. 10.). The walls of the capillaries are highly hydrophilic to ensure that the flow rate of sweat is not negatively influenced by the channels. The sweat passes a T-junction (Figure 4.3, nr. 8) at a certain moment. At this junction the sweat needs to flow down into the reservoir. By creating sharp edges at the junction and by directing the left branch of the junction upwards, it is ensured that the sweat goes straight into the reservoir. The materials were cut in the desired shapes with a CO₂ laser system (Merlin Lasers, Lion Laser Systems, The Netherlands). The film is rinsed with demineralized water (to remove

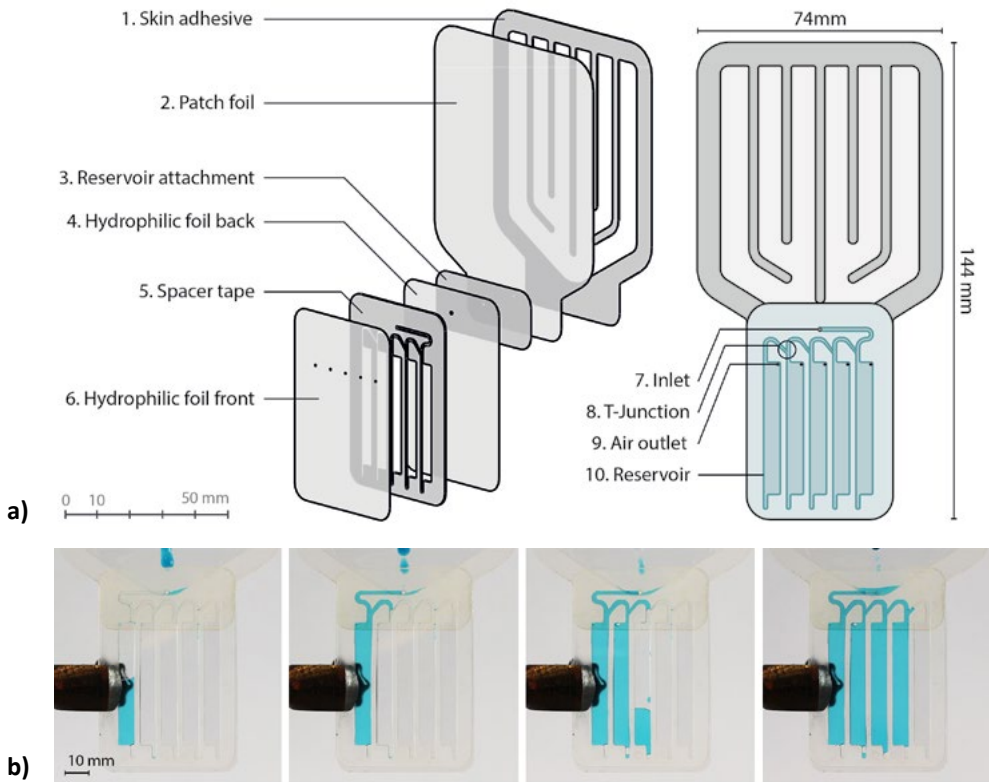


Figure 4.3. Design of the sweat patch: a) left: exploded view, right: front view of the patch. b) The filling process of the reservoirs. When the reservoir is filled, the sweat will take the right turn and will flow to the next reservoir by capillary forces. Entrapment of air is prevented by placing air outlets (Figure 4.3, nr. 9) at the corner of each reservoir.

surfactant that was applied to the film by the manufacturer, because it influenced the sodium measurements in preliminary experiments). Samples of the foil and adhesive were placed in vials with demineralized water (3ml, 24 hours), and ion concentrations (Na⁺, Cl⁻ and K⁺) in these vials were analysed to ensure the absence of background contaminants from the materials. No significant Na⁺, Cl⁻ and K⁺ peaks were detected in these samples. Contact angles of the materials were measured with optical tensiometry (KSV Instruments Ltd). The spacer tape has an average contact angle of 50.5° and the hydrophilic foil has an average contact angle of 92.2° (Figure A1, appendix).

Simulations

Gravitation and capillary effects are used to make sure that the sweat flows into the reservoirs at a similar or faster volumetric flow rate than the sweat rate. The capillary effects depend on the surface tension and the geometry of the channel. A relation between the capillary pressure and the contact angle and dimensions of the microchannel with a certain height (*h*) and width (*w*) is given by the Young-Laplace equation:

$$P = -\gamma \left[\frac{\cos\theta_t + \cos\theta_b}{h} + \frac{\cos\theta_l + \cos\theta_r}{w} \right] \quad (4.1)$$

44

Where *P* is the capillary pressure, γ the surface tension of the liquid and θ_t , θ_b , θ_l , and θ_r are the contact angles of the top, bottom, left and right microchannel walls. For the design of capillary channels, there are a few practical guidelines. First, contact angles smaller than 60° are preferred (Berthier, 2013). Secondly, some of the walls of a microchannel can be made of a hydrophobic material if one takes into account that the ratio between for example the hydrophobic height and the hydrophilic width of the channel is very low. Furthermore, fluid flow near corners needs to be considered since it can affect the filling of the channels negatively by entrapment of air bubbles (Wu et al., 2018). It can be prevented by rounding edges and corners of the channels for example.

Several designs were made and CFD simulations with COMSOL Multiphysics software were performed to test the functioning of the devices. For the simulations it was assumed that water can flow freely into the channel (ideal case). The transport of the fluid interface was given by a level set function (Comsol Inc, n.d.). This function was coupled with the Navier Stokes equations to describe mass and momentum transport of the fluid. The velocity of the fluid was dependent of convection, pressure, diffusion, the surface tension and gravity in this model.

Initially, a small reservoir at the beginning of the microchannels was filled with water and the rest of the channels and the big reservoir were filled with air. The initial velocity is 0. A hydrostatic pressure was placed at the inlet of the channels ($P=p^*g*y$) and the pressure at the outlet was 0. Atmospheric pressure could be omitted since it is acting on both the inlet and the outlet. The gravity was added to the model as a volume force. The wetted wall feature was used to identify hydrophobic and hydrophilic walls. First, the influence of the

4. Wearable fluidic collection patch for sweat monitoring during exercise

spacer tape and corner flow effects were simulated with a straight channel. Second, parts of the collection patch were simulated to test if the reservoirs fill in the right way and to prevent entrapment of air.

Syringe pump experiments

A syringe pump experiment was executed to test if the reservoirs will fill one after the other and to research if the sweat flow in the collector was the same as the actual sweat rate. The syringe pump (KDSscientific 200, USA) was set at a rate of $48 \mu\text{l}/\text{min}$. Via the funnel-shaped structure, the sweat dropped down towards the inlet of the reservoirs. The collector was designed to be placed at the back of an athlete. The back was chosen, because of the high sweat rate and the presence of eccrine sweat glands at this location. Smith and Havenith (2011) measured a sweat rate at the back of $1.2 \text{ mg}/\text{cm}^2/\text{min}$ during a running exercise at around 155 bpm of 30 min ($25.6 \pm 0.4^\circ\text{C}$, $43.4 \pm 7.6\%$ relative humidity). The patch has a collection surface of 40 cm^2 , which means that the sweat rate will be around $48 \mu\text{l}/\text{min}$. Collector filling was recorded with a camera. After the experiment, stills were taken from the movie. Due to the blue colorant that was added to the fluid, it was possible to count all blue pixels in the image to derive the volume that was filled with fluid. This process was automated with a MATLAB program.

Physiological Experiments

45

The physiological experiments were approved by the Human Research Ethics Committee of Delft University of Technology. The participants gave informed consent before the experiment. Healthy recreational athletes ($n=5$, 20-30 yrs.) that play sports 2 till 5 times a week are asked to cycle for one hour at a cycling ergometer. The ergometer was equipped

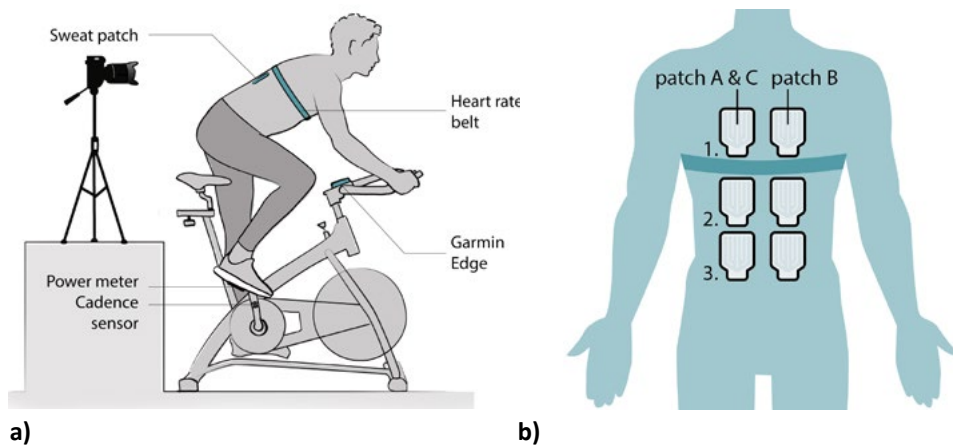


Figure 4.4. a) Setup of the physiological experiment (reproduced from (Steijlen et al., 2020b)). b) Placement of the patches in the final experiment. The patches A (location 1,2 and 3) are placed at the start. Patches B (1,2 and 3) are placed when patches A start filling. Patches of C (1,2,3) are placed when A is filled.

with a cadence meter, power meter (Garmin Vector 3s) and cycling computer, the Garmin Edge 820 (Garmin, USA), that was placed at the handlebar (Figure 4.4a). The subject wore a heart rate monitor and sweat collectors were placed at the back. A camera was placed behind the cyclist and focused on the sweat collectors to measure the filling speed. After placement of the heart rate belt and the first sweat patches, the subject was asked to cycle for one hour at a constant cadence and power output (in the final experiment a cadence of: $M=91$, $SD=5$ rpm, heart rate: $M=158$, $SD=11$ bpm and power: $M=284$, $SD=28$ W were measured (Figure A2), the temperature of the room was 20 °C). Two preliminary tests were performed before the final experiment to improve the test setup. Preliminary results (Figure A3) showed the importance of a strict and optimized test protocol. In the final experiment, the skin was cleaned with a sterile gauze pad that was wetted with demineralized water. This was executed two times before each patch was placed to avoid accumulation of old sweat constituents.

In the first two series of experiments the collectors were replaced at the same location, when a collector was filled completely. Unfortunately, a replaced collector does not start filling immediately (it can take approximately 10 minutes). To improve the continuity of the sweat measurements, the patches were placed as shown in Figure 4.4b in the final experiment. Patch B can now be placed 10 minutes before patch A is filled and more sweat can be collected. It is assumed that the sweat rates at locations left and right of the spine are identical.

Chemical analysis

After sweat collection, transfer to vials was done by perforating the bottom tip of the reservoir on one side. A syringe with air was placed at the air inlet of the reservoir and the sweat was forced out through the perforated tip to the vial. Before each perforation of a reservoir, the outside of the collector was cleaned to prevent that one sample contaminates the other (Figure A4). Approximately 5% of the sweat in each reservoir was lost during transfer. The sweat was diluted with 3 ml of ultra-pure water. The samples were stored in a fridge at 7°C. The day after, the sweat was analysed using ion chromatography/high pressure liquid chromatography (IC/HPLC) (Doorn et al., 2015). The IC system consisted of a Metrohm 881 Anion system and an 883 Basic IC plus system (Metrohm, Switzerland). The two systems worked independently. Both devices contained an HPLC pump that pumps the eluent through a column that separates the ions. After separation, the conductivity of the fluid was measured by a conductivity detector.

To analyse the cations, a Metrosep C6 - 150/4.0 column was used for separation with a solution of 3 mM HNO_3 as eluent. The flow rate is set at 0,9 ml/min. For the anions, a Metrosep A supp 5 - 150/4.0 column was used, and chemical suppression was performed by the Metrohm Suppressor Module, which is regenerated with 150 mM H_3PO_4 . The eluent of the anion system contained 1 mM NaHCO_3 and 3.2 mM Na_2CO_3 . The flow rate in this system was 0,7 ml/min. A sample loop of 20 μl was used in both systems.

Before each analysis, standards needed to be made for all the ions of interest. Solutions

with 0.1 till 100 ppm were made. The measurements of the standards were used for calibration. After assigning manually the right retention times to the peaks, the MagIC Net software automatically created a calibration graph based on the peak areas which can be applied to the measurements. To quantify the accuracy of our method, standard deviation experiments were executed. Standard solutions with 0.1 to 100 ppm Na⁺, NH₄⁺ and K⁺ ions and separate solutions with Cl⁻ ions were created. The solutions were divided in 5 samples and measured one by one to obtain an idea of the standard deviation of the method at different concentration levels.

4.2. Results & discussion

The results of the simulations and lab experiments are presented first. Thereafter, the results from the physiological experiments are discussed.

Design & simulations

A first simulation was executed to find out what the effect of the hydrophobicity of a spacer tape (sidewalls of the channels) is on the volumetric flow rate in the channels. The dimensions of the simulated channel were 2*0.25*4 mm. Contact angles of $\theta = 112.5^\circ$ and $\theta = 67.5^\circ$ are chosen for the hydrophobic walls and the hydrophilic sidewalls, respectively.

To study the effect of corner flow, channels with rounded corners and the same dimensions as the previous channel were simulated as well. One channel had hydrophobic rounded sidewalls and the other had hydrophilic rounded sidewalls. Figure 4.5a shows the influence of the rounded and sharp, hydrophilic, and hydrophobic sidewalls on the contact point position of the fluid-air interface over time. The volumetric flow rate decreases significantly when the hydrophobic sidewalls have rounded corners. Since the laser cut spacer tape is placed on top of another layer of foil, the corners will be relatively sharp.

Simulations were also performed to test whether the T-junction works properly. In Figure 4.5b can be seen that the fluid first flows down and once the water reaches the bottom ($t=5$ ms), it goes left to the next reservoir. Lastly, a simulation was performed to check if entrapment of air would be a problem in the reservoirs. Figure 4.5c shows that the fluid does not block the air outlet during the filling process, so that air bubbles can be released. The filling time of a reservoir with a height of 10 mm, is now very small. This is due to the infinite supply of water at the inlet. The sweat rate will limit the fluid supply in reality. However, the simulation showed that even with an infinite supply of water, the reservoir fills in the right way. This accounts for the T-junction as well.

Syringe pump experiments

Figure 4.3 shows stills from one of the movies that is made during the syringe pump experiments, which prove that the reservoirs fill consecutively. The measurement results of the experiment are shown in Figure 4.5d. A delay of 50 to 80 seconds is observed before the fluid is in the reservoirs and recorded by using a camera. The average volumetric flow rate in

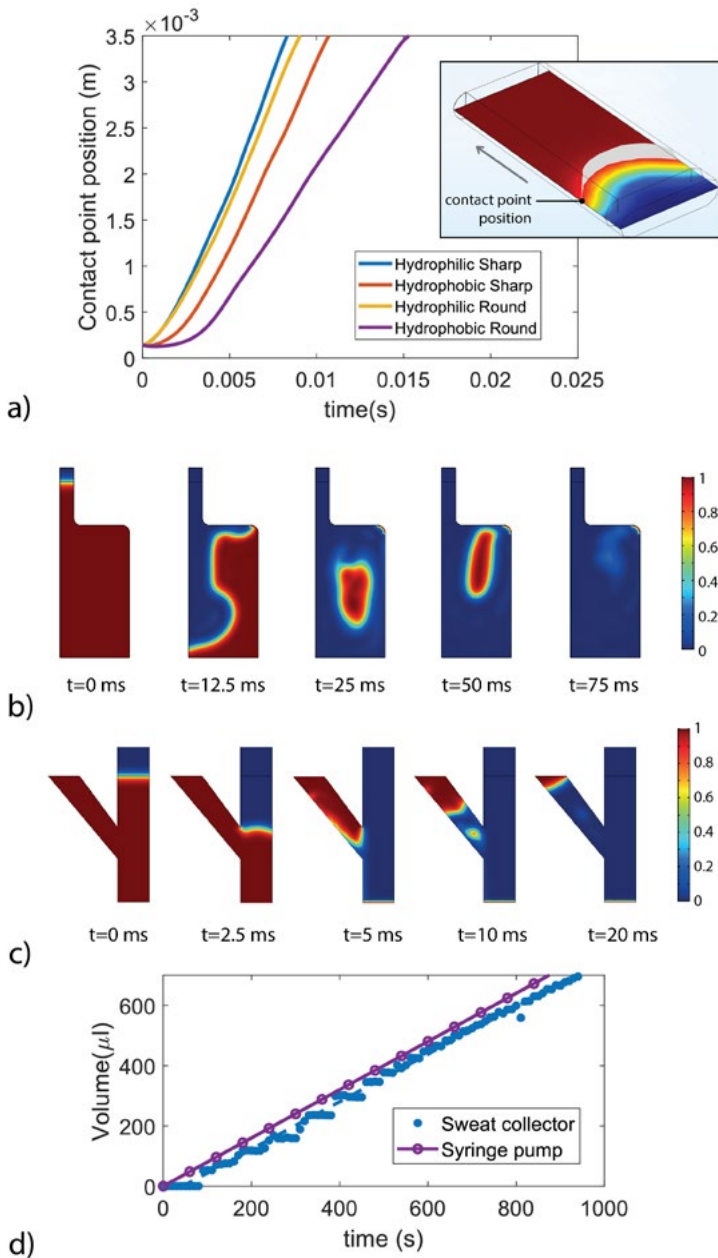


Figure 4.5. a) Contact point position of the fluid-air interface over time of designs with rounded and sharp, hydrophilic and hydrophobic sidewalls. b) Simulation of the T-junction: volume fraction of air at different time points. c) Simulation of the reservoir: volume fraction of air at different time points. d) Volumetric flow rate of the syringe pump vs. the volumetric flow rate in the collector.

4. Wearable fluidic collection patch for sweat monitoring during exercise

the collector is 47 $\mu\text{l}/\text{min}$, which means that the flow rate in the collector is 2% lower. From this we can conclude that the fluid inflow is not significantly inhibited by the resistance of the channels.

Physiological experiments & chemical analysis

After sweat collection during the physiological experiments, the sweat in the collectors was analysed using ion chromatography/high pressure liquid chromatography (IC/HPLC). In the chromatographs of our sweat samples, the peaks are nicely separated and there are no significant unknown peaks that interfere with the peaks of the selected ions (Figure A5).

To get an idea of the standard deviation that is introduced by the IC measurement method, standard deviations of the method were included. These were determined by analysing five samples of each standard (0.1-100 ppm) and plotting the average relative standard deviations (RSDs) in a graph (Figure 4.6a). The fitting curve was used to determine the SDs in the actual measurements. For Cl^- and Na^+ the SDs are relatively small, for K^+ , the concentrations in sweat are around ten times lower so the RSDs of the measurement method become important to consider. The measured concentration levels of Na^+ , Cl^- and K^+ of patch location 2 are shown in Figure 4.6b. The Na^+ and Cl^- concentrations show an initial steady increase which levels off. However, Cl^- levels are systematically lower by on average 16.4 mM (SD=2.5 mM) than the Na^+ levels. This deviation can possibly be explained by the presence of other negative ions like lactate and bicarbonate ($\text{C}_3\text{H}_5\text{O}_3^-$ and HCO_3^-) in sweat.

In Figure 4.6c, the Na^+ , Cl^- and K^+ levels of patch location 1 (between the shoulder blades) and 3 (lower back) are added. The Na^+ and Cl^- levels are very similar for collector 2 and 3 (Cl^- : M=1.6, SD=2.9, Na^+ : M=0.4, SD=3.4 mM) while the Na^+ and Cl^- levels of collector location 1 are significantly higher (Cl^- : M=10.3, SD=2.4, Na^+ : M=10.4, SD=2.9 mM). One of the reasons for this difference between the absolute concentrations of collector 1 and collector 2 and 3 is the variation in sweat rate across the different locations. Smith and Havenith (2011) measured at the sides of the upper back a median sweat rate of 0.84 $\text{mg}/\text{cm}^2/\text{min}$, while at the sides of the lower back this sweat rate was 0.75 $\text{mg}/\text{cm}^2/\text{min}$. Higher sweat rates decrease ion reabsorption per unit volume and therefore higher concentrations can be measured at the upper back.

Figure 4.6d shows the K^+ levels at the three locations over time. A decrease was measured over time and no difference between the three locations was detected within the error margin. To test whether the trend is still a decreasing line, when taking the large SDs into account, random samples and their linear fits ($n=1000$) were created, assuming a normal distribution. Within the 95% confidence interval, the fits for location 1 and 2 were always a decreasing line. However, from literature it was assumed that only minimal changes in K^+ levels occur in sweat (Baker & Wolfe, 2020). Therefore, it is expected that elevated values after the start of the exercise are due to the presence of old sweat or residue in the channels or other physiological effects that need further research.

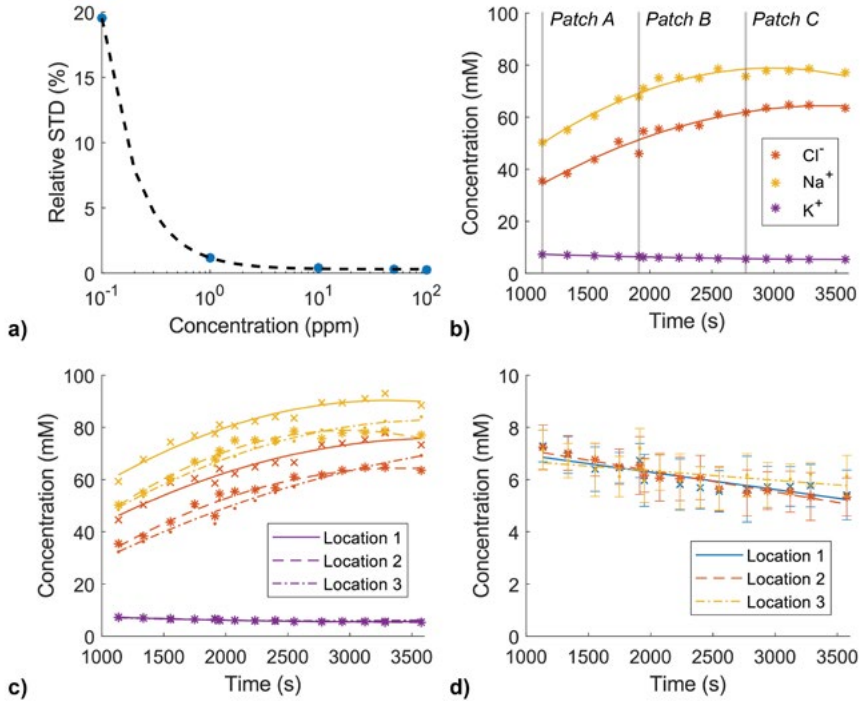


Figure 4.6. a) The accuracy of the IC method: relative standard deviation at different ion concentration levels of standard solutions. b) the Na^+ (top), Cl^- (middle) and K^+ (bottom) levels of patch location 2. c) the Na^+ (top), Cl^- (middle) and K^+ (bottom) levels of patch locations 1,2 and 3. d) Potassium concentrations over time for patch locations 1,2 and 3.

Because an increased sweat rate leads to less ion reabsorption in the reabsorptive duct, sweat rate measurements are important as well. The sweat collection rate is measured at location 2 during the experiments with the help of a camera. The average sweat rate is $1.19 \text{ mg/cm}^2/\text{min}$. The sweat collection rate varied between 0.74 and $1.54 \text{ mg/cm}^2/\text{min}$ (Figure 4.7a). The sweat rate was plotted against the concentration of Na^+ and Cl^- , to check whether this relation was visible. The data allows us in principle to verify a possible relation between sweat rate and Na^+ and Cl^- concentration. Although the plot of Figure 4.7b suggests a mild increase in ion concentrations with increasing sweat rate, the scatter in the current data is too large to draw a solid conclusion. In a next phase of this project, other sweat rate measurement techniques will be explored, by for example conductive or capacitive measurements. It would also be interesting to compare this new way of sweat rate measurement with conventional methods like the ventilated capsule measurement and the absorbent patch method in the same physiological experiment (Morris et al., 2013).

4. Wearable fluidic collection patch for sweat monitoring during exercise

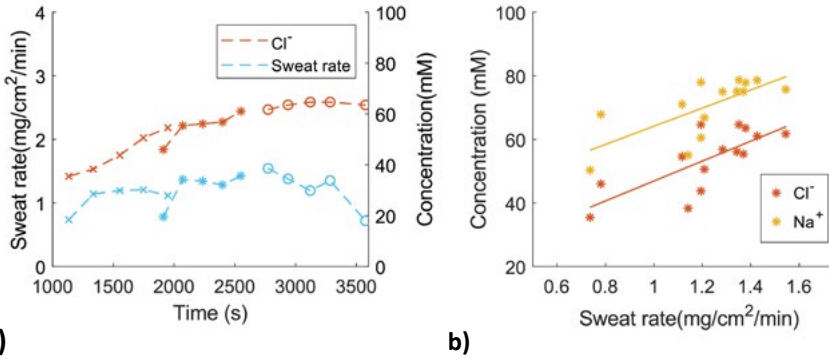


Figure 4.7. a) Sweat rate and Cl⁻ variation over time b) Relation between sweat rate and Na⁺ and Cl⁻ concentration

4.3. Conclusions

The results of the final physiological experiment showed that Na⁺, Cl⁻ and K⁺ can be measured accurately with this new collection system in combination with ion chromatography. Although the Na⁺ and Cl⁻ concentrations differ when the collector is placed at the upper back, all three collector locations show a similar trend in Na⁺ and Cl⁻ levels. K⁺ measurements are also reproducible, and a decreasing trend was measured.

In the current study, data from only one physiological experiment of a single individual were compared, because it is well known that sweat analyte concentrations can differ considerably between individuals and that the day-to-day variability in sweat analyte concentrations can be large. Therefore, comparing, and interpreting data between individuals in small scale experiments, would be less relevant.

However, the presently developed device will facilitate more systematic larger studies on the inter-individual variability as well as the daily variations of a single individual in sweat electrolytes. In this way, the new device can contribute to a better understanding of sweat mechanisms and their relation to blood values, to find useful biomarkers in sweat to monitor the status of an athlete.

5

Sweat patch for continuous analyte monitoring and offline analysis

52

In the previous chapter, a new sweat collection concept was developed that enabled chronological sweat sampling and offline analysis using ion chromatography. The aim of this study is to develop and present a new version of the sweat collection patch that enables continuous *in situ* monitoring of sweat composition and maintain the function of controlled sampling of sweat in reservoirs for offline analysis. The new patch consists of an analysis chamber that hosts a conductivity sensor for measuring ionic content continuously. Once the sweat passes this chamber, it flows into a sequence of reservoirs which include level indicator electrodes. The level indicator electrodes measure the filling speed, which is dependent on the sweat rate. The sweat in the reservoirs can be analysed offline. In this way, *in situ* sweat composition measurements of the patch, can be directly compared with lab measurements. The new sweat patch is made with accessible fabrication techniques. This means that the patch can be easily reproduced and other novel electrochemical can be placed in the analysis chamber to perform controlled validation experiments in a physiological setting.

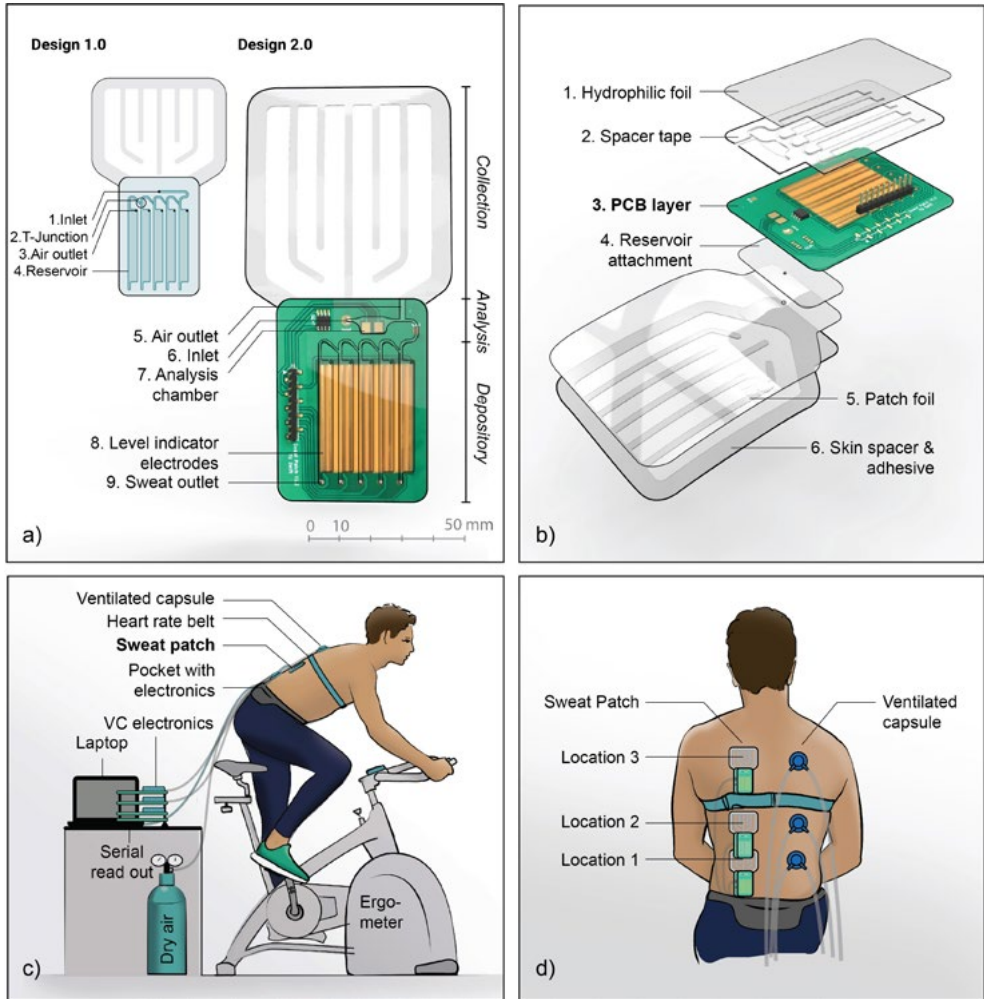
To test the performance of the collector patch, lab validation experiments are executed followed by physiological experiments in a climate chamber. In these experiments, the relation between *in situ* sweat conductivity measurements and $[Na^+]$ and $[Cl^-]$ of the samples, measured by ion chromatography in the lab, is researched. Thereafter, sweat rates measured with a ventilated capsule measurement system are compared with the conductivity measurements and filling rate measurements from the patch.

5.1. Materials & methods

The sweat patch

The new patch design was based on the sweat patch presented in chapter 4. Figure 5.1a shows the first patch on the left. The patch consists of a funnel-shaped structure that guides the sweat to the collector inlet. By capillary and gravitational forces, the sweat will flow to the first reservoir. Once, this reservoir is filled, the new fluid will pass to the subsequent reservoir. The patch is designed to be placed at the back of a person. This version has

5. Sweat patch for continuous analyte monitoring and offline analysis



53

Figure 5.1. a) Front view of the design of the preliminary collector patch (left) and the new patch with integrated sensors (right). An extra reservoir is added near the inlet (no.7). All sweat will pass this reservoir. Electrodes in this reservoir measure sweat conductivity. Level indicator electrodes are placed in the in the bottom reservoir sequence. b) Exploded view of the new patch. c) Setup for physiological tests with the new sweat patch. The patch is placed at the subject's back and electronics are placed in a waist pocket. For the ventilated capsule system, dry air flows through a capsule at the subject's back and the humidity and temperature are measured by the sensors that are connected to the outlet of the capsule. d) Measurement locations of the patches (left) and the capsules (right)

a collection surface of 40 cm² and can collect 5 samples of 130 µl. Sample volume and collection surface can be adjusted to the type of physiological experiment.

After testing the first patch in a physiological setting, a redesign was made (Figure 5.1a, right). An extra chamber, the analysis chamber (Figure 5.1a, no. 7), was placed near the inlet of the reservoir system. This chamber has rounded corners so that there is constant renewal of sweat. Preferred marker specific electrodes can be placed in this reservoir. The extra air outlet in the top (Figure 5.1a, no. 5) ensures that electrodes stay covered with sweat. In this design, the back foil layer of the reservoir system was replaced with a thin printed circuit board layer (0.6 mm) with gold electrodes. The gold electrodes are located in the new chamber to measure the sweat conductivity over time. Furthermore, electrodes were added in the sequence of reservoirs to measure the filling rate which depends on the sweat rate (Figure 5.1a, no. 8). Two parallel elongated gold electrodes were positioned in each of the five reservoirs which allows us to measure a conductance change, when the reservoirs are filling up. A temperature sensor (LM35, Texas Instruments, USA) was placed at the PCB as well. Since the PCB materials are less hydrophilic, contact angle measurements and new syringe pump experiments were performed to test whether the new collector fills at the same rate as the sweat rate. Contact angles of the gold electrodes and the solder mask are 69.8° and 73.1° respectively, while the contact angles for the adhesive tape and the hydrophilic film are 92.2° and 50.5° (measured with water at t=10 s after contact with the surface, with optical tensiometry (KSV Instruments Ltd)).

54

For both sensors, the AD5933 impedance converter (Analog Devices, USA) is used to measure the impedance. The integrated circuit contains a frequency generator (up to 100 kHz, V_{pp}: 0.2 to 2 V), and a 12bit ADC to sample the impedance. The chip also holds a DSP that performs a discrete Fourier transform to return the magnitude of the impedance and the phase of the impedance at the defined output frequency. An 8-channel multiplexer (ADG1408, Analog Devices, USA) is used to switch between the conductivity sensor, sweat rate sensors and a calibration resistor. The excitation voltage is set at 0.2 V_{pp}, to prevent saturation of the ADC at lower resistances and the frequency is set at 80 kHz to minimize double layer effects. The AD5933 and the multiplexer are placed in a pocket that can be carried around the waist. The patch is connected to the readout electronics via simple header pins. Figure 5.1b. shows an exploded view of the patch design.

To calibrate the conductivity sensor in the lab, different solutions of NaCl (from 10 mM to 150 mM) were placed in the top reservoir of a patch. The impedance was measured for each solution to find the relationship between the NaCl concentration and the conductance in the analysis chamber. The functioning of the level indicator electrodes was tested using the syringe pump (KDScientific 200, USA). Pump rates ranging between 12 and 60 µl/min were chosen. For patches with a collection surface of 40 cm², this translates to sweat rates of 0.15 till 1.5 mg/cm²/min. For these experiments, a NaCl solution of 75 mM was used.

Reference measurement

To research the performance of the sweat collector patch in the physiological setting, two types of reference measurements were performed. First, the continuous *in situ* conductivity

measurements were compared to ion chromatography measurements of the samples that were collected and stored in the sequence of reservoirs. Second, to investigate whether sweat conductivity measurements and patch filling rate relate to the actual sweat rate, these measurements were compared against sweat rate measurements with the ventilated capsule technique.

Ion chromatography

This paragraph describes the procedure for offline chemical analysis. In each collection patch, tiny outlets are made in the PCB layer at the bottom of each reservoir (Figure 5.1a, no. 9). These holes are covered with adhesive tape during collection. Once the patch is removed, the tape can be removed and the sweat can be pushed into a vial by injecting air in the reservoir with a syringe at the air inlet. The sweat volume was weighed and diluted with ± 3 ml of ultrapure water, after which the vials are stored at -20° and analysed in the laboratory. In this study, we focused on analysis of electrolytes using ion chromatography/high pressure liquid chromatography (IC/HPLC). $[\text{Na}^+]$, $[\text{Cl}^-]$ and $[\text{K}^+]$ were measured. For the anions, a Metrohm 881 Anion system with a Metrosep A supp 5 – 150/4.0 column was used. The cations were analysed with the 883 Basic IC plus system and a Metrosep C6 – 150/4.0 column (Metrohm, Switzerland). A more detailed description of this method can be found in the previous chapter.

Ventilated capsule measurement

The most common method for measuring local sweat rate in a lab setting are the ventilated capsule (VC) technique and the absorbent patch technique (Morris et al., 2013). Using absorbent patches requires a lot of repetitive work and a limited number of samples can be collected over time. Therefore, the VC measurement is more suitable to measure sweat rate continuously (Rutherford et al., 2021). Capsules with a collection surface of 5.3 cm^2 , made from a flexible 3D-printed photopolymer on a Connex 3 3D printer (Objet 350, Stratasys Ltd., Israel), were placed at the skin. The capsule is connected to a dry air cylinder and air flows through the capsule at a volumetric flow rate between 0.1 and 1.2 l/min. The flow rate is measured with a variable area flow meter (Keyinstruments, USA). A humidity sensor and temperature sensor (HDC1080, Texas Instruments, USA) are connected to the outlet of the capsule. The sensors are controlled with an MSP430 microcontroller (Texas Instruments, USA). We used the Antoine equation in the conversion of relative humidity to absolute humidity. Knowing the dry air flow rate, absolute humidity and sweat collection surface, the sweat rate was calculated.

Lab measurements were executed to test the performance of our VC system. A detailed description of these experiments and the results can be found in Appendix B (B1). To test whether the VC system measures all sweat in the capsule and to test if there are no leakages, a predetermined amount of water was placed in a closed capsule and the total amount of sensed water was calculated by numerical integration of the evaporation rate measurements. It was concluded that the deviation was adequately small (1- 5%). Furthermore, the response and recovery time of the VC system were calculated. At a dry

air flow rate of 1.2 l/min, the response time is 118 s and the recovery time is 353 s. Because sweat rates will always increase or decrease gradually, the actual response time will be even faster in a physiological setting. This means that the VC system can be used for continuous monitoring of sweat rate. The maximal sweat rate that can be measured with the current system is 2.75 mg/cm²/min.

Physiological experiments

Healthy recreational athletes (n=6, 20-30 years) cycled (Lode Excalibur, The Netherlands) in a climate chamber (b-Cat, The Netherlands) that was set to 33 °C and 65% relative humidity. Figure 5.1c shows the setup of the physiological experiments. The patches were placed at three locations at the back on the left side of the spine. Three ventilated capsules were attached to the right side of the spine at the same heights, as can be seen in Figure 5.1d. The locations were chosen based on the study of Smith and Havenith (2011), which showed relatively high sweat rates at the back and similar sweat rates at the left and right side of the sagittal plane. The capsules were placed from the start of the exercise and the dry air flow rate was set at 1.2 l/min to allow for the detection of the expected high sweat rates in this climate. Heart rate was measured with a heart rate belt (Polar H10, Finland) and body core temperature was measured with a rectal temperature probe (Yellow Springs Instruments, USA) during the experiments. The participants cycled 30 minutes at 40-50% of their maximum heart rate (HRmax), followed by 20 minutes at 60% HRmax and 20 minutes at 70% HRmax. Afterwards, the participant stopped cycling and a cooling down period of 20 minutes at the stationary bike was included. Sweat tests were approved by the Human Ethics Research Committee of Delft University of Technology. The initial 30 minutes included the 20 minutes wash out period of the skin (Baker & Wolfe, 2020). The first sweat patch was placed after this initial 30 minutes. Once all reservoirs were filled with sweat, the patch was replaced with a new one. Collectors with 10 reservoirs of 70 µl and a collection surface of 20 cm² were used.

56

5.2. Results & discussion

Characterization of the collection patch

During the patch characterization experiments two topics were addressed. First, it was researched if the conductivity sensor in the analysis chamber can measure NaCl concentrations in the desired range. Figure 5.2a shows the impedance magnitude of the conductivity sensor in the top reservoir when it is filled with different solutions of NaCl (10 till 150 mM). The frequency sweep (5-100kHz) results show that undesired capacitances do not influence the measurement above approximately 50 kHz for all solutions. The magnitude of the impedance lies between 3.6 kΩ and 250 Ω for all measurements.

Figure 5.2b shows the relationship between the conductance measured with the conductivity sensor in the top reservoir and the concentration NaCl of the standard solutions. A linear relationship was found and the sensitivity of the sensor system was 24 µS/mM.

5. Sweat patch for continuous analyte monitoring and offline analysis

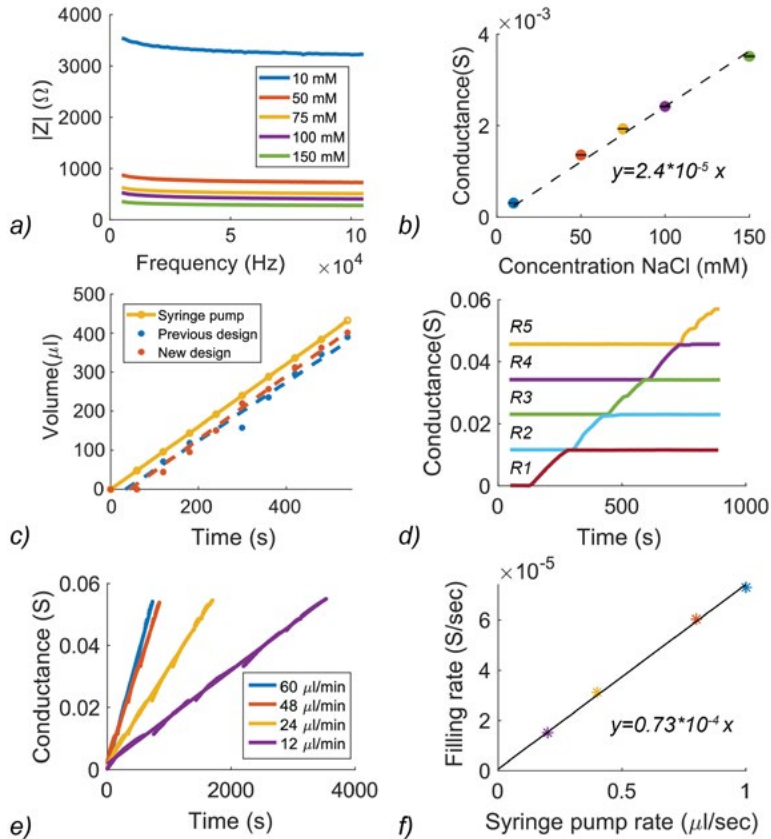


Figure 5.2. a) Impedance magnitude during the frequency sweep for different solutions of NaCl in the analysis chamber. b) Calibration plot of the sweat conductivity sensors in the analysis chamber at different NaCl concentration levels. c) Volume flow rate of in the new design vs. the previous design from video recordings. d) Results of a filling rate measurement when the syringe pump is set at 12 $\mu\text{l}/\text{min}$. Each colour represents the measurement of a separate pair of filling rate electrodes in a single reservoir. Cumulative results show the course of the filling process. e) The conductance over time at 4 different pump rates f) Relationship between the syringe pump rate in $\mu\text{l}/\text{sec}$ and the filling rate in S/sec.

Using the molar conductance of NaCl in water (Chang & Thoman), a cell constant of 5.223 /cm was calculated. Second, to monitor the filling process of the collector, a syringe pump (KDSscientific 200, USA) is set at a rate of 48 $\mu\text{l}/\text{min}$. This rate is based on the size of the patch (40 cm^2) and an average sweat rate at the back of an athlete during exercise (1.2 $\text{mg}/\text{cm}^2/\text{min}$ (Smith & Havenith, 2011)). The pump is connected to a tube which is placed close to the inlet of the collector. The filling process of the collector was filmed with a camera. Afterwards, stills were extracted from the movie, a selection of the area that contains fluid was made and pixels are counted in each image. The pixel area was converted to volume, since the

dimensions of the patch are known. Figure 5.2c shows the volume plotted against time. A delay of around 50 s is visible, before the fluid of the pump starts entering the reservoirs. In the graph can be seen that the volume flow rate of the fluid in the second design is similar to the flow rate of the syringe pump and the first design (with two hydrophilic layers). The differences in flow rate are not significant. The camera images show that entrapment of air and formation of droplets can temporarily delay or accelerate the inflow of sweat. This emphasizes the importance of real-time measurement over a timespan that is larger than several minutes, to find the actual sweat rate.

Furthermore, the performance of the collection system was tested with the level indicator electrodes. It was researched whether the reservoirs fill consecutively, and if the conductance change measured with the level indicator electrodes is linearly related to the volumetric flow rate settings of the syringe pump. To test the consecutive filling of the reservoirs, the syringe pump was set at a flow rate of 12 $\mu\text{l}/\text{min}$. Figure 5.2d shows the results of the measurement of the separate electrode pairs in pre-wetted reservoirs. Once a previous reservoir is filled, the total conductance is added to the next measurement, to see the course of the filling process. Figure 5.2e shows that the collectors fill at a constant speed at increased pump rates as well and a linear relationship between the different pump rates and the filling rate in Siemens per second was obtained (Figure 5.2f).

58 Physiological Experiments

All 6 participants completed the protocol in the climate chamber. For most participants the patches started filling typically around 8 minutes after placement. Once a patch was completely filled, it was immediately replaced by a new one. Sweat rates highly varied among participants. For one participant at 2 locations at the back 3 patches of 10 reservoirs were completely filled, while for another participant, only 3 reservoirs were filled during the entire exercise. Body core temperature increased $1.03^\circ \pm 0.72^\circ$ during the exercise. Figure B2 shows real-time rectal temperature and heart rate of participant 1 during the exercise. A picture of the experimental setting is presented in Figure B3. Figure 5.3a shows the sweat rate over time measured with the ventilated capsule system for the three different locations at the back of participant 1. The sweat rate was calculated using the air flow rate, humidity, and temperature measurements. Data were filtered with a Savitzky-Golay sliding window filter (Savitzky & Golay, 1964), using a second order polynomial and a window size of 150 data points. The sample frequency of the measurements was 1 Hz. In Figure 5.3b, the conductivity measurements in the patch analysis chamber at the same locations on the left side of the back of participant 1 are plotted. Low conductance values ($< 0.5 \cdot 10^{-3} \text{ S}$) and abrupt changes in conductance, attributed to air bubbles in the system, were removed. Subsequently, a similar sliding window filter was used to remove high frequency noise components (window size: 50, sample rate: 0.3 Hz, 2nd order polynomial). Unfiltered data can be found in the appendix (Figure B4). Temperature changes over time varied from 0 to 1.5 $^\circ\text{C}$ for each patch from the start of the filling process. The temperature coefficient of conductivity of electrolyte solutions is around 2 %/ $^\circ\text{C}$ at 25 $^\circ\text{C}$ (Robinson & Stokes). Thus the conductivity change due to temperature effects would be estimated between 0% and

5. Sweat patch for continuous analyte monitoring and offline analysis

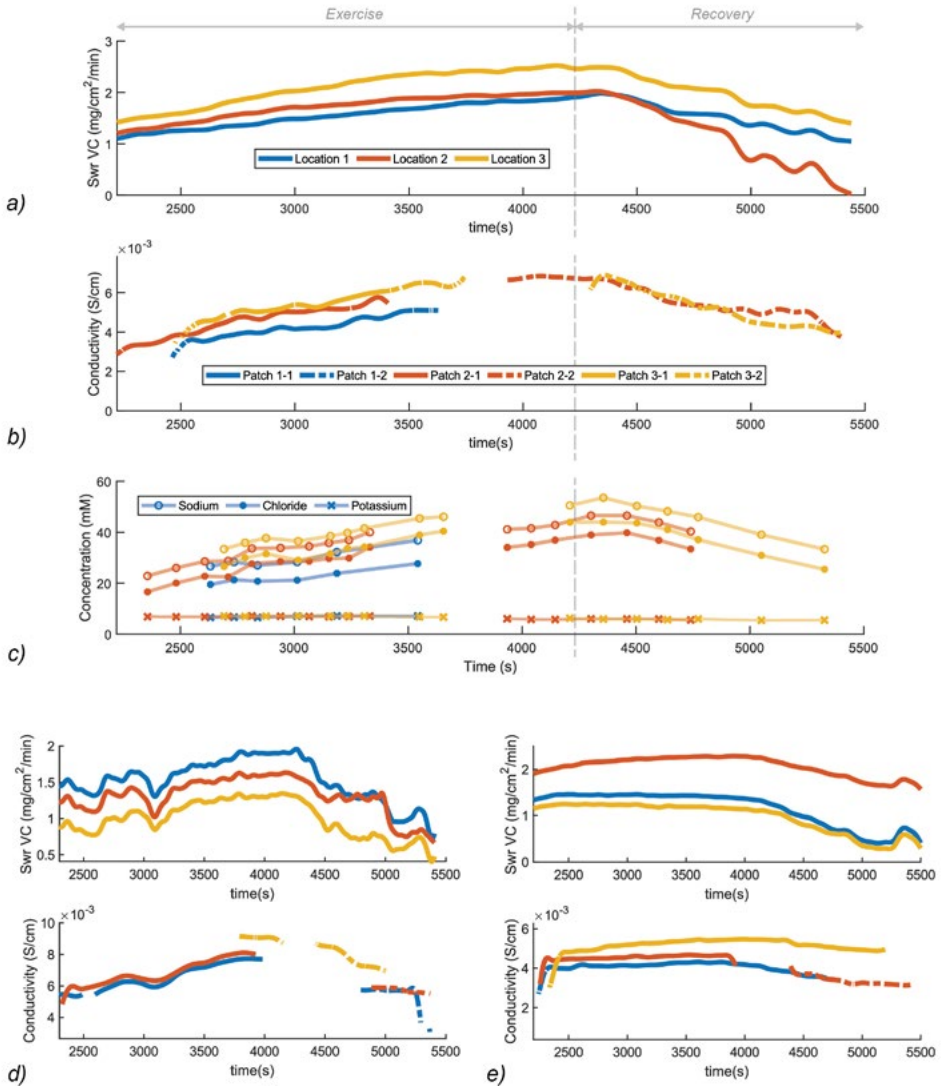


Figure 5.3. a) Continuous sweat rate measurement from the VCs placed at the 3 locations at the back of participant 1. The incremental exercise was performed until $t=4200$ s, followed by a recovery period of 1200 s. The patches were placed at $t=1800$ s. b) Conductivity measured in the analysis chamber of the patches at the 3 locations of participant 1. Gaps are due to patch replacement (e.g. patch 2-1 is replaced by patch 2-2). c) $[Na^+]$, $[Cl^-]$ and $[K^+]$ data from chromatographic analysis of the samples from the individual reservoirs. Timestamps were derived from the filling rate measurements. Lines indicate that the samples are from the same patch d,e) Sweat rate from ventilated capsules (top) and conductivity measurements from the analysis chamber (bottom) of d) participant 3 and e) participant 4. Location 1 is blue, location 2 is orange and location 3 is yellow.

3% maximum. Given that the conductivity increased more than 100% during the course of the exercise of participant 1, temperature changes have limited influence.

It can be noted that all 3 graphs from participant 1 show a similar trend during the exercise. The sweat rate increased as the heart rate increased. After a few minutes from the start of the cooling down period $t = 4200$ s, the sweat rate decreases again. When the sweat rate increases, a lower percentage of ions will be reabsorbed by the sweat duct (Baker, 2019). Therefore, the conductivity measurement shows an increasing trend when the sweat rate increases. This corresponds to the ion chromatography results from the samples that were collected in the reservoirs. In Figure 5.3c. can be seen that $[Na^+]$ and $[Cl^-]$ increase, and when the participant stops exercising, the concentrations decrease again. $[Na^+]$ are on average $6.84 \text{ mM} \pm 0.98 \text{ mM}$ higher than $[Cl^-]$. This difference is presumably being caused by the abundant presence of other negative ions in sweat such as lactate and bicarbonate. $[K^+]$ concentrations show a slight decreasing trend during the entire exercise. For K^+ , secretion mechanisms are partly known and probably these ions are not reabsorbed in the duct and therefore not influenced by changes in sweat rate (Klous et al., 2020). Parrilla et al. (Parrilla, Ortiz-Gómez, et al., 2019) also compared the results of newly developed sweat sensors during physiological tests with ion chromatography measurements. However, because they used the labour-intensive absorbent patch method and they used a different physiological protocol, the number of samples that were collected over time were limited to 1 for every 10-12.5 minutes. Figure 5.3d shows the VC measurements and conductivity measurements of participant 3 at the three different locations. For this participant, the trends of the different measurements correspond as well. The dip around 3100 sec, originated from a deviation in the execution of the exercise protocol. Probably, due to a technical error of the bike, the participant stopped exercising for a moment and sweat rates decreased almost immediately. It is remarkable to see that this change is detected by the ventilated capsule measurement system as well as the conductivity sensors. Figure 5.3e shows the results of participant 4, with again corresponding trends of the different measurement methods.

60

Sweat conductivity and $[Na^+]$ and $[Cl^-]$

In this study, it was aimed to test the performance of the sensor patch *in situ*, by validating if the lab measurements of the samples from the reservoirs can be used as a reference for the sensor in the analysis chamber. Therefore, a comparison between all ion chromatography results and conductivity measurements was made, by investigating the relationship between sweat conductivity and $[Na^+]$ and $[Cl^-]$ in sweat. First, the time intervals of the filling process of each reservoir were identified, by detecting the starting times and end times of filling each reservoir. Subsequently, the time that it takes for the sweat to move from the top reservoir to the bottom reservoirs was subtracted from the time intervals. The mean conductance values of the top electrodes at the resulting time intervals were compared with the ion chromatography results. Because each electrode pair covers 2 reservoirs, concentration levels of 2 samples were averaged. In Figure B5 the results including an error estimation of the three locations for each participant can be found. A large range of concentrations was measured (from 18 mM to 105 mM).

Figure 5.4a. shows all measurements in one graph. $[Na^+]$ and $[Cl^-]$ are plotted against conductivity and a strong linear relationship ($R^2=0.97$) for both ions was found. From these results, it can be concluded that the collector patch showed good performance, because the continuous measurements in the analysis chamber were well related to the offline measurements. Furthermore, it can be concluded that a 2-point AC conductivity measurement with gold electrodes can be used to obtain $[Na^+]$ and $[Cl^-]$ levels with good accuracy in these physiological conditions. Because of the higher stability and less complex fabrication process of the electrodes, conductivity sensors might be more accessible choice than potentiometric sensors (Choi et al., 2017; Mazzaracchio et al., 2021; Pirovano et al., 2020) for integration in smart sweat patches that are aimed to monitor $[Na^+]$ and $[Cl^-]$ levels of healthy individuals. To find out if conductivity measurements can be used to obtain $[Na^+]$ and $[Cl^-]$ concentrations in other physical or specific dietary conditions, further research is required.

Sweat conductivity and sweat rate

The filling rate of the reservoirs of the patch can be used as an indicator of the sweat rate. Therefore, it was researched whether this filling rate correlates well with the sweat rate derived from the VC technique. To obtain the actual filling speed from the level indicator readings, several data processing steps are required. The conductance will increase during the course of the filling process, but ionic content changes influence the conductance measurement as well. The cumulative average of the conductance data from the analysis chamber are used to compensate for the change in sweat conductivity due to ionic content change. Equation 5.1. shows the relation between the level indicator conductance (C_2) and the cumulative average of the conductance in the analysis chamber (C_1):

$$C_2(t) = \frac{K_2}{K_1} * C_1(t - \Delta t) * \frac{V(t)}{V_{tot}} \quad (5.1)$$

In which K_1 and K_2 denote the cell constant in the analysis chamber and the cell constant of the level indicator electrodes respectively. V is the current volume, t is time, V_{tot} is the total volume of the sweat that is covered by 1 level indicator electrode pair. A time delay (Δt), which is the time that it takes before incoming sweat at the inlet reaches the reservoirs, is included as well. In Figure B6, a graph of the filling rate (volume plotted against time) of two patches can be found. The abrupt changes in conductance over time are caused by droplet formation and a linear fit was made to derive the average filling rate of a collector. The slope of this fit, or the filling rate, is plotted against the average VC sweat rate. For one participant, who had exceptionally high sweat rates, sweat rates were above the maximum evaporation rate of the system. So these data were excluded. Patches that showed leaks, or patches that collected less than 4 samples were excluded as well. As can be seen in Figure 4b, the data of both techniques correspond reasonably well. However, a wider range of sweat rate measurements should be performed to draw a solid conclusion about the correlation. The

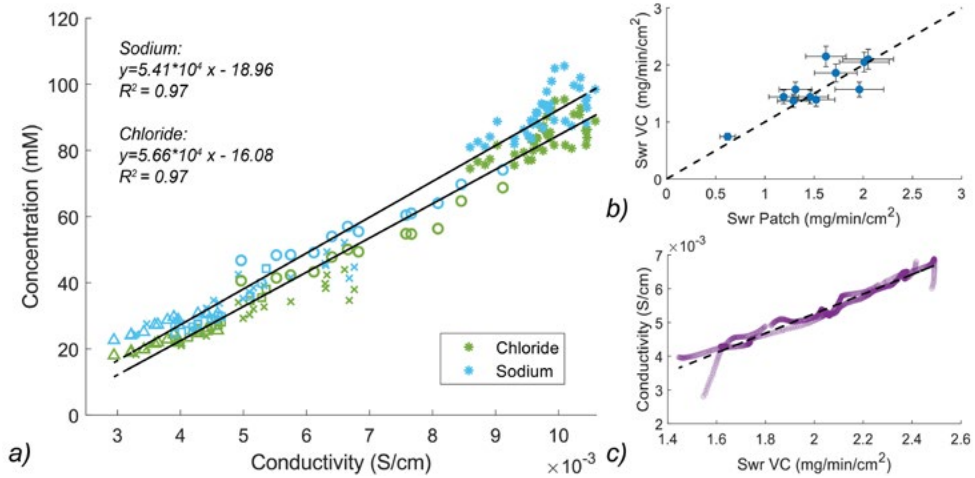


Figure 5.4. a) $[Na^+]$ and $[Cl^-]$ plotted against conductivity of all samples ($n=97$) of the physiological experiments. b) Sweat rate of the VC plotted against the sweat rate of the patch. The dashed line represents the identity line c) Relation between sweat conductivity and sweat rate of the VC at the upper back of participant 2.

62

main source of error appeared to be caused by reading accuracy of the flow meters. Reading errors can result in an offset of maximum 8.3% of the measured sweat rate. These errors are represented by the horizontal error bars in Figure 5.4b. Furthermore, the errors of the filling rate occur when small air bubbles are enclosed in a reservoir. The R^2 value relative to the regression line of the best fit is 0.71 and relative to the identity line ($y=x$) is 0.65.

Lastly, the relationship between the sweat conductivity and the VC data was studied. The time interval of continuous flow of sweat through the reservoir was identified and the continuous measurements at this time interval were compared for each patch location. Figure 5.4c. shows the results at one location of participant 1. A significant relation was found for all patch locations (mean $R^2= 0.87$), except for 1 case. In this case, the sweat rate did not increase significantly. The results show that conductivity is directly related to sweat rate. When sweat rate increases, the relative ion reabsorption rate changes and sweat conductivity increases, which corresponds to the theory described by Baker and Wolfe (Baker & Wolfe, 2020). Thus, the patches can be used to accurately monitor sweat rate changes during exercise.

To summarize the results, the physiological experiments showed that the new patch can be used to test continuous sweat monitoring techniques and to simultaneously collect and store this sweat for separate, offline analysis. The sweat collection system enabled collection of 38 samples of 70 μ l on average per participant during the physiological tests of 90 minutes. It was found that the $[Na^+]$ and $[Cl^-]$ of the samples were linearly related to conductivity, and conductivity data were related to VC sweat rate data as well. The current version of the patch was shown to work well, but the system can possibly be expanded with

an extra sensor for semi-continuous absolute measurement of sweat rate with the patch. A new narrow microfluidic channel with a small collection surface could be integrated, to minimize droplet formation and enclosure of air during sweat rate measurement. The filling of this new channel could be detected by placing tiny electrodes at multiple places along the channel and counting the moments that the fluid passes the channel, like in the patch of Yuan et al. (Yuan et al., 2019). The current filling rate electrodes should be maintained in this alternative version of the patch, to use them for timing purposes.

The simple fabrication process of the collection patch enables other researchers to easily replicate this system to compare their own sensors, such as electrochemical glucose sensors (Oh et al., 2018), or lactate sensors (Alam et al., 2020), against a reference. Furthermore, the reservoir volume and collection surface can be easily adapted to physiological tests performed in alternative conditions that evoke sweat rate levels of a different order of magnitude. Figure B7 shows an example of how an external screen printed potentiometric sensor can be integrated in the system and in Figure B8, a technical drawing is shown. With this new patch, novel sweat sensors can be validated. Thereafter, the sensors can be used by physiologists, to learn more about the mechanisms behind sweating and to identify new sweat biomarkers.

5.3. Conclusions

In this chapter, we presented a new version of the sweat collector patch for both continuous monitoring of analytes and chronological sampling of sweat for offline analysis. A conductivity sensor was integrated in the patch for continuous measurement and level indicator electrodes measure the filling rate of the sweat in the sequence of reservoirs that store sweat for offline analysis. The new sweat patch was characterized in the lab. The sensitivity of the conductivity sensor was $24 \mu\text{S}/\text{mM NaCl}$, and the reservoirs fill at the same speed as the sweat rate in the desired range (12 to 60 $\mu\text{l}/\text{min}$). In physiological experiments, continuous conductivity measurements were successfully compared to ventilated capsule (VC) sweat rate measurements and offline analysis of $[\text{Na}^+]$ and $[\text{Cl}^-]$ by ion chromatography. Results ($n=6$, 3 locations for each participant) showed that VC sweat rate data were related to the conductivity measurements. Furthermore, sweat conductivity data were linearly related to $[\text{Na}^+]$ and $[\text{Cl}^-]$ from the samples stored in the reservoir sequence of the patch ($R^2=0.97$). Thus, the new sweat collector patch allows to continuously measure sweat analyte concentrations during physiological experiments and to store the sweat in a sequence of reservoirs for offline reference measurement, as an *in situ* validation strategy for new sweat sensors.

6

Continuous sweat NH_3 , Na^+ and Cl^- monitoring

In the previous chapter, a sweat sensor patch with a conductivity sensor for continuous measurement of ionic content, was presented. This chapter focusses on sensor system concepts for continuous measurement of specific analytes. A selection of three sweat constituents was made based on the insights from the physiological review in chapter 2. As described in chapter 2, it is hypothesized that NH_4^+ in sweat can be used to measure muscle fatigue. Since NH_4^+ quickly evaporates from sweat, a novel device is developed that measures evaporated $[\text{NH}_3]$ underneath a ventilated skin capsule. Secondly, a new potentiometric sensor patch is presented that measures $[\text{Na}^+]$ and $[\text{Cl}^-]$ for potential sweat rate and hydration monitoring. Being the most abundant ions in sweat, real-time $[\text{Na}^+]$ and $[\text{Cl}^-]$ monitoring can also provide more insight in the physiological mechanisms behind sweating.

64

6.1. NH_3 capsule

Measuring muscle fatigue would be an interesting aspect of monitoring an athlete's health status and monitoring efficiency of training programs. To find a relationship between muscle fatigue and sweat constituents, more physiological research is required. Although lactate levels in blood are a well-known indicator of muscle fatigue (Skinner & McLellan, 1980), it is known that lactate is a by-product of sweat gland metabolism as well (Derbyshire et al., 2012), and no significant relationship between lactate levels in blood and lactate levels in sweat have been found in literature (Klous et al., 2020). As an alternative, several researchers highlighted the possibility of using NH_4^+ in sweat as a potential biomarker for muscle fatigue (Alvear-Ordenes et al., 2005; Guinovart et al., 2013). NH_4^+ concentrations in sweat are relatively high (between 0.5 and 25 mM (Harvey et al., 2010)). To research if NH_4^+ levels in sweat are related to blood levels, and if sweat $[\text{NH}_4^+]$ can be used as a biomarker for muscle fatigue, reliable real-time NH_4^+ monitoring systems are required.

Since $\text{NH}_3(\text{aq})$ is evaporating quickly, we propose to measure the NH_3 levels evaporated from sweat in a sensing capsule that is placed at the skin. A controlled air flow through the system is necessary to calculate the concentration in sweat based on the concentration

measured in the sensing capsule. Therefore, the sensor is integrated in a ventilated capsule system, which is commonly used by physiologists for measuring sweat rate (Morris et al., 2013).

Sensor system design

It is estimated that a sensor with a detection range between 0 and 100 ppm is required, by using data about $[\text{NH}_4^+]$ in sweat found in literature (Harvey et al., 2010), sweat rate and volumetric flow rate of air through the capsule. Based on measurement range, price, and ability to integrate this sensor in a wearable, the MICS-5914 semiconductor metal oxide gas sensor (SGX Sensortech, Switzerland) was selected. This sensor consists of a Si/SiO₂ substrate with 4 gold-platinum electrodes. Two electrodes are used for heating the sensor and two are for performing the measurement. The metal oxide sensing layer including tungsten nano-plates, is placed on top (Krivec et al., 2015). When the sensor is exposed to NH_3 , the resistance across the sensing electrodes will drop. Next to NH_3 , the sensor is sensitive to ethanol, hydrogen, propane and butane. These gases will not be formed during sweating in general conditions. Figure 6.1 shows a schematic overview of the entire measurement system. We use a series-series feedback circuit to read-out the sensors (Figure 6.2). This circuit has a linear response, which facilitates calibration. It also reduces noise, distortion, and variations due to temperature influences. The circuit includes the precision operational amplifier LTC2057 (Analog Devices, USA) and the MCP3421 (Microchip, USA) analog to digital converter with differential input is used. These electronics with a single NH_3 sensor and a humidity and temperature sensor (HDC1080, Texas Instruments) are placed at a small PCB (34 mm × 28 mm), that is designed to fit in a capsule (Figure 6.2b and Figure 6.2c). The capsule can be taped to the skin of the athlete. The sensors are placed inside the capsule and the other supporting electronics of the readout circuit are placed at the other side of the PCB, outside the capsule. The capsule PCB is connected to a shield that contains the current source for the heater circuit, the connection to a power supply and a multiplexer.

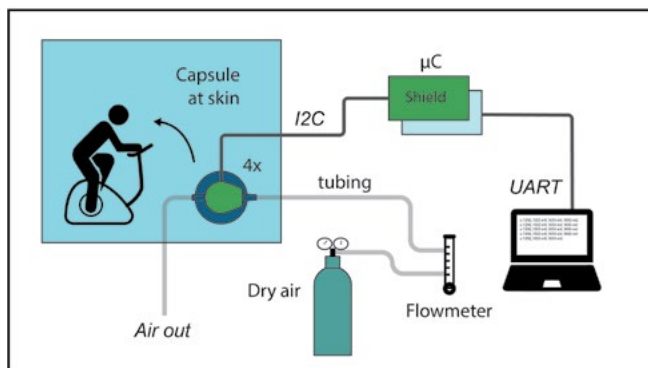
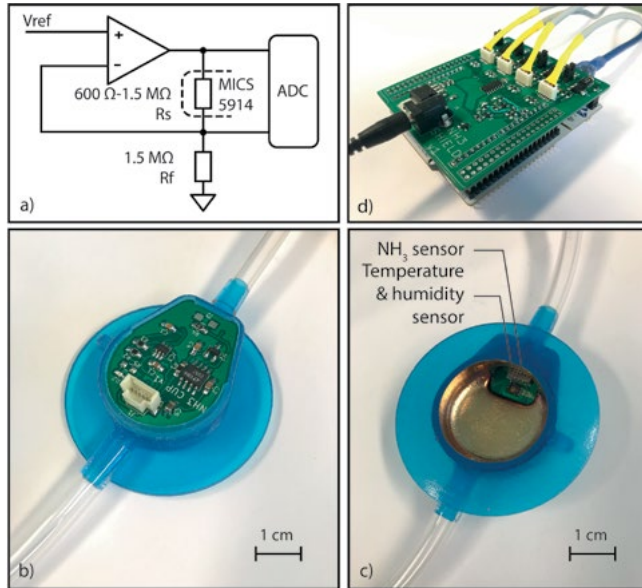


Figure 6.1. An overview of the sweat NH_3 measurement system. Four capsules with sensors can be read out by the microcontroller. Data can be retrieved through a UART connection.



66

Figure 6.2. a) The series-series feedback circuit used to read out the MICS-5914 sensor. b) Top view of the capsule. c) Bottom view of the capsule. d) The shield for reading out 4 capsules. to switch between different capsules.

Data of four sensor capsules can be read out with an STM32F411RE microcontroller board (STMicroelectronics, Switzerland) (Figure 6.2d). It was chosen to place the sensors as close as possible to the collection surface, to prevent that NH_3 is absorbed by the materials of the capsule and the tubing, before the NH_3 molecules are detected. A thin gold layer was sputtered on the inside of the capsule to prevent absorption in this area. The capsule itself is made of a 3D printed flexible photopolymer (Connex 3, Objet 350, Stratasys, Israel) and has a collection surface diameter of 26 mm. The airtight capsule will be placed at the skin with a double-sided acrylate adhesive (3M 1522, (3M, 2013)). During the *in situ* experiments, the capsule can be ventilated with dry air at a flow rate between 0.2 and 1.2 l/min, depending on the type of exercise test that will be performed.

Lab validation

Each of the MICS-5914 sensors has a different resistance in air and the sensitivity will also differ (SGXSensortech, 2014). Therefore, each individual sensor needs to be calibrated. A calibrated electrochemical NH_3 sensor for air quality monitoring (S900, Aeroqual, New-Zealand) was purchased to calibrate the sensors. The sensor modules and the reference sensor are placed in a closed box with tubing to an Erlenmeyer flask. The air is circulated with a small fan through the glass and through the box. First, the sensor resistance must stabilize before NH_3 can be measured reliably. Therefore, the sensors are started up 2 h before the measurement. One sensor is covered with aluminum foil, to keep an eye on the effects of

temperature changes. An ammonia solution is made in the Erlenmeyer flask from household ammonia and demineralized water. With this solution, different NH_3 concentration levels can be created in the closed box. Measurements of 30 to 40 minutes are performed at concentration levels of 3, 5, 10, 20 and 30 ppm NH_3 . Figure 6.3a shows the raw data of the resistance change of the sensors when environments with different concentrations NH_3 are created. The temperature is 25 °C and the humidity level is 60%. The baseline resistance highly differs for each sensor (from 360 k Ω to 1140 k Ω). Furthermore, the sensor readings show a transient behaviour. In literature it was found that metal oxide gas sensors have a fast response time compared to other types of gas sensors (Dey, 2018), and in experiments with ethylene, the MICS-5914 has a sorption and desorption time constant of $\tau_s = 29$ s and $\tau_d = 43$ s (Krivec et al., 2015). On top of that, the reference sensor shows a very similar transient response. It is expected that the transient is mainly originating from the rising NH_3 concentration in air, since the NH_3 is evaporating from a flask, and it will take some time before an equilibrium at a certain concentration is reached. The small peaks between each concentration level originate from the moment that we change the flask and box is circulating air from the environment for a few minutes. During this moment, $[\text{NH}_3]$ and humidity levels will decrease, and sensor resistance will increase. When a new flask with an NH_3 solution is connected, the resistance will immediately decrease again.

A calibration plot can be made using data from the MICS-5914 sensors (baseline resistance, R_0 and sensor resistance, R_s) and the reference sensor measurements (Figure 6.3b). A clear difference in sensitivity between sensors can be seen, which emphasizes that each individual sensor needs to be calibrated. In all experiments, it was found that the baseline sensor resistance drifts over time. This drift varies in each measurement. In further experiments, these measurements will be repeated multiple times, to test the stability of the sensors during NH_3 measurements. A sensor with excellent stability would be beneficial if physiologists and clinicians want to know the absolute concentration levels in sweat.

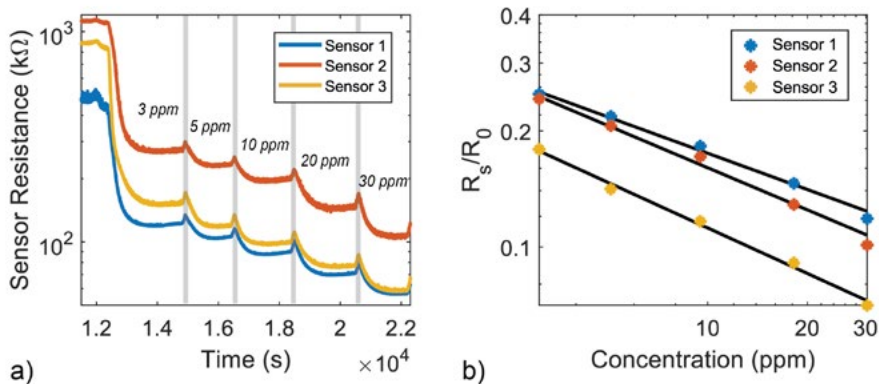


Figure 6.3. a) Sensor resistance plotted over time during the calibration experiment. The sensors are exposed to an environment with different concentrations of NH_3 . b) Sensor resistance (R_s) divided by baseline resistance (R_0) plotted against $[\text{NH}_3]$ in ppm measured by the reference sensor. Data were fitted using a power function: $y = a \cdot x^b$.

However, in studies about the relationship between $[\text{NH}_3]$ and muscle fatigue, measuring relative changes in $[\text{NH}_3]$ would already give valuable information. When exposing the sensor to a changing humidity level from 38% to 50%, a clear drop in resistance, which varies between sensors (from 25% to 60%), can be seen. These changes are comparable to the changes measured by Krivec et al. (2015). Water molecules can be adsorbed at the sensor surface in a similar way as the volatile gas. These molecules reduce the baseline resistance and the sensitivity of the sensor because the available surface area for adsorption of NH_3 molecules decreases. The humidity measurements show the necessity of compensating for humidity influences during sweat NH_3 measurements.

After quantifying temperature and humidity effects in the expected conditions in the lab, it can be decided if the current sensor can be used with humidity change compensation or another, electrochemical sensor needs to be selected. Once the lab validation is concluded, the sensors will be tested in physiological experiments in which athletes will perform a high intensity cycling exercise. In these experiments we will validate the use of our NH_3 ventilated capsule system for NH_3 sweat measurement. Trends in NH_3 levels in the capsule during exercise at a cycling ergometer will be researched. Based on the insights from these experiments, further improvements of the system can be made. The current system is not a wearable, because measurements are restricted to a lab environment. Once it is known that NH_3 in sweat can be used as a biomarker, the system can be made wearable.

6.2. Potentiometric sensor patch

From a technological perspective, real-time sweat sensors provide new opportunities for monitoring personal health status (Bariya et al., 2018). However, little is known about the relationship between blood and sweat composition (Klous et al., 2020) and how sweat can be used in diagnostics and health monitoring. The cardiovascular system is circulating blood at a speed of 5 l/min, which results in a blood composition that reflects the functioning of the body at an instant. For sweating, the story is completely different. The epidermis including the sweat glands has an important role in maintaining homeostasis as a physical barrier to the circulating nutrients and solutes in the body (Heikenfeld et al., 2018). Furthermore, the composition of sweat is location and sweat-rate dependent, which makes interpretation of sweat composition measurements more complex. To learn more about sweat secretion mechanisms and to identify sweat biomarkers, real-time ion-specific sweat sensors can provide new time-dependent information (Ghaffari et al., 2021; Parrilla, Cuartero, et al., 2019). For example, to research relationships between blood and sweat composition with certain time delays. As a starting point Na^+ and Cl^- were selected to be analysed because they are the most abundant ions in sweat and they show potential to be used in sweat rate and hydration monitoring. Furthermore, real-time $[\text{Na}^+]$ and $[\text{Cl}^-]$ measurements can be used in monitoring medicine effectiveness in the diagnostic process of cystic fibrosis (Bakker, 2019).

Sensor system design

Potentiometry is the most common measurement method to retrieve real-time Na^+ and Cl^- measurements with wearable sensors (Parrilla, Cuartero, et al., 2019). An accessible alternative would be colorimetry (Zhou et al., 2016). However, this technique does not enable continuous digital measurement. A potentiometric sensor contains two electrodes. The reference electrode is an Ag/AgCl electrode in a saturated NaCl or KCl solution resulting in a stable potential. The sensing electrode is selective to a certain ion. In this case the Na^+ sensing electrode contains Sodium Ionophore X and the Cl^- sensing electrode contains an Ag/AgCl layer for selectivity to Chloride. When the electrodes are immersed in an analyte solution, the difference in potential is measured under static conditions. As described by the Nernst equation, the cell's potential (E) is proportional to the logarithm of the activity of the primary ion ($a_{i(aq)}$):

$$E = E^0 + \frac{RT}{nF} \log(a_{i(aq)}) \quad (5.1)$$

Where E^0 is the standard electrochemical cell potential, R is the universal gas constant, T the absolute temperature, n the number of electrons in the reaction and F the faraday constant (Parrilla, 2016).

Figure 6.4 shows a top view and an exploded view of the design of the sensor. The layers were screen printed. During the sensor development process several iterations were performed. First the sensors were printed by hand in a small chemical lab environment in house. In a next stage, a series of sensors was printed by an external party specialised in printed electronics (Holst Centre, The Netherlands). The membranes were drop casted by hand. Table 6.1 shows the materials used for the final sensors. The detailed fabrication process was described by del Rio Garcia (2021). The sensors were printed on PET film.

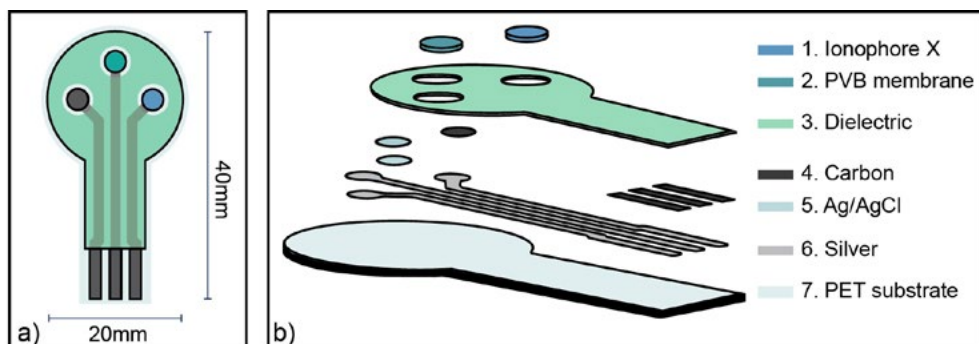


Figure 6.4. a) Top view and b) exploded view of the potentiometric sensors. Adapted from (Bakker, 2019).

Table 6.1. Materials for potentiometric [Na⁺] and [Cl⁻] sensors

Material	Manufacturer	Productcode	Function
Silver ink	DuPont	5025	Conductive tracks
Carbon ink	DuPont	BQ226	Conductive pads/Solid contact interface
Silver/silver chloride ink (ratio: 32/68)	DuPont	5876	Chloride electrode/Reference electrode
Dielectric	Dupont	BQ10	Encapsulation
Sodium ionophore X	Supelco	71747	Sodium membrane: ionophore
Bis(2ethylhexyl) sebacate (DOS)	Supelco	84818	Sodium membrane: plasticizer
Na-TFPB	Sigma Aldrich	692360	Sodium membrane: catalyzer
Polyvinyl chloride (PVC)	Supelco	81392	Sodium membrane: structure
Tetrahydrofuran (THF)	Supelco	87369	Sodium membrane solvent
Polyvinyl Butyral (PVB)	Sigma Aldrich	P110010	Reference membrane: structure
Methanol	Sigma Aldrich	34860	Reference membrane: solvent
Sodium chloride	Sigma Aldrich	746398	Reference membrane

70

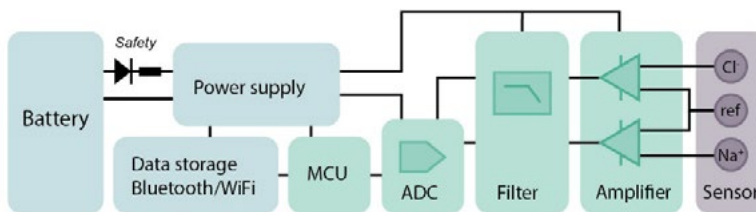


Figure 6.5. Circuit overview of the potentiometric sensor system. Adapted from (Bakker, 2019).

A schematic overview of the readout electronics of the system is presented in Figure 6.5. The STM32F103RB microcontroller (STMicroelectronics, Switzerland), an INA333 instrumentation amplifier (Texas Instruments, USA) and a 16-bit ADC (ADS1115, Texas Instruments, USA) were selected. A filter was added to reduce noise and interference.

6. Continuous sweat NH_3 , Na^+ and Cl^- monitoring

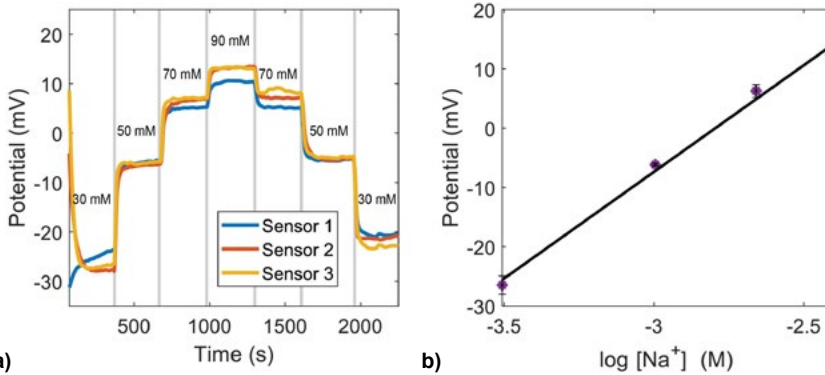


Figure 6.6. Calibration experiment of the sodium sensor: a) the potential in mV of three pre-wetted sensors in different NaCl solutions (30-90 mM). b) The mean potential of the three sensors plotted against $\log[\text{Na}^+]$.

Sensors were characterized in the laboratory with different NaCl solutions (20-90 mM). Figure 6.6a and Figure 6.6b show calibration examples of the Na^+ sensor. The sensors show a Nernstian response with a mean sensitivity of 36.0 ± 2.8 mV/log[M].

To reliably transport the sweat from the skin surface to the sensors, a sweat collection system needs to be designed as well. Figure 6.7 shows an example of a collector designed for continuous athlete monitoring (del Río García, 2021). Fluidic channels were created by laminating TPU film (Dupont Intexar TE-11C, Dupont, USA) and two types of adhesive tapes (3M 9469PC, 3M 1522, 3M, USA). Sweat flows from the collection surface (50 mm²) into a microfluidic channel. Subsequently it is transported to the analysis area through capillary effects. In the analysis area, the sensors are positioned. The outlet area effectuates removal of sweat after analysis. In this concept, a tesla valve (Tesla, 1920) was added in the outlet area to control the flow (by slowing down fluid flow when the sweat has a high flow rate among others).

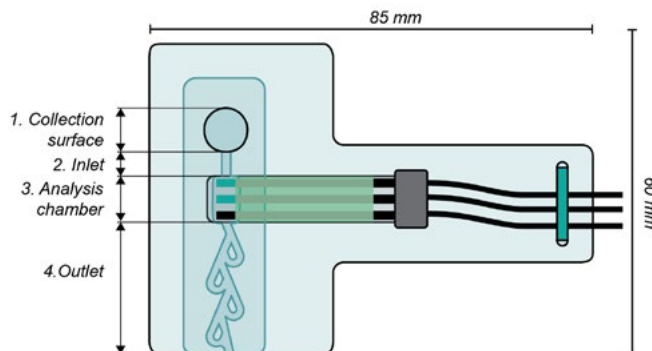


Figure 6.7. Concept of a sweat collection patch for use on the back of an athlete during exercise.

Further microfluidics research is needed to quantify the effects of the Tesla valve in the sweat collector. The electronics were integrated in a box and connected to the patches via an FFC connector for a preliminary physiological experiment. The experiments showed that the sweat collection system enabled successful collection and removal of sweat. In future physiological experiments, the shielding and connection to the readout circuitry need to be improved to derive reliable continuous ion concentration measurements.

6.3. Conclusions

In this chapter two different sensor system concepts for continuous measurement of specific sweat analytes were presented. The first sensor system uses a gas sensor that analyses evaporated sweat NH_3 levels. A ventilated capsule system was used to control air flow through the NH_3 capsule and measure sweat rate at the same time. From the sweat rate measurements, and gas sensor measurements, the absolute concentration of NH_3 can be derived. The second sensor system comprises potentiometric sensors that are integrated in a sweat collection patch for continuous measurement of $[\text{Na}^+]$ and $[\text{Cl}^-]$. It needs to be emphasized that the sensor concepts are still under development. First sensor validation experiments are performed, but more research is required to fully characterize the sensor systems for larger physiological studies. For example, the influence of humidity changes on the metal oxide gas sensor needs to be quantified to derive the absolute NH_3 concentrations at different sweat rates. Furthermore, the stability of the potentiometric sensors needs to be measured and the integration of the readout electronics and potentiometric sensor patch needs to be improved before new physiological experiments can be performed.

Summarizing conclusions for sweat sensing

In this section, a series of novel sweat sensor systems was developed to continuously collect and reliably measure sweat rate and sweat composition during exercise. The most important contribution of this work is the design and validation of a sweat collection patch that enables real-time sweat monitoring as well as offline analysis for reference measurements. The development of the patch was divided in two parts. First, the fluidic collection system was created from hydrophilic foils and a double-sided adhesive using low-cost fabrication techniques. The patch consists of a funnel-shaped collection area and a sequence of reservoirs that store the samples for further analysis. The design of the fluidic system was validated using CFD simulations and benchtop experiments with a syringe pump. A successful proof of concept study in a physiological setting was performed to validate the sequential filling and offline analysis of the collected samples by ion chromatography.

Second, a redesign of the patch was made. A thin PCB layer was integrated into the patch. The patch consists of an analysis chamber, hosting a conductivity sensor, and a sequence of 5 to 10 reservoirs that contain level indicators that monitor the filling speed. The sensors were successfully validated in lab experiments using a syringe pump and different NaCl solutions. A ventilated capsule measurement system was built for reference measurement of sweat rate and a more elaborate physiological experiment was performed in a climate chamber. The physiological validation study proved that the patch enables to reliably compare real-time sensor measurements with lab analysis of chronologically collected samples. Real-time sweat conductivity was linearly related to $[\text{Na}^+]$ and $[\text{Cl}^-]$ of the collected samples for all six participants. Furthermore, changes in sweat rate measured with a ventilated capsule related to changes in sweat conductivity.

The abovementioned sensor system can continuously measure the total ionic content of sweat. Although $[\text{Na}^+]$ and $[\text{Cl}^-]$ from the sweat samples showed a strong relationship with the conductivity measurements, different physical and dietary conditions can influence the conductivity measurements. To learn more about the analyte-specific concentrations in sweat, two other sensor systems were developed. We presented a new ventilated capsule to measure NH_3 that is evaporated from sweat. Additionally, an electrochemical sensor system was created that can measure sweat $[\text{Na}^+]$ and $[\text{Cl}^-]$. Initial characterization experiments of these sensors were performed. Further research is required for the optimization of these systems for physiological testing. By testing these systems in physiological experiments in an early stage of development, we aim to create sensor systems that can reliably measure in the intended user setting.

III

Movement Tracking in Field Sports

.....
*The movement tracking section is based on the following publications:

Steijlen, A., Burgers, B., Wilmes, E., Bastemeijer, J., Bastiaansen, B., French, P., . . . Jansen, K. (2021). Smart sensor tights: Movement tracking of the lower limbs in football. *Wearable Technologies*, 2, e17. doi:10.1017/wtc.2021.16

Steijlen, A. S. M., Bastemeijer, J., Plaude, L., French, P. J., Bossche, A., & Jansen, K. M. B. (2020). Development of Sensor Tights with Integrated Inertial Measurement Units for Injury Prevention in Football. Paper presented at the Proceedings of the 6th International Conference on Design4Health, Amsterdam.

Motivation

Over the years, the physical demands of football have increased. In the English Premier league for example, high intensity running distance and sprinting distance increased by more than 30% between 2006 and 2012 (Barnes et al., 2014). Likewise, in World Cup Soccer finals between 1966 and 2010, ball speed and passing rate increased by 15% and 35%, respectively (Wallace & Norton, 2014). The high physical demands in football lead to a substantial injury risk. In professional football 8.1 injuries per 1000 hours of play were reported based on epidemiological data of 44 studies (López-Valenciano et al., 2020). Most injuries occur during competitive matches (Owoeye et al., 2020), and almost one-third of all time-loss injuries are muscle related. More than 90% of all muscle injuries are lower limb injuries, of which 37% concern the hamstrings (Ekstrand et al., 2011). Several studies conclude that increased age and previous injury significantly increase the risk of hamstring injury (Arnason et al., 2004; Freckleton & Pizzari, 2013). Moreover, Ekstrand et al. reported more cases of injury at the end of each half of a football game (2011), which suggests that fatigue is also an important risk factor. Therefore, investigating physical player load and its relation to hamstring injury prevalence can expand the knowledge on the aetiology of hamstring injuries, and can help to develop new methods to prevent these injuries in the future.

76

The use of wearable electronic measurement equipment was approved by the FIFA in 2015 (Dunn et al., 2018). Several commercial systems that can track individual athletes by GPS (Global Positioning System, e.g. Zephyr Performance Systems, US, Catapult Sports Ltd, Australia and JOHAN Sports, The Netherlands) or RFID technology (Radio Frequency Identification, e.g. Inmotio Object Tracking, The Netherlands) have been developed. In addition, the systems contain a 3-axis accelerometer. Based on the data from these systems, the total distance covered can be calculated, whole-body acceleration and deceleration data can be derived (Barrett et al., 2014) and activities can be classified (Datson et al., 2017). However, these data do not provide insight in the kinematics of the lower limbs. For detailed kinematic analysis of the lower limbs, the current practice is to use an optoelectronic measurement system (Cuesta-Vargas et al., 2010; Malfait et al., 2016; Schache et al., 2012), which is restricted to a lab environment and does not allow for on-field measurements during training or competition. Kinematic measurements outside the lab are commonly performed using inertial measurement units (IMUs), which are attached to body segments. IMUs measure linear accelerations (accelerometer), angular velocities (gyroscope) and the earth magnetic field (magnetometer) in three different axes making the 9 degrees of freedom (Ahmad et al., 2013). The orientation of an IMU can be derived by combining these measurements using a sensor fusion algorithm. After a calibration of the sensors to each limb segment, the lower limb kinematics can be obtained (Luinge et al., 2007; Roetenberg et al., 2007).

Recently, several applications of IMU systems have been presented. These IMUs consist of a box, typically with a size of 30 mm x 40 mm x 10 mm, containing all electronics including the battery. In most cases, the modules are tied around the limbs, chest, or hands (Anwar

.....

et al., 2018; Chen et al., 2020; Rawashdeh et al., 2016; Stiefmeier et al., 2008; Teague et al., 2020). Other researchers attach them to the skin with an adhesive at predetermined locations (Gaidhani et al., 2017; Hu et al., 2020). These sensor units are less suitable for long-term monitoring studies and little attention is paid to the integration of the IMUs in clothing in these papers. The company Xsens developed a motion tracking suit including software to derive body kinematics (MVN Link, Xsens, The Netherlands). Although, they found an elegant way to place the hardware in pockets in the garment, the electronics are relatively large, and it takes time and additional help to position all the electronics in the right locations when wearing the suit. The integration of electronics in textile is part of another research field that is more focused on materials science (de Mulatier et al., 2018; Komolafe et al., 2019; Varga, 2017). In this field some researchers have integrated IMUs in textiles. For example, Wicaksono et al. created a suit with an IMU on a flexible printed circuit board right below the sternum for measuring heart, and breathing activity (Wicaksono et al., 2020), and Wang and co-workers created a garment with integrated IMUs for posture monitoring (Wang et al., 2015). However, in all of the abovementioned monitoring systems, either the sensor modules are relatively large and not integrated in the garment, or the IMU sampling rate and detection range are limited (100 Hz or below, and 16 g or lower, respectively). Therefore, as far as we are aware of, a garment for unobtrusive monitoring of lower limb kinematics in everyday training situations which is accurate enough and can be used without the need of technical assistance does not yet exist.

To enable reliable long-term monitoring at the football field, we are developing an easy-to-use wearable monitoring system with integrated IMUs, which will be referred to as smart sensor tights. This is an embedded system with IMUs integrated in textile on each segment of the lower limbs. The sensors are connected by flexible wiring to a central processing unit at the waist band that contains a single microprocessor and a power source. The advantages of this specific architecture are that the sensor modules are small, unobtrusive and of low weight. Moreover, no additional synchronisation of the sensors is needed, since they are all read out by one microprocessor. To the best of our knowledge, this is the first IMU system that has the sensors integrated in shorts or tights, which allows for easy on-field measurements of fast movements of the lower limbs. By making use of a real-time operating system, high sample rates can be reached to track fast football-specific movements accurately. The measurement range of the IMUs is larger (± 4000 °/sec for the gyroscopes and $\pm 30g$ for the accelerometers) than in the systems presented above. The tights can be easily put on by the players themselves and can be worn in regular matches and trainings. The integration of the sensors in a garment facilitates long-term monitoring of players and larger scale studies outside a lab environment, which are required to find injury risk factors for injury prevention.

This section presents the design and development of the smart sensor tights. First, the research approach is explained. Four prototypes of the sensor tights were created during the course of the research project. Each prototype showed new improved functionality. This is presented in the subsequent chapters.

Research approach

Hamstring injuries are among the most common injuries in field sports that involve explosive actions like jumping and sprinting (Woods et al., 2004). These injuries in most cases happen near the end of the match (Ekstrand et al., 2011), which suggests that the accumulation of these explosive actions results in a higher injury risk. The common aim of this multidisciplinary research project is to design a wearable system, the so called ‘Smart Sensor Shorts’, that tracks the load on the hip-related muscles accurately, to prevent hamstring and adductor overload. Starting from a clear user need from elite football and field hockey, a consortium with human movement scientists and engineers was formed to research this. The sensor shorts are called sensor tights in this study, because multiple longer versions of the garment were created to also measure movement around the knee joint for researching the aetiology of hamstring injuries.

Project overview

Figure 7.1 presents an overview of the different research aspects in this project. Our team from the TU Delft is responsible for system design and development of the sensor tights (Figure 7.1, no. 1). This includes design of the electronics, software development and the integration in textiles.

78

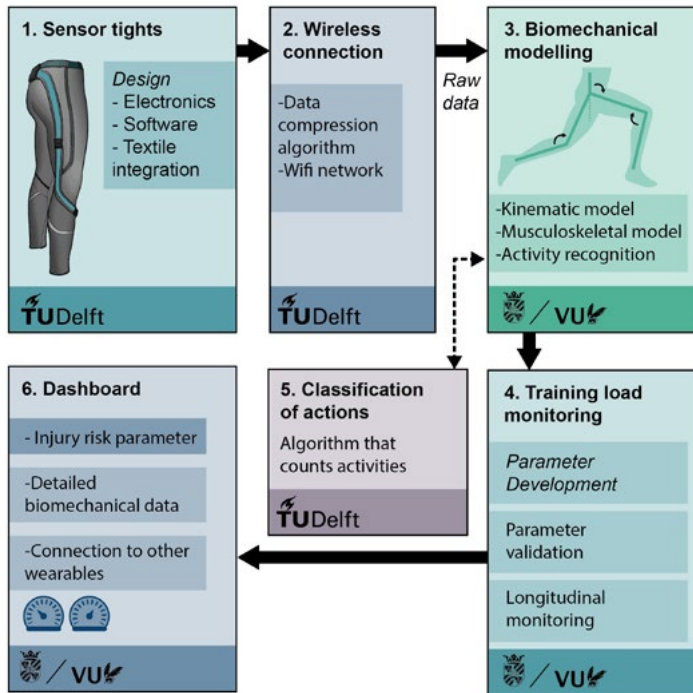


Figure 7.1. Project overview of the Smart Sensor Tights for movement tracking.

The most important design criteria for the sensor tights are (Steijlen et al., 2020):

1. Five IMUs should be integrated in tights: one at the trunk, one at each upper leg and one at each lower leg. They gather accelerometer data, gyroscope data and magnetometer data in x,y,z directions.
2. Raw data should be saved and should be read out at a computer.
3. The electronics should not harm the wearer and fellow players during a match.
4. The product should be comfortable to wear and should not restrict the athlete's movements.
5. The IMUs should not move with respect to the skin.

The data of the tights will be stored at an SD card, but for near real-time monitoring, a wireless connection to a central computer is required as well (Figure 7.1, no. 2). This computer will receive and store the data of all players in the team. It will show the data near real-time on a dashboard and via a web interface or hardware connection (e.g. a universal serial bus) the raw accelerometer, gyroscope and magnetometer data can be derived by the human movement scientists from the University of Groningen and the VU Amsterdam, who are responsible for translating these data to biomechanical models (Figure 7.1, no. 3). With the help of biomechanical models, a parameter for training load monitoring and injury risk will be developed (Figure 7.1, no. 4). This parameter should be easy to understand, so that in the future coaches and medical staff can use this parameter in daily practice. A potential parameter for the load around the hip joint that is part of current research, is the vector norm of the angular accelerations in three directions around the hip joint (α_{hip}) in $^{\circ}/s^2$, divided by a scaling factor. $|\alpha_{hip}|$ is squared to emphasize high intensity movements, which are expectedly increasing the risk of injuries.

$$Hip\ load = \frac{|\alpha_{hip}|^2}{10^8} \quad (7.1)$$

The accelerations are directly related to the forces around the hip, which would possibly give a good indication of the hip load. The parameter needs to be validated at different levels of play and during longitudinal monitoring studies. This research is performed at the campus of the Royal Dutch Football Association. Furthermore, the sensor data can be used for football activity recognition (Figure 7.1, no. 5), for example to count the number of shots or sprints that are performed during a match. At the mathematics department of the TU Delft, an algorithm is being developed to accomplish this (Cuperman et al., 2022).

As a last step in this project, a dashboard will be created that shows the new injury risk parameter in a user friendly way to coaches and medical staff (Figure 7.1, no. 6). This dashboard can be a completely new interface, or it can be added to existing dashboards (such as the dashboard of Inmotio Object Tracking) that show heart rate and GPS data. Detailed biomechanical data can be retrieved via the dashboard for more detailed investigation as

well. Finally, the new information derived from the sensor tights can be combined with other measurements such as heart rate data and GPS data, to obtain a more detailed view on the health status of the athlete.

Prototype planning

During the design process of the sensor tights, an iterative design approach was followed. Within a time-span of four years, four prototypes were created (Figure 7.2). The prototypes were tested in user studies and technical validation studies. Based on the insights of those studies, improvements were identified for the next prototype. In the following chapters the four prototypes including main design considerations and design validation are described.

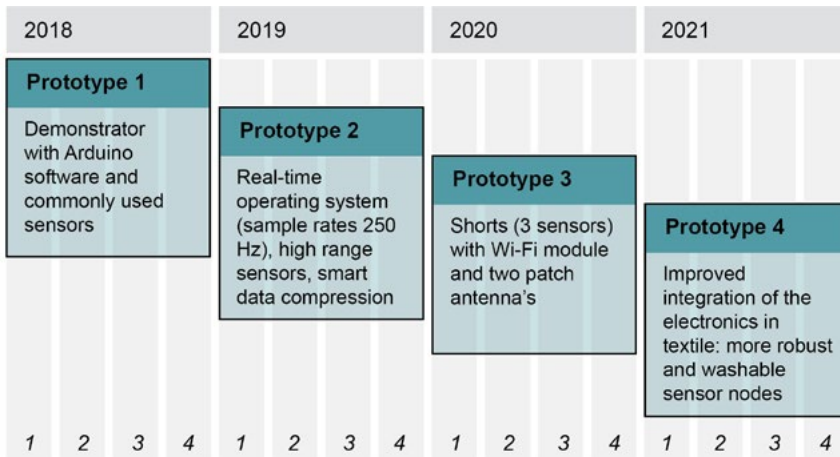


Figure 7.2. Prototype planning.

7

Smart sensor tights 1.0: a proof of concept

At the start of the project a first concept of the system architecture was made, starting from the list of criteria. Commercially available IMU sensor modules are in most cases independent sensor nodes that contain a microcontroller, battery and an IMU sensor integrated in one device (e.g. the Shimmer3 IMUs, Shimmer Sensing, IRL). We choose to use a single microcontroller to read out all five sensors. This microcontroller, including power supply and user interface are placed in a central pocket at the waistband of the tights. An advantage of using a single microcontroller is that the sensors can be easily synchronized. Moreover, centralizing the power supply minimizes the mass of the sensor modules, to limit artefacts due to inertia of the modules. Furthermore, less components are required and the system becomes less bulky and obtrusive.

81

7.1. Interconnects

Centralizing the microcontroller and power supply, means that a relatively long distance (>50 cm) needs to be bridged to connect the sensor modules. The interconnects need to be highly deformable to not restrict the athlete during sports activities and to avoid disconnection. Zeng et al. (2014) described three approaches to make largely deformable interconnects. The first approach is to create new stretchable and flexible conductive materials. Several different types of composite materials were developed, such as carbon nanotube flexible materials. For example Sekitani et al. (2008) developed a material with single-walled carbon nanotubes in a copolymer matrix, covered by PDMS (polydimethylsiloxane). Additionally, graphene composites were developed, like graphene in PDMS (Someya et al., 2004). PEDOT:PSS/PDMS composites (Teng et al., 2013) and (liquid) metal films or particles (e.g. silver and gold) on or in stretchable membranes or fibres (Park et al., 2012) can be found as well. The second approach is to make stretchable interconnects from rigid inorganic materials by designing a smart structure. Several researchers used horseshoe/ meander-based patterns on a flexible organic substrate to make stretchable interconnects (Gonzalez et al., 2007; Verplancke et al., 2012). An example of meander-based structure is shown in Figure 7.3a. Furthermore, net shaped structures (Someya et al., 2005) and out-of-plane wrinkles (Xu et al., 2012) of rigid conductors are developed. The third approach is the

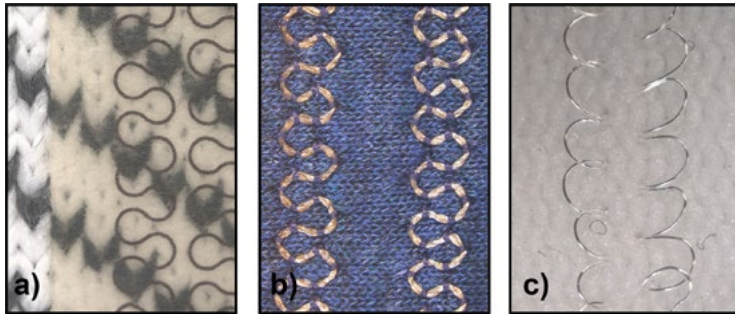


Figure 7.3. Integration of wiring in textile: a) a meander-based pattern of copper traces on TPU, laminated on a knitted sample. b) Carbon based conductive yarn embroidered on a knitted sample. c) Enamelled copper wire knitted in textile.

creation of elastic textile structures. Metal wires can be woven (Locher & Tröster, 2008) or knitted (Li & Tao, 2011) in textile structures. Knitted structures are preferred over woven structures, because these are much more stretchable (20-30 % strain for woven structures and more than 100% strain for knitted structures). Figure 7.3c. shows an example of a knitted sample.

82

Zeng et al. (2014) performed a benchmark analysis for the three types of interconnects. They investigated the ability of the different structures to maintain conductance at a certain strain in repeated loading-unloading cycles (also called fatigue resistance). It was found that the knitted interconnects, in which copper wiring was knitted in textile, performed best. These knitted interconnect maintain function over 100.000 loading cycles, up to a 60% fabric strain, while the resistance is almost unchanged (0.09%).

Because the third category, integrating wiring in textile structures, shows at this moment a much higher fatigue resistance, it was chosen to embroider stranded copper wiring in a serpentine pattern on the textile. For the first versions of the tights, integrating the wiring was performed by hand.

7.2. Proof of concept

The first prototype was designed in a very early phase of the project. Prototype 1 served as a proof of concept and was meant to identify the main challenges towards designing a reliable product. Therefore, this prototype was built with the userfriendly Arduino platform. An Arduino Due development board with 32-bit ARM core microcontroller (Arduino, USA) was used to readout 5 widely used inertial measurement units with an integrated magnetometer (MPU-9250, InvenSense, CA). The sensors were connected to the Arduino via an 8-channel I²C switch (TCA9548A, Texas Instruments, USA) with PVC insulated stranded copper wires. The wires and sensor modules were sewn in a serpentine pattern to a pair of tights (Figure 7.4). Solder connections were made to the break-out boards and the sensors were encapsulated in silicone (Shore (A) 15-40, two-part silicone elastomer, Siliconesandmore,

NL) to protect the electronics. Data were stored at an SD card. An important challenge that was encountered was that the sample frequency was not well controlled and limited to 165 Hz. Furthermore, the sensor range was limited to 2000 °/s for the gyroscope and 16g for the accelerometer and clipping can occur during high intensity sprints and shots.

To test whether accurate limb tracking was possible with the new garment, a preliminary validation study was performed to compare the sensor tights against the optoelectronic measurement system (Vicon Motion Systems Ltd., UK). Raw IMU data were translated to orientation data with a preliminary version of the sensor fusion algorithm (Wilmes et al., 2020). Three different football specific movements (10 m sprint, kick and jump) were executed at 2 different intensity levels (“jog” and “maximal”). It was observed that root mean square differences between the optoelectronic measurements and IMU measurements of the hip- and knee angles increased with intensity. To reduce the errors at higher intensity movements, several improvements were identified. First, measurement at higher sampling frequencies may gain more accurate results for higher intensity movements. Second, the sensor fusion algorithm can be optimized by tuning filter parameters. And third, the weight of the sensor modules can be reduced and integration in textile can be improved to limit the movement of the sensors with respect to the skin.

7.3. Sensor locations

During the development of prototype 1 of the sensor tights, a study was performed to identify the best location of the sensors. Two considerations are important in optimizing sensor location. On the one hand, the sensor needs to be placed at the most comfortable and safe location and on the other hand, soft tissue artefacts (STAs) need to be minimized

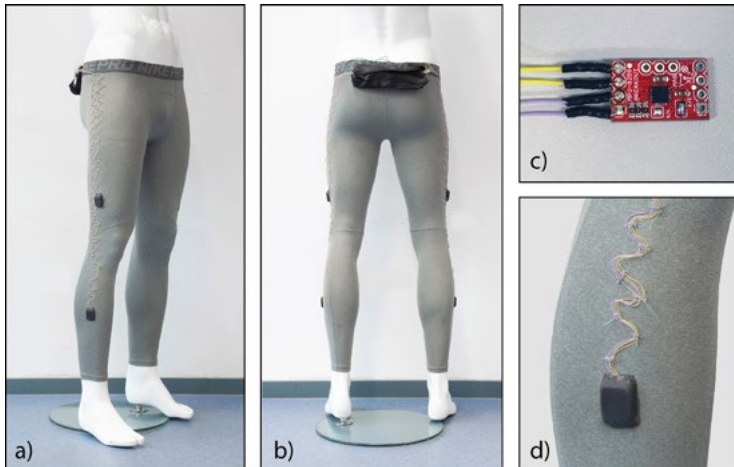


Figure 7.4. Pictures of prototype 1. a) side view b) back view c) the IMU sensor module d) encapsulated sensor module connected to the insulated copper wire embroidered in a serpentine pattern at the tights.

(Barré et al., 2015). STAs are defined as measurement errors that arise from the relative motion between bone and sensor, for example due to muscle bulging during a contraction.

To study the most safe and comfortable locations of the sensors, an observational study was performed, a survey was held among professional athletes and experts were interviewed (Ahsmann et al., 2019; Steijlen et al., 2020). In the observational study, a series of typical football interactions was identified that could cause problems with the electronics in clothing. A series of professional football trainings was observed via video recordings (87 minutes in total) and the occurrence of these types of interactions was quantified. It was found that face-to-face duels (0.082 times per player per minute), face-to-back duels (0.051 x per player/min.), and side-to-side duels (0.031 x per player/min.) occur most. The potential sensor locations at the medial and lateral sides of the thighs and at the upper part of the lower legs were least involved in the interactions. From the results of the observations and survey, the locations shown in Figure 7.5a. were chosen for further study.

To identify the locations with minimal STAs, a test was performed with the optoelectronic measurement system (Vicon Motion Systems Ltd., UK). 16 Markers were placed at bony landmarks, to identify joint centre coordinates. Seven markers were placed at potential sensor locations that were chosen based on the outcomes of the abovementioned tests. Four subjects performed an acceleration run (0-100%) and deceleration run (100%-0%). From the bony landmarks, a reference frame was created and perpendicular movement and parallel movement of the sensor location markers with respect to the reference frame was measured (see Figure 7.5b). Parallel movement was converted to movement relative to the segment length, because the segment length will vary during limb movement. From the study it was found that sensor locations at the outer sides of the thighs and the sides of the tibia show the lowest shift. Although this study gives an insight in the locations that have a larger influence of STAs, movement of the reference frame markers with respect to the skin

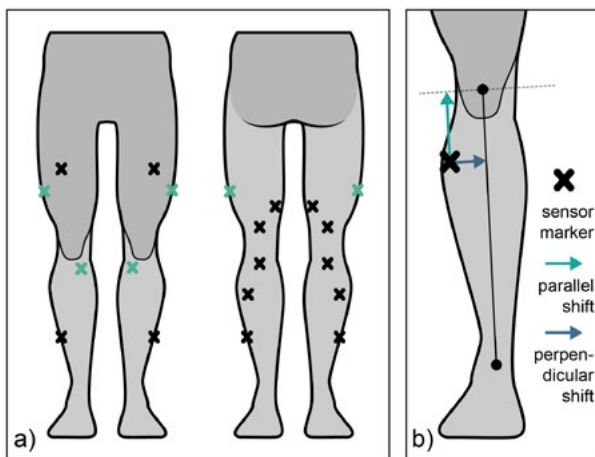


Figure 7.5. Identification of the best sensor locations. a) sensor locations for the STA study (black markers) and the chosen sensor locations (green markers). b) The marker shift was measured perpendicular and parallel to the reference frame.

will influence the outcomes and bone-fixed markers or röntgen stereophotogrammetric data are required for more accurate measurements. Based on the outcomes of the different tests the final sensor locations were chosen. In Figure 7.5, these locations are highlighted in green.

7.4. Conclusions

During the development of the first prototype, several design decisions were made. At first, it was decided to centralise sensor readout, power supply and data storage, to reduce the weight of the sensor modules and to facilitate synchronization. Second, state-of-the-art flexible and stretchable interconnects were identified. For the prototypes, it was decided to embroider insulated stranded copper wire in a serpentine pattern on the textile. A proof of concept prototype was created to identify main improvements for the next prototype. These included, increasing sampling rates and measurement range and reducing the weight of the sensor modules. Lastly, a study was performed to identify suitable sensor locations at the lower limbs. Based on the outcomes of a soft tissue artefact experiment and an observational study, the best sensor locations (Figure 7.5a) were chosen. The sensor locations are implemented in the next prototypes.

8

Smart sensor tights 2.0: a validation study in a football context

86

To improve the technical reliability and user acceptance of the new system, an iterative design approach was followed. Multiple prototypes were made to enable simultaneous improvement of the hardware and software, as well as improvement of usability and comfort. Prototype one included widely used IMUs (MPU-9250, InvenSense, USA) and an easy-to-use microcontroller development board (Arduino Due). With this prototype, a proof of concept was created and based on field tests, major improvements were identified. These improvements included increasing the sampling rates, increasing the measurement range, and improving the robustness of the electronics. This formed the starting point for the design of the 2nd prototype that is presented here.

First, the new smart sensor tights system design is presented, followed by the detailed design of hardware and software. Secondly, a controlled test with football specific movements was executed in the lab to concurrently validate the novel sensor tights with an optoelectronic measurement system. Third, the sensor tights were worn during football specific exercises to test the performance in the field. Lastly, user experience is assessed.

8.1. Materials & methods

Design

The design of the sensor tights had to meet several requirements. To investigate the kinematics of the legs, 5 IMUs are integrated in this design as well. IMUs are placed on the thighs, shanks, and pelvis. The exact locations are explained below. Since the product will be used by researchers in biomechanics to derive lower limb kinematics, it is important that the IMUs have a sample rate of 250 Hz in each direction and that raw data can be obtained via an SD card. At a later stage, a wireless connection will be integrated. Furthermore, the risk that the electronics harm the wearer or fellow players during a match should be negligible. The garment should not restrict the players movement and it should be comfortable to wear. Lastly, the IMUs need to be tight to the skin and of low mass, to prevent shaking due to inertia of the sensors.

Hardware Design

For the hardware, it was chosen to centralize the data acquisition electronics and the power supply. This resulted in tiny and low weight sensor modules that reduced the measurement artefacts due to inertia of the sensors. Figure 8.1 shows an overview of the new system. The two subsystems are referred to as the IMU node and the central unit. A new PCB was designed for each subsystem. Linear accelerations and angular velocities are measured by the ICM-20649 (InvenSense, USA). This IMU was selected based on the wide measurement range of ± 4000 °/sec and $\pm 30g$, which enables more representative analysis of kinematics of highly dynamic movements. Preliminary experiments showed that with sensors with a smaller measurement range (16g), clipping occurred at moments of impact with the ground. Via an I²C bus, a magnetometer (AK8963) with a range of ± 4900 μ T (Asahi Kasei Microdevices, Japan) is connected to the ICM-20649. The central unit is responsible for reading out the sensor, power handling and data storage at an SD card. The microcontroller that was chosen for the central PCB is the Arm Cortex-M4 with FPU processor (STMicroelectronics, Switzerland) which runs at 100 MHz maximum. The STM32F411 Nucleo-64 development board was used for software development (STMicroelectronics, Switzerland). Lastly, a CE marked power bank (1350 mAh, Xqisit, Germany) was used as a power supply. Data acquisition from the sensor nodes occurs via a Serial Peripheral Interface (SPI). The SPI bus was chosen, because the ICM-20649 can then directly be read out through SPI and no extra electronics are needed. Furthermore, the SPI bus is less prone to errors over long distances at high data transfer rates than the I²C protocol.

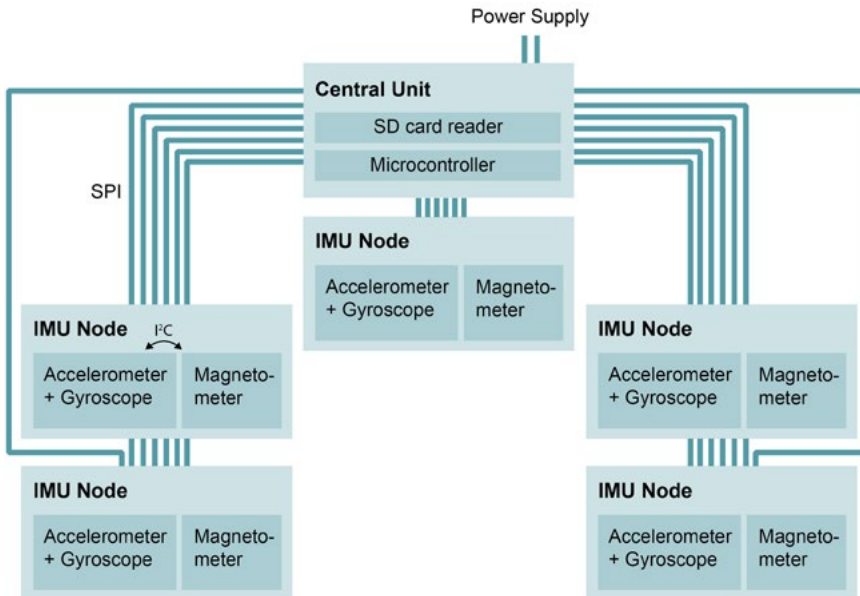


Figure 8.1. System overview.

Sensor locations

Based on observation of training sessions and a soft tissue artefact (STA) study (chapter 7), the best sensor locations were chosen. The upper leg sensors are placed halfway the hip and knee joints on the lateral side of the thighs. STAs were expected to be relatively low because of the stiff underlying connective tissue. The lower leg sensors are placed at the inner sides of the shanks, close to the knees. The trunk sensor is placed in the waistband and the central unit, including the battery, is placed in a pocket located above the sacrum (Figure 8.2).

Software Design

To make sure that each sensor node can be read out with a sample rate of 250 Hz for the gyroscopes and accelerometers and 100 Hz for the magnetometers, a real-time operating system (FreeRTOS) was used for this design. An RTOS was used to implement a pre-emptive priority-based scheduling scheme (Guan et al., 2016). Pre-emptive scheduling means that a task with lower priority can be interrupted by a task with higher priority. Once the task with a higher priority is finished, it will continue with the lower priority task. Table 8.1 shows the different tasks and their priority level. With this software, the required sample rates can easily be reached. When the microcontroller is running at 100 MHz, it turns out that the microcontroller only needs 40% of available time to execute all tasks. The power consumption is around 110 mAh, which means that with the current battery the system can run for 12 hours.

Lossless data compression

Future prototypes must be able to send data wirelessly to the football coach or medical staff. Given that the total amount of bits per sample is 16, the data rate of one prototype is 144 kbit/s. This implies that, when 22 players at the field are wearing the system, a data rate of 3.168 Mbit/s would be required. Based on the overview of different wireless protocols for a local network and their maximum bit rates and ranges by Kos et al. (Kos et al., 2019), it can be concluded that only Wi-Fi protocols would be suitable. On top of that, experimental findings from literature show that the presence of a human body between the transmitter and receiver can lead to significant disturbances in the radiation pattern (Kurusungal et al., 2010; Sivaraman et al., 2010). To improve the reliability of wireless data transmission for future versions, the amount of data retrieved from the sensors can be compressed.

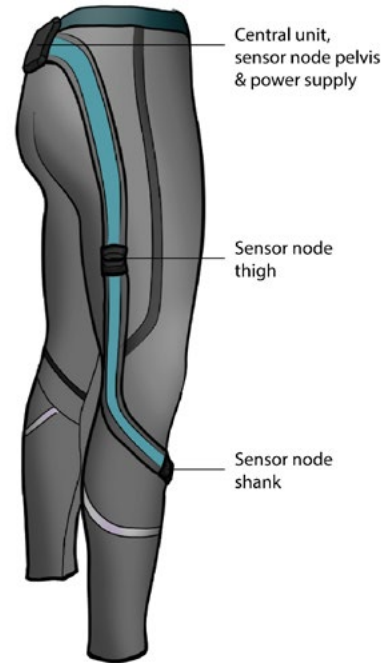


Figure 8.2. Location of the electronics in the tights.

8. Smart sensor tights 2.0: a validation study in a football context

Table 8.1. Scheduling scheme for microprocessor.

Task	Frequency	Priority
Read out accelerometers and gyroscopes for all IMUs	250 Hz	Real-time
Store accelerometer, gyroscope & magnetometer data into a buffer (size: 4kb)	250 Hz	Real-time
Read out magnetometers for all IMUs	100 Hz	High
Create SD card file and handle the user interface	5 Hz	Above normal
Write the buffer to the SD card	Event-based	Normal

Therefore, the FELACS data compression algorithm (Kolo et al., 2015) was implemented in the software. The performance of the algorithm was thoroughly tested in a football specific setting.

Prototype

Figure 8.3. shows images of the tights and important details. As can be seen in Figure 8.3g. an insulated stranded silver-plated copper conductor with a conductor area of 0.03 mm^2 was chosen and laced in a serpentine pattern to allow for stretchability on top of a base garment (stretchable running tights, Under Armour, USA). PTFE was chosen as insulation material, because of its high chemical inertness, hydrophobicity and mechanical strength, which will be of great value when the tights will absorb sweat and when they are washed. Miniature connectors for use in wearables are not yet commercialized. As an alternative, a regular miniature wire-to-board connector (Pico-clasp, Molex, USA) was chosen to connect to the central unit PCB and IMU node PCBs. To test the impact of washing with soap and water on the reliability of the connections, a washing test ($40 \text{ }^\circ\text{C}$, 1200 RPM, including other sports clothes) was performed with these connectors ($n=12$) and a 4-point resistance measurement was performed after each washing cycle. The resistance slightly increased after 7 washing cycles. However, it stayed below $1 \text{ }\Omega$. The PCBs were placed in 3D-printed casings made from a photopolymer (Connex 3, Objet 350, Stratasys Ltd., Israel). The sensor nodes weigh 3.6 grams. The sensor nodes and central unit were placed in sleeves, which have a waterproof lining, to protect the electronics against sweat. For washing the tights, the sensors and central unit, can be disconnected. The wiring and connectors remain embedded in the garment. The central unit has an interface with three coloured LEDs and 2 buttons, to start and stop recording and to indicate a special event. Figure 8.3d shows the interface.

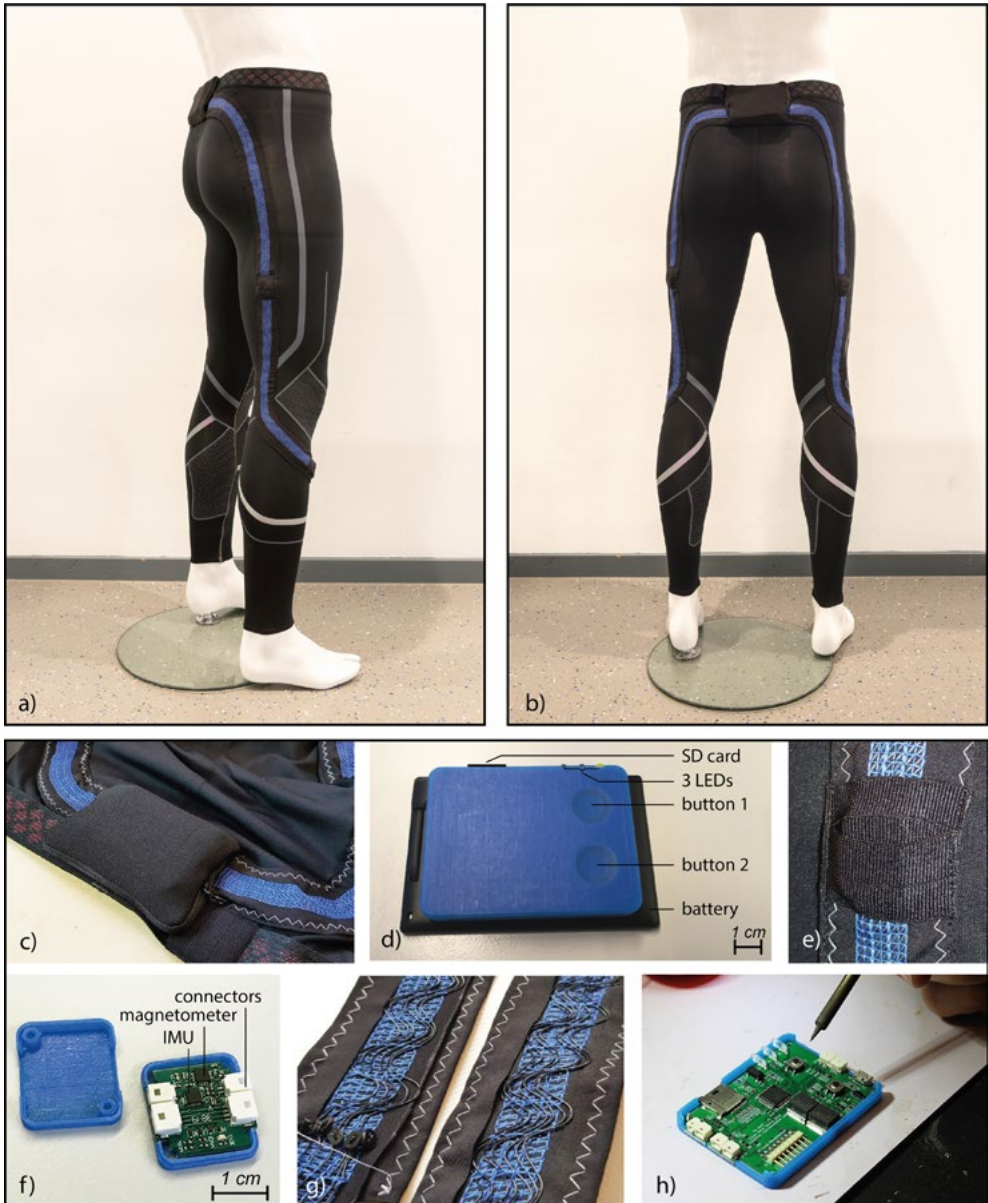


Figure 8.3. a) Side view sensor tights. b) Back view sensor tights. c) Pocket with central unit PCB and battery. d) Battery and central unit with user interface. e) Pocket of a sensor node. f) A sensor node. g) Interlaced wiring that allows for 100% stretching. h) Central unit during assembling.

Validation study

The validation of the design was split in two parts. The first part was a validation test in the lab. The aim of this test was to assess the concurrent validity of the prototype with the golden standard optoelectronic motion analysis system. The second part was a validation test of the system on the football field. In this experiment, the functioning of the device was tested, and user experience tests were performed. It was verified if the datasets are complete, and the performance of the data compression algorithm for different football specific movements was measured. The study was approved by the Human Research Ethics Committee of Delft University of Technology. All participants gave informed consent.

Lab validation

As explained in the introduction, detailed lower limb kinematics can be derived by applying sensor fusion algorithms to the IMU data and performing sensor-to-segment calibration (Roetenberg et al., 2007). Recently, a paper has been published which explains the model that we use to derive lower limb kinematics with the sensor tights (Wilmes et al., 2020). In that study, individual sensor modules that are taped to the skin were used to validate the models and good concurrent validity with an optoelectronic system was shown. To validate the novel sensor tights, a similar protocol was performed. Since the previous study was already performed with 11 participants, it was chosen to compare the previous results and the results with the new garment of 1 participant to validate the new product. In the current experiment, one male participant (age: 23 years, height: 1.89 m) was wearing the garment with integrated IMUs, and the measurements of the garment were compared with the optoelectronic system measurements. The sensor-to-segment calibration consists of two steps. First, the participant is asked to stand still for 5 seconds in a neutral upright pose to identify the longitudinal axis of each segment by using the direction of gravity. Thereafter, the participant performs three movements in the sagittal plane to determine the frontal axis of each segment; a rise of the right upper leg, a rise of the left upper leg, and a bow forward of the trunk. A gradient descent Madgwick algorithm is used to estimate the sensor orientation during the measurements (Madgwick et al., 2011).

The optoelectronic system used eight cameras (Vicon V5 cameras, Vicon Motion Systems Ltd., UK), and 20 reflective markers were placed at the lower body. More information about marker placement can be found in Figure C1 (appendix). The motion capture area was 25 m². Five types of football-specific movements were executed: an acceleration run, a run with a cutting movement, a run with a 180 ° turn, kicking a ball (preceded by a few steps) and a jump. Each movement was performed at 3 different intensities (50%, 80% and 100% of maximum effort respectively). Each trial was repeated 3 times. A more detailed description of the protocol can be found in Wilmes et al. (2020). Data were processed in MATLAB (The MathWorks, USA). Hip and knee joint angles and angular velocities were calculated with the data from the optoelectronic system, and with the data from the sensor tights. Thereafter, the root mean square differences (RMSDs) and coefficients of multiple correlation (CMCs) were calculated between the sensor tights and the optoelectronic system for all types of movements separately.

Field tests

Five male participants (recreational football players, age: 21.8 ± 1.3 years) were asked to wear the garment and to perform a high intensity football-specific training drill (Kelly et al., 2013). This training drill is aimed to replicate the physical movements and technical actions during match-play. The drill was performed at least 2 times for each participant. Next to the training drill, two participants performed an extra series of isolated football specific movements at 50%, 80% and 100% of maximum effort. These movements included an instep soccer kick, running, jumping vertically, running with the ball, and running sideways. After the field experiment, all participants were asked to fill in a short questionnaire about their experience with wearing the tights. Data were processed in MATLAB (The MathWorks, USA). Differentiated signals and probability distributions of the decompressed accelerometer, gyroscope and magnetometer data were calculated to check the completeness of the dataset, and functioning of the sensors. Furthermore, compression ratios for each type of movement were calculated, to test the performance of the data compression algorithm. The compression ratio (CR) is defined as:

$$CR = 100 * \left(1 - \frac{\text{compressed filesize}}{\text{original filesize}}\right) \% \quad (8.1)$$

92

8.2. Results & discussion

This part describes the results and discussion of the validation study. First, a comparison of football specific movements measured by the optoelectronic system and by the prototype is made. Secondly, the results of the recorded training sessions and user tests are discussed.

Lab validation

One participant performed six types of football-specific movements, and these were tracked with the IMU system and the optoelectronic measurement system at the same time. To compare the IMU data with the optoelectronic measurement results, the raw IMU data were converted to joint angles and joint angular velocities. An example of the comparison of the joint angles and angular velocities of the right leg during a kick and a jump measured with the prototype and the optoelectronic system, is shown in Figure 8.4 and Figure 8.5 respectively.

To evaluate the comparison, the root mean square differences (RMSDs) and coefficients of multiple correlation (CMCs) were calculated for each joint respectively. An overview of all RMSDs and CMCs at the different intensities and types of movement, is given in appendix C2. As shown in the tables of C2, RMSDs of the knee joint angles for all types of actions (each movement at a certain intensity) ranged between 14.11° and 2.98° , and CMCs between 0.911 and 0.997. For hip joint angles for all types of movement, RMSDs ranged between 18.46° and 7.07° and CMCs between 0.830 and 0.983. Errors in hip joint angles are likely to be larger than errors in knee joint angles, because the hip has a larger range of motion. RMSDs of joint angular velocities for all separated actions ranged between $168.2^\circ/\text{s}$ and $59.1^\circ/\text{s}$ for the hips and between $141.2^\circ/\text{s}$ and $37.7^\circ/\text{s}$ for the knees, respectively.

8. Smart sensor tights 2.0: a validation study in a football context

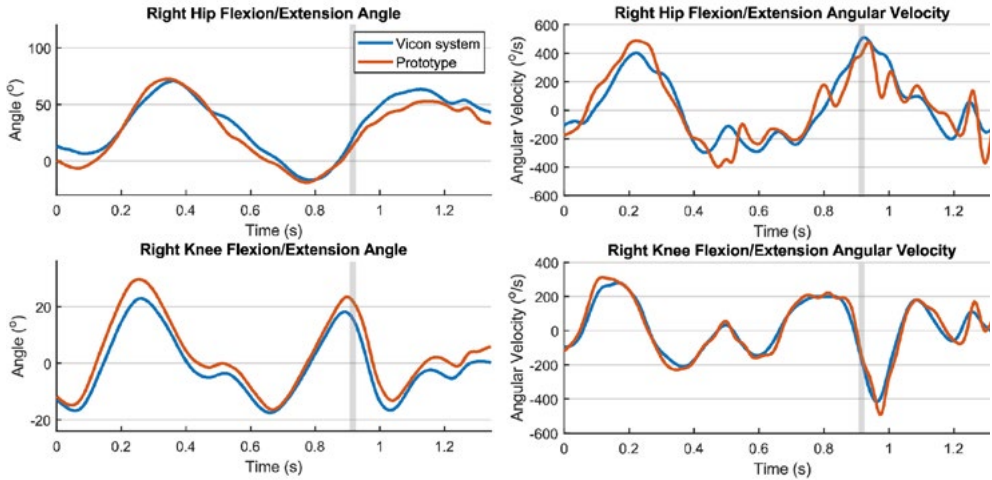


Figure 8.4. Joint angles and angular velocities of the right leg during a kick. The vertical grey line indicates the moment of ball contact.

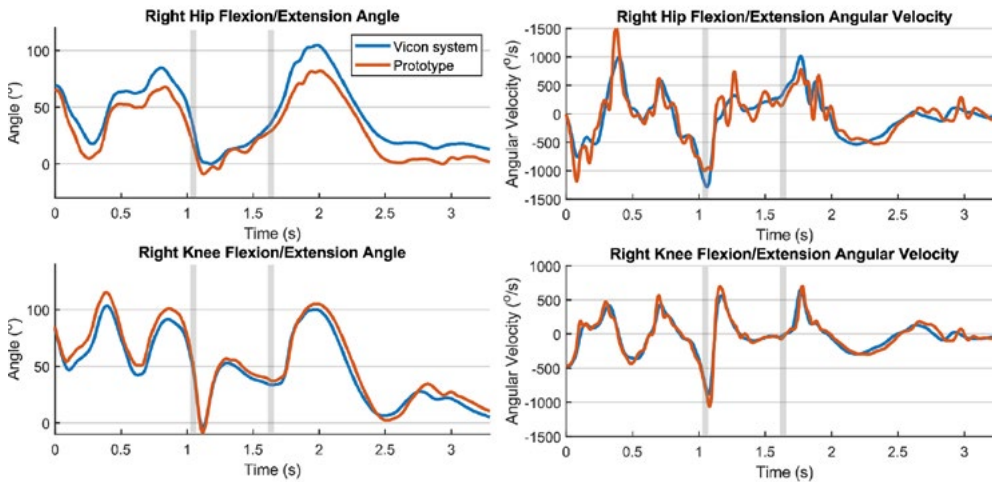


Figure 8.5. Joint angles and angular velocities of the right leg during a jump. The first vertical grey line indicates the time of push-off and the second indicates the landing.

CMCs ranged between 0.809 and 0.968 for the hip and between 0.979 and 0.9938 for the knee joint angular velocities. In general, It was found that the RMSDs and CMCs for all types of movement are within the same range as in the previous measurements of 11 players with the taped IMUs (Wilmes et al., 2020). In some cases (e.g. Figure 8.5, upper right) it seems that the differences are related to stronger filtering (peak suppression) by the Vicon

system, rather than measurement accuracy. Furthermore, the RMSDs and CMCs of joint angles found in the previous study by Wilmes et al. and in this study were comparable to the results from other studies. For example, Nüesch et al. measured RMSDs of 27.6° for the hip and 17.9° for the knee during jogging (~2.9 m/s), before they performed an offset correction (Nüesch et al., 2017). Additionally, Tadano et al. (2013) measured RMSDs of 9.0° for the hip and 7.1° for the knee during walking. Errors are expected to be higher for high intensity movements due to soft tissue artefacts and errors originating from the orientation filter. During this study, the participants performed higher intensity movements than reported in the other studies (e.g. acceleration runs with a mean running speed up to ~6.6 m/s), and the new IMU system still provides valid joint angle measurements (CMCs > 0.8) during these higher intensity movements. The advantage of the garment compared to the taped IMUs is that it is easier to use, comfortable to wear, and allows for longer-term monitoring studies during trainings and matches in the field.

Field tests

This part describes the results and discussion of the field tests. First, the technical validation results are discussed. Second, user experience insights are shown.

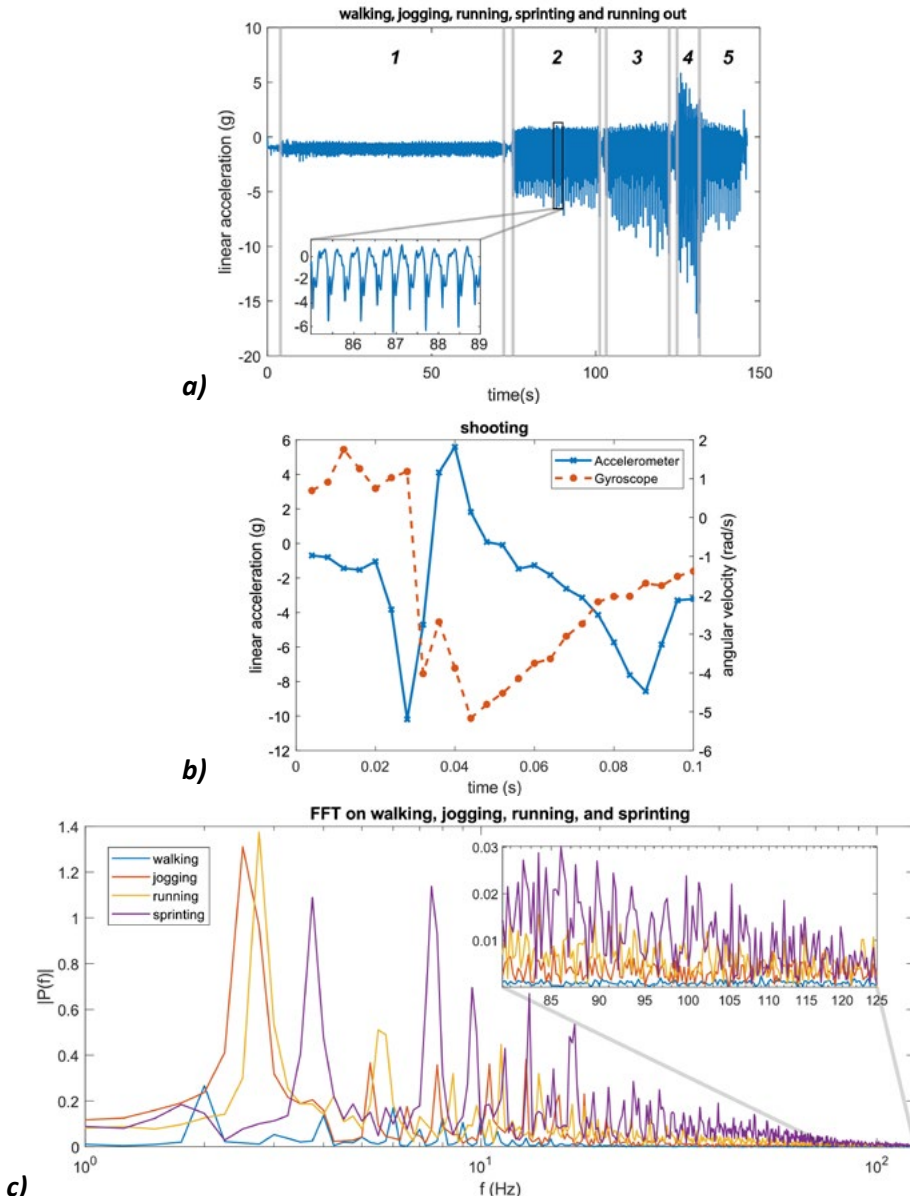
Technical validation

Datasets of the training sessions of the five participants were checked for completeness by plotting the probability distributions of the differentiated signals and visually inspecting the sensor data. It was found that for one participant, malfunctioning of a connector resulted in data loss of one of the lower leg sensors. For the other measurements, the differentiated signals of the sensors showed a Gaussian distribution. Figure 8.6a shows typical accelerometer data of the left lower leg in a single direction for the accelerometer. They were recorded during execution of a series of isolated movements. The figure shows results at different running intensities.

The training session measurements showed that the accelerometers and gyroscopes worked properly and data transfer using the SPI bus through the laced wiring appeared to be no problem. However, the magnetometers occasionally showed double readings. Most likely, this is caused by a not-updated register of the sensor itself. In future versions, the magnetometer can be replaced with a newer version, which may improve reliability of the readings.

Detailed analysis showed that the compression ratios varied with movement intensity as expected. Lower compression ratios were reached at higher movement intensities, whereas the lowest compression ratios were observed while sprinting (~24%). During walking the compression ratios were around 48%. As a comparison, Chiasson et al. (2020) were able to achieve compression ratios of ~16% of IMU data during walking in a recent study. It should be noted that their data were converted using the CR definition presented in the methods section, because they used another CR definition. The sample frequency of their dataset was 60 Hz, with a lower measurement range, which probably explains the large difference with our data. On top of that, the encoding part of the FELACS algorithm

8. Smart sensor tights 2.0: a validation study in a football context



c) Figure 8.6. a) Results from the left lower leg accelerometer (x-axis) of participant 1, during walking (1) jogging (2) running (3) sprinting (4) and running out (5). The spacings between each movement type indicate that the player is standing still or turning. b) A recording of a shot. Results from the right lower leg accelerometer and gyroscope in a single direction. c) Power spectrum analysis of accelerometer recordings (left lower leg, x-axis) at different running intensities (walking, jogging, running, and sprinting). For each running intensity, a recording of 1000 samples (4 sec) is used. A zoomed-in view of the range between 80 and 125 Hz is shown at the top right.

improves the representation of the quotient, most likely outperforming normal Golomb-rice encoding used by Chiasson et al. In this study, the average compression ratios of all sensors during the training session were between 43-45% for the different participants. In other words, the files of the training session data were 43-45% smaller than the original data set, which is beneficial for wireless data transfer in future prototypes. The algorithm for data compression adds only 1.6% to the total power consumption. These results are promising for wireless data transfer because the algorithm would markedly reduce the amount of data to be transferred at only a very small energetic cost.

At the start of this research, it was assumed that high sample rates (of 250 Hz) are required to prevent aliasing, and to ensure that the resolution is high enough to track all football specific movements accurately. First, when inspecting the raw data of the recordings of the isolated movements, sudden large changes were observed during high intensity movements such as sprinting and kicking. Figure 8.6b shows the data of the gyroscope and accelerometer of the right lower leg during a shot. The recording comprises 25 samples. Due to the limited number of samples, no transient behaviour was recorded during impact with the ball. The accelerometer measured a difference of almost 15g within 12 ms. This indicates that maybe even higher sampling rates than 250 Hz could be beneficial for high intensity actions like shooting. In lower intensity movements like walking, transient information and even noise were measured during a stride, so the sample rate is high enough for this type of movement.

Secondly, to analyse if the high sampling rate of 250 Hz is sufficient, a fast Fourier transform (FFT) was used to represent the data at different running intensities in the frequency domain. 1000 samples of each running intensity were used for a separate power spectrum analysis. The results are plotted in Figure 8.6c. The first peak in the power spectrum corresponds to the dominant movement frequency of the different activities. As can be seen from Figure 8.6c, for walking, jogging, running, and sprinting, the dominant frequencies increase from 2.0, 2.5, 2.75 to 3.75 Hz respectively. When zooming in at the last part of the graph, it can be seen that between 80 and 125 Hz the amplitude is higher for sprinting than for walking. A shock usually consists of a high magnitude main peak, associated with lower magnitude components at the higher frequency part of the spectrum. The high frequency components observed in Figure 8.6c are therefore attributed to these associated lower magnitude components. From the power spectrum analysis in combination with the abrupt changes in accelerometer and gyroscope data during shooting (Figure 8.6b) and sprinting, it can be concluded that this high sample rate adds information in case of high intensity movements. Further research is needed to find out if this extra information adds accuracy in deriving kinematics and estimating player load. Furthermore, a balance between high sample rates and practical implementation needs to be found. High sampling rates will increase the load on a wireless link in the future and it will increase energy use. Based on these considerations, a sampling frequency of 250 Hz is a justified choice. Future work may also include the use of adaptive sampling. For sprinting and shooting, the sample rates maybe even higher than 250 Hz, while the sample rates could be reduced for walking without losing accuracy.

User Experience

To investigate user experience, each participant filled in a short questionnaire. Table 8.2 summarizes the results. Testing the prototype in the field provided insight not only in user experiences, but also in reliability of the prototype and efficiency and effectiveness of the movement monitoring system. User experience scores on comfort and freedom of movement were relatively high. For both attributes a rating of 4 was given on average (Likert 5-point scale). A tight fit of the tights is required for minimizing motion artefacts of the sensors. Four subjects experienced the tightness of the garment as a positive aspect. One subject, with the largest clothing size, experienced the garment as too tight. In the future, multiple sizes and shorts need to be developed to enhance comfort and freedom of movement for every player. In general, the subjects did not feel restricted in their movements by the electronics in the tights. However, one subject noted that the garment would seem too fragile for sliding's. In future versions, connections will be made more robust to enable the players to make sliding's. Furthermore, the thickness of the sensor modules will be reduced, and the use of a cushioning layer can be explored.

When a novel prototype is developed and a wireless module is added to the tights, it would be beneficial when the athletes can activate the sensor tights themselves. Therefore, future work will include optimization of the user interface to start and stop measurements for use by athletes. Future work should also include better integration and miniaturization of the sensor nodes and central unit to enhance safe use and comfort. Furthermore, the connections with the sensor nodes need to be improved. During the tests, it was found that even after very short instants of disconnection, for example during dressing, the data collection is interrupted for this sensor. Since the connectors chosen were not designed for use in clothing, alternative solutions need to be explored. A very robust, yet not very sustainable solution, is to solder the wires to the PCB and encapsulate sensor nodes with an acrylate or silicone material. An alternative solution would be to develop a new type of connection, for example based on inductive coupling. In the current version of the garment, a waterproof textile layer was placed in the pockets between the electronics and the skin to protect against sweat. When the sensor nodes are encapsulated, the central unit casing is sealed, and an extra waterproof layer will be placed between the environment and the body, the system will also be resistant to rain. Lastly, although power consumption did not cause feasibility issues, it can be optimized to minimize the size of the battery. A smaller battery can enhance comfort and reduce safety issues. Power consumption can be reduced by optimizing the software and reducing power dissipation through the wiring.

Table 8.2. Results of the user experience tests. Positive feedback is indicated with a (+) and negative feedback with a (-).

Subject	Size waist (cm)	Size inseam (cm)	Comfort (5-point Likert scale)	Freedom of movement (5-point Likert scale)	Qualitative feedback
1	79	86	4	5	+ Can be worn underneath football shorts - Garment feels very tight
2	76	81	3	2	+ Garment is tight - Not suitable for sliding's
3	76	81	4	5	+ Very stretchable - Sensors seem fragile
4	79	81	3	4	+ Not too tight - Probably not suitable in summer
5	76	81	5	5	+ The same as ordinary tights - Feels hot during exercise
Mean (SD)	78 (2)	82 (2)	4 (1)	4 (1)	

8.3. Conclusions

In this study the second prototype of the sensor tights was developed for monitoring lower limb kinematics during every day, on-the-field training situations. Attention was paid to the aspects of unobtrusiveness, ease of use, as well as the accuracy and reliability of the recorded signals. In a human performance lab, hip and knee joint angles and angular velocities recorded with the tights were compared with the same measurements obtained with an optoelectronic measurement system and good validity was shown. The validation study with the prototype demonstrates that the sensor tights can be used to accurately monitor lower limb kinematics. During the field tests, the tights scored high on ease of use, comfort, and freedom of movement, which allows the sensor garment to be used in field training sessions and matches, and this shows that the tights can be used for long term monitoring studies. Improvements for the next prototype will focus on making a wireless connection to a dashboard for the coach and medical staff. This dashboard should show physical player load parameters.

9

Smart sensor tights 3.0: wireless data transmission

For prototype 2, data were stored at an SD card. However, to visualize data near real-time, wireless data transfer is required. In prototype 3, this extra functionality was added. This chapter describes the development of this prototype including selection of the wireless data protocol and hardware. Furthermore, a first version of a dashboard is presented, that shows the raw data and quality of the connection.

9.1. Wireless communication protocol

99

Several wireless communication techniques can be used to send data wirelessly to a central computer at the side of the football field. The following criteria were formed to identify the best wireless communication technique.

1. *Bit rate:* Each IMU contains an accelerometer and gyroscope that are sampled at 250 Hz and a magnetometer at 100 Hz, the three sensors have 3 DOF and each sample is 16 bits. This means that the total sample rate per player is 133 kbit/s. Having 22 players in the field this would lead to a required bit rate of at least 3.168 Mbit/s.
2. *Coverage:* The wireless network should cover a football field of 120 m x 90 m (the maximum size of a football field according to the International Football Association Board)
3. *Reliability:* Data loss due to bad connection should be minimized to 10 ms for proper functioning of the biomechanical modelling algorithm. All data should still be saved at an SD card for detailed post-analysis.
4. *Energy consumption:* Energy consumption of the transmitter should be optimized, to minimize the size of the battery. The power consumption of the measurement system is 110 mAh. When the required measurement time is 3 hours, at maximum 340 mAh is left for wireless transfer with the current battery (1350 mAh).
5. *Unobtrusiveness:* Antennas and wireless transfer modules should be unobtrusive to wear in clothing.

It was decided to focus on creating a local network, which is stand-alone and works in crowded stadiums as well as in rural areas. Recently, Kos et al. (2019) researched the potential of different wireless communication protocols for connected sensors and wearable devices. By comparing the different standardized wireless technologies (e.g. ZigBee, Bluetooth and IEEE 802.11) on maximum range, transmit power and bit rate, it was found that IEEE 802.11n, IEEE 802.11af or IEEE 802.11ah can be used for our application.

9.2. Hardware selection

An important influence on performance of the wireless network is path loss between transmitter (the tights) and receiver. In high frequency bands (in GHz range) path loss is increased when people are present in the transmission path. This effect is called body shadowing (Januszkiewicz, 2018). The effect of body shadowing mainly depends on the environment, the location of transmitter and receiver and the frequency band. To give an example, Januszkiewicz (2018) measured path loss in an indoor environment. When transmitter operating at 2.4 GHz with a dipole antenna and a receiver were placed one meter from each other and a person was placed in between, path loss increased from 45 dB to 55 dB. In the application of the sensor shorts, data transfer occurs in an outdoor environment over larger distance. In a dynamic football situation, more people may obstruct the transmission path which may increase path loss. To minimize the effect of body shadowing, the switched diversity technique is implemented. A switch diversity system in our case uses two antennas on the transmitter side. Once, the signal strength is below a predetermined threshold, the transceiver will switch to the other antenna (William, 1974). A small Wi-Fi module that supports antenna switching (every 300 ms) is the xPico 240 (Lantronix, USA) and can use the IEEE 802.11n protocol. The module can be easily integrated in the waist pocket, since the dimensions are 22 x 35.5 x 2.73 mm including the edge card (Lantronix, 2021).

Two types of antennas were tested for integration in the sensor tights: a dipole antenna (FXP74.07.0100A, Taoglas, IE) and a patch antenna (W3230, Pulse Electronics, USA) (Figure 9.1). The antennas were placed at the front and back on the sagittal plane at the height of the waistband of the sensor tights on a test person. With an EAP-225 access point (TP-LINK Technologies, CN), radiation patterns were mapped out. Furthermore, a test was performed to measure the received signal strength indication (RSSI) at different distances.

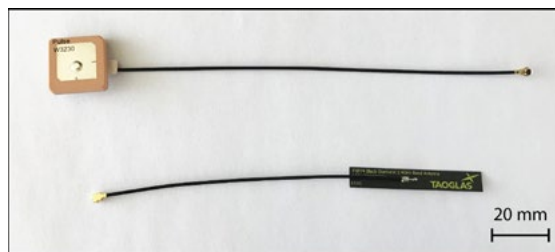


Figure 9.1. The patch antenna (top) and dipole antenna (bottom) that are tested in prototype 3.

For the dipole antenna configuration the gain increases on average 9.3 dB in the back and front of the athlete when using two antennas. For the patch antenna the gain increases 10.3 dB on average in the back and front of the athlete when an extra antenna is used. Figure 9.2.a shows the ideal radiation pattern of the dual configuration of the dipole and patch antenna.

The RSSI was measured at different distances between the transmitter and receiver (0 to 50 m), while the two types of antennas were placed at opposite sides of a bucket of water (to simulate the body) and at opposite sides of a piece of wood. From this test it was concluded that the patch antenna outperforms the dipole antenna with 15 dB (Figure 9.2.b.) and is less prone to interference of conducting materials present on the backside of the antenna (such as our body). Based on these insights, it was concluded to use the patch antenna for prototype 3.

To test the performance of the wireless network in the field, 11 prototypes were created. This time, a short version with three sensors was created. Figure 9.3 shows an overview of the network and two images of this prototype.

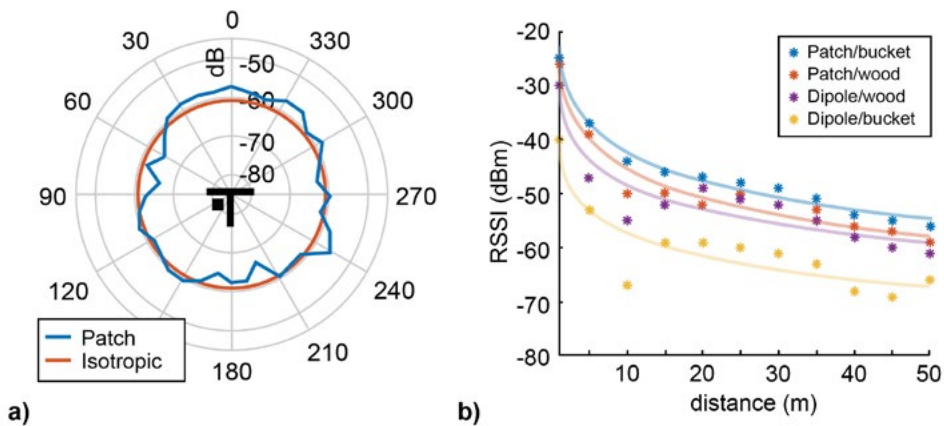


Figure 9.2. a) The ideal radiation pattern of the configuration with two patch antennas. Two separate measurements of the antennas mounted at a waistband at the front and back of a person combined. The “T” represents the person viewed from above, with the front side of the body pointed to 0°. The black square represents the location of the pocket with electronics. b) RSSI at different distances between sender and receiver, for the dipole antenna and patch antenna placed mounted at a bucket of water and at a piece of wood. Data were fitted using the logarithmic function: $y=a+b*\log(x)$.

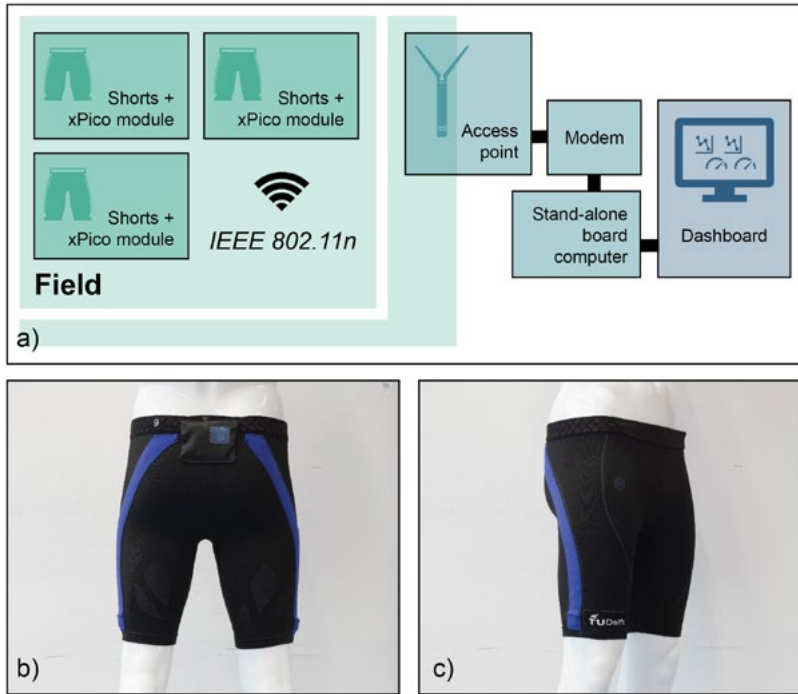


Figure 9.3 a) The wireless network b) Back view of the sensor shorts c) Side view of the sensor shorts.

9.3. Dashboard

As shown in the overview, the data need to be collected by a central computer. As a first prototype, a Raspberry Pi 4B was used to collect the data. The data were shown near real-time on a connected display and they could also be downloaded via a universal serial bus. The shorts can be controlled via a start and stop interface (Figure 9.4, no. 1). For this preliminary version of the dashboard, raw data are displayed using dynamic bar charts (Figure 9.4, no. 2). Furthermore, received signal strength for each pair of shorts can be shown (Figure 9.4, no. 3). In a later stage, more userfriendly visualisations of the data and the new injury risk parameter can be implemented for use by coaches and medical personnel.

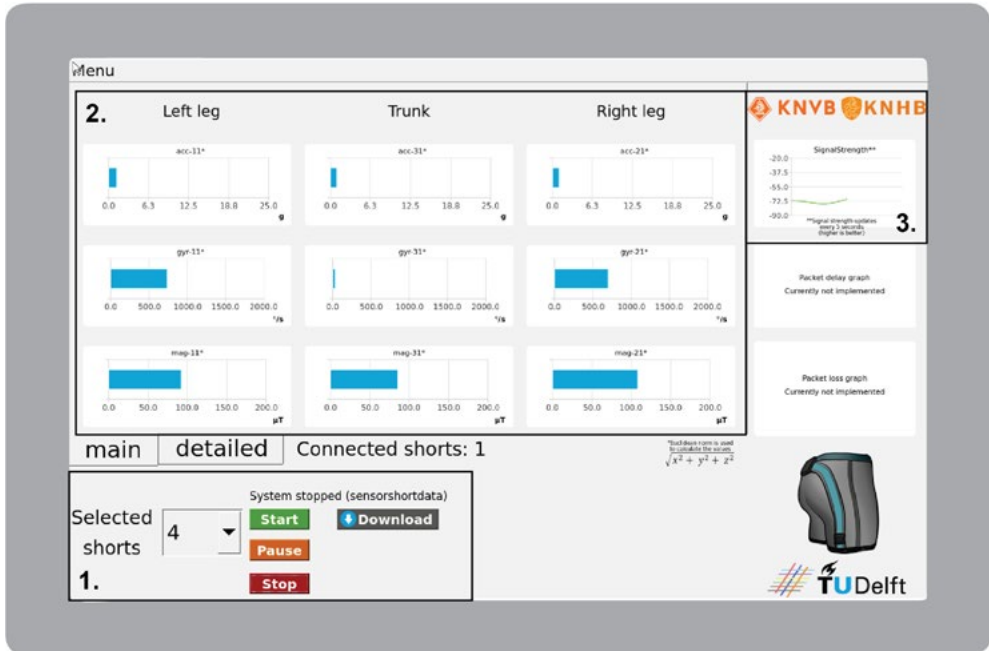


Figure 9.4. A preliminary version of the data dashboard.

9.4. Conclusions

In this chapter, we presented a prototype that can send the movement tracking data wirelessly to the side of the field. It was chosen to set up a local network using a Wi-Fi protocol. A series of prototypes with a Wi-Fi module and two patch antennas was created that can be used for further testing of the reliability of the network and finding the optimal configuration of the base station(s). Furthermore, a preliminary version of a dashboard was created. This dashboard can be used to observe the quality of the connection and to inspect the raw sensor data.

10

Smart sensor tights 4.0: washable integrated sensor modules

In the previous prototypes, commercial miniaturized connectors were used. These connectors introduced practical problems during measurements in the field, because they are not intended for integration in flexible and stretchable systems. Furthermore, the connectors are not intended for frequent connection and disconnection. Therefore, an alternative solution was implemented for the final prototype. It was decided to integrate the sensor modules even more in the clothing and to make the entire sensor string washable. The central unit including the microprocessor and the battery was kept as an independent module that needs to be removed for charging and before washing the tights. The connectors to the sensor modules were removed and solder pads were placed at the sensor PCBs. Elastic conductive wire tapes with stranded polyurethane coated copper wires (Amohr Technische Textilien, DE) were tinned in a solder bath and soldered to the sensor PCBs. An encapsulation material with a thickness of approximately 1 mm was dispensed on top of the PCB to protect all electronic components and connectors against moisture and detergent (Figure 10.1a). On the other side of the sensor string, a connector to the central unit was designed. Designing a completely new connector did not fit the scope of this research project. Therefore, it was decided to use a micro SD card 8 way push/push connector (Würth, DE) for the design, because it has a durability of 10 000 mating cycles. A micro SD card was replicated on a 0.8 mm PCB and solder pads for the wiring were connected (Figure 10.1b).

104

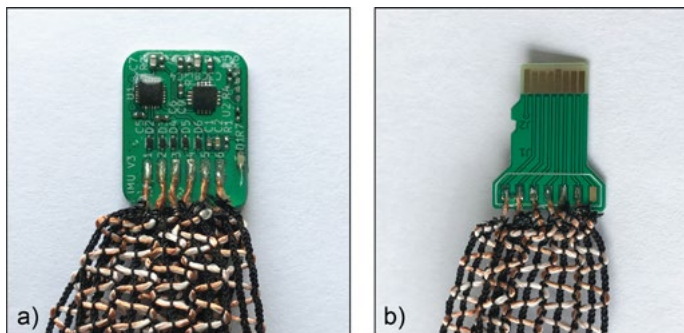


Figure 10.1. a) The sensor module. b) The connector to the central unit.

10.1. Encapsulation tests

In collaboration with Linxens Wijchen (NED), a company specialized in connectors and electronics packaging, 5 potential materials were selected for encapsulating the sensor modules and solder joints of the SD card connectors (Table 10.1). These materials included acrylate based encapsulants, an epoxy encapsulant and a silicone encapsulant.

Table 10.1 Encapsulation materials

Material	Manufacturer	Product code	Young's Modulus (MPa)	Shore A/D Hardness	Viscosity (mPa·s)
Acrylate encapsulant	Delo Industrial Adhesives	Dualbond AD4950	41	75 (A)	26000
Acrylate encapsulant	Delo Industrial Adhesives	Dualbond AD4930	30	80 (A)	14000
Acrylate encapsulant	Henkel	Loctite Eccobond UV 9060F	2200	76 (D)	11000
Epoxy encapsulant	Henkel	Loctite Eccobond EN 3838T	466	27 (D)	6700
Silicone encapsulant	Henkel	Loctite Ablestick ABP 8035	n.k.	n.k.	7880

To test the reliability of these encapsulants in a washing test, a test PCB was designed. This test PCB had the same dimensions as the sensor node PCB (20 mm x 20 mm) with 13 cm conductive wire tape connected. 6 traces were placed on the PCB with three 1 MΩ resistors and a 0 Ω component linking two different traces. The design including the different measurement locations can be seen in Figure 10.2a. Three 0 Ω measurements, to test if the interconnects stay intact, and three MΩ measurements, to test whether moisture affected the electronics, are performed. Each encapsulant was placed on three test PCBs. Reference measurements were performed and the samples were inspected with a microscope prior to the washing test. It was found that all materials adhere well to the wiring, but for the silicone material small air bubbles were found near de wiring. All samples were washed with detergent at 30 °C, 800 rpm and for 45 minutes, 8 times. Resistance measurements were performed after 1 washing cycle, after 3 cycles and after 8 cycles. Lastly, the samples were again inspected with a microscope (S8 APO, Leica, DE).

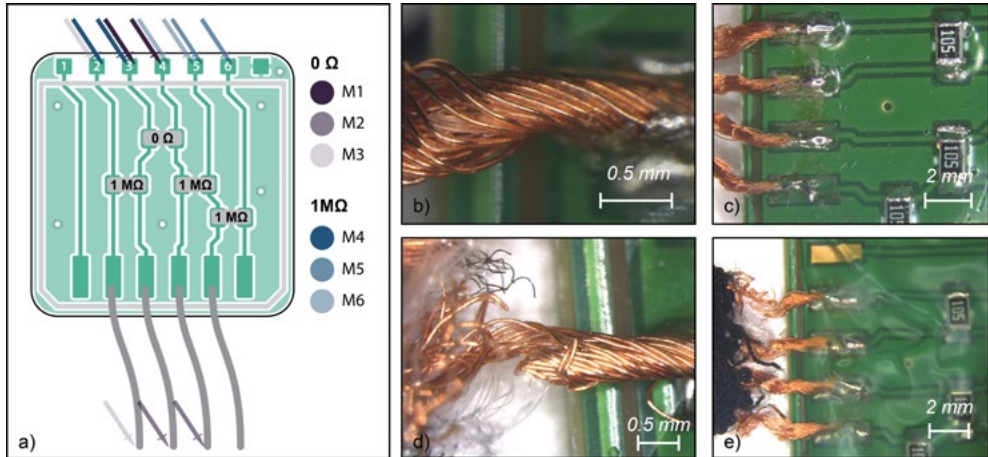


Figure 10.2. a) The test PCB for reliability of the encapsulants after washing. The light grey lines on the PCB indicate the boundaries of the encapsulated part. Three 0 Ω measurements and three 1 MΩ measurements can be performed. b) and c) Microscopic pictures of the wires of the PCBs encapsulated in the acrylate encapsulants AD4950 and AD4930 after 8 washing cycles. d) and e) Microscopic pictures of the wires of the PCBs encapsulated in the acrylate encapsulant 9060f after 8 washing cycles.

From the tests, it was found that all resistance measurements for all samples did not change significantly after the washing tests. Measurements 1 till 3 (Figure 10.2a) were below 1 Ω, so the interconnects stayed intact. Measurements 4 till 6 were all below 0.999 MΩ, which means that moisture did not cause shorts. When inspecting the samples with the microscope, differences were found. For the AD4930 and AD4950 encapsulants, the wires stayed intact (Figure 10.2b and Figure 10.2c) but for the other encapsulants, several strands of the copper wires were broken (Figure 10.2d and Figure 10.2e). The materials have a different viscosity of the uncured material ranging from 26000 mPa·s to 7600 mPa·s. Materials with a low viscosity flow easier through the stranded wire and when the material is very stiff and hard, this may result in wire breakage. The hardness of the cured material varies from Shore 75A to 76D, the Young's modulus from 30MPa to 2200 MPa for the different materials. The materials that showed the best performance (AD4930 and AD4950) have the lowest Young's moduli and hardness. It was decided to use the AD4950 for encapsulation of the sensor modules for the prototypes. At this moment, we just used passive components in the tests. In future studies the reliability of the encapsulated sensor modules can be determined by testing on a larger scale using multiple tests to simulate different conditions. For example, by performing a salt spray test (International Organization for Standardization, 2017) to research resistance to sweating and rain, mechanical tests and temperature/humidity cycling.

Once, the right encapsulant was identified. Prototype 4 was built. Figure 10.3a shows a sensor string for prototype 4 with encapsulated sensor modules. These strings were integrated in a pair of tights. Figure 10.3b shows that the sensor modules and wiring are barely noticeable. The central unit is still a separate module (Figure 10.3c).



Figure 10.3. a) The sensor module assembly. b) Detail of the sensor tights: the sensor of the right thigh is covered with a blue textile. c) Central unit of prototype 4.

10.2. Future improvements

By creating 4 prototypes during 4 years of research and development, several important iterations were performed. It was proven that the IMUs can be read out at high sample rates (250 Hz) through stretchable interconnects using the SPI. The SPI bus is one of the most widely used buses for communication between sensors and microcontrollers. SPI enables to connect multiple slaves to one master and the hardware is simple. Furthermore, it supports higher clock frequencies than I²C. However, it has no error-checking mechanism by default and is not intended for use over long distances. Although the sensor tights system works well and the design of the electronics is simple, there is a risk that parasitics such as stray capacitances and self-inductance of the wiring will change significantly due to movement or moisture, which can result in bit errors. Figure 10.4 shows an oscilloscope measurement at the end of the clock line near the lower leg sensor. Although, at this moment no errors occur, the self-inductance effect is clearly visible. To make the system more reliable, it can be investigated if it is worth to implement RS-485 communication, which is more suitable for communication over longer distances and includes an error detection mechanism. The downside of implementing RS-485, is that more electronics are required at the sensor module and central unit.

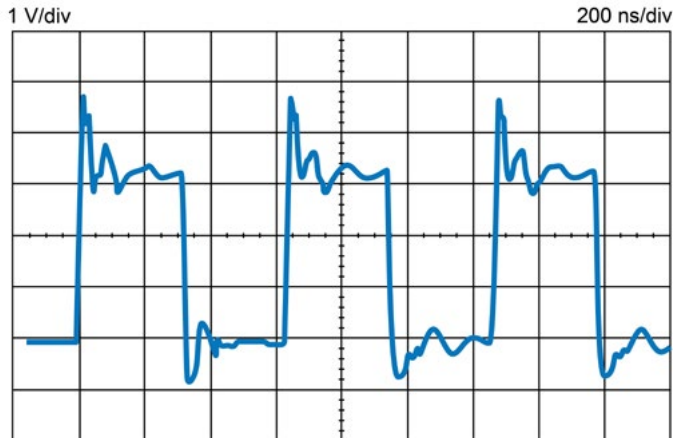


Figure 10.4. Oscilloscope measurement at the clock line near the lower leg sensor.

In a future version, the wireless data transfer system from the tights to a central computer needs to be improved as well. At first, the patch antennas that were used for prototype 3 were not integrated in the textile yet. It needs to be researched, whether these antennas can be embedded in the textile or that a custom antenna needs to be build. Second, research will be performed to test the reliability of the wireless network on the football field when 11 players are wearing the shorts. Based on the insights from these tests, the network can be optimized by for example adjusting the base stations. Furthermore, the wearable system was not yet designed for minimal power consumption. The software and electronics can be optimized to decrease the size of the battery. When the size of the battery is determined, the waist pocket can be redesigned and mounted higher on the back of the athlete to prevent concussion when the athlete falls backwards.

In short, further product development is required for successful implementation of the sensor tights. However, more challenging research steps for successful product introduction, will focus on validating the hypothesized injury risk parameters in larger scale movement science studies. Once, one of these parameters has proven to be a good indicator of hamstring or adductor muscle load, the parameter can be presented at a user-friendly dashboard to coaches and medical personnel, to estimate injury risk real-time during match play and trainings.

Summarizing conclusions for movement tracking

The technology of using IMUs for tracking lower limb movement of football players in the field was successfully demonstrated by designing and validating four prototypes of the smart sensor tights. Each of the four prototypes showed improved functionality. In prototype 2, a real-time operating system was implemented to reach sample rates of 250 Hz for recording high intensity movements. Additionally, larger range sensors (30g, 4000 °/s) sensors were used. A technical validation study with an optoelectronic measurement system was performed. It was proven that the limb orientation data derived from the sensor tights reflect player movement well for various football specific actions.

Prototype 2 used local data storage and prototype 3 included a wireless data transfer module. Data can be send wirelessly to the side of the field with two patch antennas. Furthermore, a first version of a dashboard to control the recordings with the sensor tights was made for prototype 3. With the dashboard, the reliability of the wireless connection can be checked and the data are shown in real-time graphs as well. For prototype 4, washable sensor strings were developed an de connections between the flexible wiring and central processing unit were improved.

Further sub-system development and reliability studies are necessary to make this wearable system ready for market introduction. Compared to conventional off-the-shelf IMUs, the novel sensor tights are easy to use and facilitate measurement on the field, which is required for larger studies to investigate potential hamstring injury risk parameters.

Part III. Movement Tracking in Field Sports



Summarizing conclusions for movement tracking



IV

Discussion & Conclusions

11

General discussion

In the previous chapters, application-specific insights and future work were discussed. In this chapter, we zoom out to discuss the impact of wearable sensor development in general. First, we will reflect on the wearable sensor system design process during this project. Second, the scientific impact of this work with regard to injury prevention is discussed. And lastly, the potential impact of the new wearable sensor systems on the end users and environmental impact are explained.

114

11.1. The design process

In chapter 3, we presented our design approach towards the successful implementation of new wearable sensor systems. To identify relevant problem statements from a physiological perspective that form the starting point of sensor system development, it is of great importance to work closely together with physiologists and movement scientists. In this project, the large multidisciplinary consortium facilitated this. In the consortium, researchers worked on nine applied research lines which focused on a type of sports and the most prevalent injuries. From these projects, specific requests arose, which could form the starting point of sensor system research. For example, the movement scientists in the football and hockey research project wanted to track the movement of the lower limbs of field players accurately, to retrieve information about hamstring muscle load. They requested us to make an easy-to-use garment with movement sensors, that would enable them to track movement on the field. This need from a users' perspective gives the new wearable garment a clear *raison d'être*.

Furthermore, to create wearable sensor systems that work in the desired application environment, it is of pivotal importance to test the systems in a physiological setting in an early development stage. In the sweat sensing research, a simple collection patch was designed first. By testing this patch in a physiological experiment, challenges during physiological measurements and future improvements could be identified. Moreover, sweat composition and sweat rate in this type of experiment could be quantified. This resulted in a well-considered design of the collection surface and reservoirs and experience for future physiological tests. Continuous sweat composition sensors were integrated into the second

version of the patch. This patch was tested in a more complex physiological experiment, where the patch measurements were compared with the ventilated capsule system and offline ion chromatography results. Because experience in physiological tests was gained with previous versions of the patch, it was possible to validate the sweat sensing patch properly using different reference techniques.

As explained in chapter 3, after *in situ* sensor system validation experiments that were performed in this research, large scale physiological trials to identify injury risk factors would be the next step in wearable sensor system development. However, a challenge arises here. To perform large scale physiological studies, highly reliable measurement systems are required. The *in situ* validation studies presented in this thesis required a dedicated engineer to work with the technology. The systems would need more non-scientific development to create a product that can be used by laymen and is very robust and reliable. On the other side, non-scientific innovators would generally only invest in product development of this new wearable technology, when they know that a clear scientifically substantiated application can be identified. For this scientific basis of the application, large scale physiological studies are required, which cannot be performed when the product is not in a mature stage of development. To solve this issue, product development and production partners need to be convinced to invest in a small series of products with scientists as the first target group, so that they can perform large scale physiological trials to find this evidence.

Lastly, in wearable sensor system development, an important pitfall can be identified from an engineering perspective. Novel wearable sensors are often presented as a smart sensor that can measure a specific health parameter, such as stress or muscle fatigue. In fact, these novel sensors do not measure this abstract parameter but a measurable parameter, e.g. a specific sweat analyte or accelerations of the limbs, that potentially influences this health parameter. Since it is often not scientifically proven that this parameter is an indicator of our health, there is a possibility that a false promise is made. On one side this may lead to resistance among physiologists, movement scientist and medical experts to use these systems in further research to identify new health markers. On the other side, in the case that this research is brought a step further to commercialization with the engineering literature as a basis, the business will eventually fail when this promise cannot be fulfilled. Therefore, we believe that being careful in positioning your novel sensor system, especially in sweat sensor development, will lead to more scientific and societal impact. In many cases, the new sensor systems developed by engineering scientists will initially serve as a tool to identify new indicators for health status. They should be positioned as such, and not as a magical new device that can measure an athlete's health status directly.

11.2. Scientific impact

In the introduction of this thesis, a research aim was identified. This aim was stated as follows: "We want to develop novel wearable sensor systems that acquire physiological information of athletes in action, that can support in making injury-free exercise available for everyone." In this paragraph, we reflect on this aim and on the scientific impact of this

work. From the literature study that was performed at the start of this research, it was found that, although analysing sweat shows great opportunities to unobtrusively monitor the physical status of an athlete, little is known yet about the physiology of sweating and how sweat markers can be used to monitor health status. The new sweat collection patch that was developed, enables reliable collection of sweat during exercise for offline analysis. The information that is retrieved from these sweat measurements can be used to study the physiological mechanisms behind sweating and to identify new sweat biomarkers. Moreover, the collection patch offers a space for integration of newly developed analyte-specific sweat sensor electrodes. In this way, the patch facilitates validation experiments for these new sensor materials, to find evidence that these new sensors can be used in physiological studies to reliably analyse sweat.

For the second part of this work, the development of the smart sensor tights, a clear user need from other researchers formed the starting point of the project. To track movement of the lower limbs of football and hockey players during trainings and match-play, an easy-to-use sensor garment with integrated inertial measurement units for movement tracking of the lower limbs needed to be developed. In the project, four prototypes were developed that proved that reliable movement tracking was possible with the sensor tights. Knowledge was developed about integration of electronics in textile and its main challenges, which is valuable for wearable sensor scientists. Moreover, the tights facilitate larger scale on-field movement science studies to research the relation between movement data, muscle load and the aetiology of injuries.

In short, it can be concluded that the outcomes contribute to the initially defined research aim by providing practical tools to measure new physiological and biomechanical data of athletes in action. This information can be used to identify new injury risk factors, which can eventually be used to prevent injuries. In this research, we focused on wearable sensor system design for athlete monitoring. All subjects that participated in the physiological experiments were healthy individuals. However, wearable sensor system research with healthy subjects opens up opportunities for medical applications as well. In the case of sweat research, the physiological theory about sweating is underdeveloped compared to other body fluids such as blood. Research about sweat composition changes in healthy athletes measured with our new sensor systems can contribute to substantiating and filling the gaps in the theory. This may form a starting point for new medical applications of sweat sensors, where sweat quantities that need to be analysed can be as low as 0.02–0.3 nL/min/gland in rest (Moonen et al., 2020) and miniaturized sensor systems will be required.

11.3. Societal & environmental impact

On the one hand, the deployment of novel wearable sensor systems has societal advantages. Sensor systems such as movement trackers can be used to motivate individuals to become physically active (Girginov et al., 2020; Gualtieri et al., 2016) and they can be used to prevent injuries. This can impact our current healthcare system by reducing the risk of chronic diseases and decreasing the burden on our healthcare system. On the other hand, there

are also potential negative effects. Continuous monitoring systems that are seamlessly integrated into garments can monitor individuals without notice. When the data of these systems are stored online, this can lead to privacy issues. Solid data protection mechanisms need to be in place to maintain the user's ownership. Furthermore, wearable sensor data can also be used for performance monitoring. The athlete as well as coaches and trainers will have continuous insight into your performance. This can possibly create emotional pressure, which may have the opposite effect. Therefore, this aspect needs to be further investigated, especially during the development of intended user scenarios and designing tailored feedback systems.

The design of tailored feedback systems is a very important aspect of further research. Our new wearable sensor systems in combination with established sensing technology that measure other physiological or biomechanical parameters provide a lot of information about an athletes' physical condition. How can we translate this large amount of data into valuable metrics for the user? And can we give tailored training advice based on these metrics? Only if well-considered feedback mechanisms are in place, the sensor systems can contribute to injury prevention in recreational and elite sports.

Finally, when the sensor systems will be implemented in recreational sports, the products will be produced in large quantities which increases environmental impact. Therefore, more attention needs to be paid to sustainable design. For the sensor tights, it is important to focus on design for disassembly so that materials can be recycled. In the current product, wiring can be removed and recycled. However, the sensor nodes are encapsulated to improve washability and robustness, which complicates recycling. On the other hand, effort has been paid to the miniaturization of the sensor modules to minimize raw material consumption. However, energy consumption still needs to be optimized to minimize the battery size. This is not only more sustainable but also facilitates better integration of the electronics for more comfortable tights. For the sweat sensing concepts, more sustainable solutions need to be considered as well. At this moment the readout electronics and a power supply can be reduced, but the sensor patches are disposables. It would be interesting to research if it is possible to create a patch that is made from biodegradable elastomer films such as poly(glycerol sebacate) (Wang, 2002) and biocompatible metals (Mg, Fe) when measuring sweat that has high salinity for example. Furthermore, the sweat sensors do not consume a lot of power, so a promising research direction would be to study if we can use energy harvesting from sports activities for these sensor patches to reduce environmental impact.

12

Conclusions & outlook

In this project, we developed a vast number of wearable sensor systems to monitor athletes unobtrusively. In this chapter, we summarize the main conclusions of this research and identify opportunities for further research. First, the main insights of the sweat sensing research are addressed and second, the conclusions and outlook with respect to the movement tracking research are presented.

118 *12.1. Sweat sensing during exercise*

The aim of the sweat sensing research was to create sensor systems that can reliably measure sweat composition and sweat rate during exercise, to identify parameters that give an indication of an athletes' physical status. Different electrolytes were selected to be analysed continuously. $[\text{Na}^+]$ and $[\text{Cl}^-]$ were chosen because they can potentially be used to indicate sweat rate and dehydration during exercise (Gao et al., 2017; Rose et al., 2015). Furthermore, $[\text{NH}_4^+]$ in sweat are a potentially interesting marker, since it is hypothesized that increased NH_4^+ levels may indicate muscle fatigue (Alvear-Ordenes et al., 2005; Guinovart et al., 2013).

In recent technological literature, a large number of technically validated electrochemical sweat patches that measure electrolyte concentrations is presented (Bariya et al., 2018; Mohan et al., 2020). However, due to the absence of methods for validation using reference measurements in a physiological setting, applications are limited. Therefore, a new sweat collection system was designed that can be used to chronologically sample sweat during exercise for offline analysis. Benchtop experiments showed that the new collector enables to chronologically sample sweat in a sequence of reservoirs and that the inflow of sweat is not significantly inhibited by the channel resistance. The new collectors were tested in a physiological setting as well. $[\text{Na}^+]$ and $[\text{Cl}^-]$ of the samples were analysed offline using ion chromatography and the results from three locations at the back of an athlete showed similar trends.

In the next phase, a more advanced design of the patch was made to measure ionic content continuously. The new patch included an extra analysis chamber with a sensor that measures sweat conductivity continuously. Furthermore, filling rate electrodes were integrated in the

patch. Physiological experiments were performed to compare the conductivity and filling rate measurements with sweat rate data from a ventilated capsule system and offline ion chromatography measurements. The continuous sweat conductivity data showed a good correlation with Na^+ and Cl^- concentrations from offline analysis for all six participants ($R^2=0.97$). This means that continuous conductivity measurements can be used to derive $[\text{Na}^+]$ and $[\text{Cl}^-]$. Although it needs to be researched if this correlation between $[\text{Na}^+]$ and $[\text{Cl}^-]$ and conductivity also applies to different physiological conditions (in different dietary conditions or exercise protocols), the results are promising and it would be interesting to research in larger physiological experiments if these conductivity measurements give an indication of hydration status. Additionally, results from the physiological tests showed that sweat rate measurements with the reference ventilated capsule system were significantly correlated with conductivity measurements at the different sweat collection locations (mean $R^2= 0.87$). Lastly, the sensor patch included a filling rate sensor that measured the inflow of sweat. It was researched whether these measurements correlated with ventilated capsule sweat rate measurements. It was shown that the filling rate measurements can be used to derive an average sweat rate. Continuous measurement was not possible, because of droplet formation inside the channels. Future research should focus on the development of sensors for accurate continuous sweat rate monitoring. Reliable sweat rate sensors are of pivotal importance in continuous measurement of sweat content, because sweat composition changes with sweat rate (Baker, 2019).

The results of the physiological experiments proved that with this patch you can use the same sweat for analysing real-time during exercise and analysing offline for sensor validation experiments. This is a crucial step in the validation process of novel sweat sensors, because sweat composition and sweat rate inter- and intraindividual variability is very large, which makes it very challenging to compare measurements of different sweat sensing methods using separate sweat samples.

Above, we presented a patch that can monitor total ionic content. To learn more about the mechanisms behind sweating and for the identification of new biomarkers, it would be of interest to measure specific analyte concentrations as well. Initial steps have been made to develop analyte-specific sweat sensors. A proof of concept of a potentiometric sensor system and a ventilated capsule that measures NH_3 were created. The potentiometric sensor system measures $[\text{Na}^+]$ and $[\text{Cl}^-]$ with ion-selective electrodes. The NH_3 measurement system consists of a skin capsule with a gas sensor that measures NH_3 that is evaporated from sweat. Future research should focus on further sensor system characterization and physiological validation. Once these sensors are validated in a physiological setting using reference measurements, collaborative research projects with physiologists need to be initiated. In these studies, large scale physiological studies should be performed to research the physiological mechanisms of sweating and to identify new sweat biomarkers that can be used to monitor an athlete's health status.

A glimpse into commercial use

The work presented in this thesis focuses on measurement techniques for research purposes, because little is known yet about using sweat to monitor a person's health status. However, when looking to the future, several possible applications can be identified. The conductivity sensor patch, uses a relatively simple technique to derive total ionic content in sweat. This measurement can possibly be used to measure hydration status or electrolyte imbalance, which would especially be beneficial for endurance athletes such as marathon runners, cyclists and triathletes. The technology that is used is relatively simple and can be miniaturized for day-to-day use.

12.2. Movement tracking in field sports

The aim of this part of the research was to create smart sensor tights with integrated inertial measurement units that can track the movement of the lower limbs accurately. The system should be unobtrusive and suitable for use on the field. An iterative design approach was followed to accomplish this. Four prototypes, each with improved functionality, were developed. The first prototype served as a proof of concept to identify the main challenges in designing a reliable movement tracking system. Five common inertial measurement units (IMUs) were integrated in tights and read out by a single microcontroller. The main improvements that were identified were; enabling higher sample rates and a larger measurement range to track high-intensity movements accurately, and integrating larger range sensors that are well integrated into the tights to minimize soft tissue artefacts.

In prototype 2, these improvements were implemented. Sample rates increased to 250 Hz and larger range sensors (4000 °/s, 32 g) were used. The sensor tights were concurrently validated with an optoelectronic measurement system. IMU data were converted to orientation data and subsequently compared with the kinematic data from the optoelectronic measurement system. The systems showed good concurrent validity (CMCs >0.8) for different football-specific movements. Furthermore, from the results of field tests, it was found that users experienced the tights as comfortable to wear and they did not feel restricted in their movements.

The sensor tights will be used during trainings and matches on the football field. A wireless connection would enable near real-time visualization of the data so that a trainer or medical staff can use the data during play. A third prototype was made which enabled wireless data transfer to a central computer and user dashboard. It was found that the quality of the wireless connection is significantly decreased when a person is present in the transmission path. Therefore it was chosen to integrate two antennas in the tights and use antenna switching when the signal strength is below a threshold.

For the final prototype, we focused on seamlessly integrating washable sensor modules in the tights. The sensor modules were encapsulated in an acrylate material to make them resistant to water and detergent. In this part of the research, we reached an advanced stage in product development (technology readiness level 6 (Mankins, 1995)). Further development is required for creating a wireless network that can transfer the data of two football teams

in one football field reliably. In field experiments, multiple tights will be equipped with a wireless module that sends the data to a central computer. The effects of body shadowing, antenna configurations and the location of the base stations will be quantified. Moreover, the user interface needs to be improved. Once these product improvements are made, a small series of for example 50 tights could be made in collaboration with a production partner. These tights can be used in longitudinal movement science studies. When participants can be equipped with a pair of these user-friendly tights, they can record movement data themselves during trainings and matches over time. These large datasets are required to research the aetiology of muscle injuries and to identify a load parameter that estimates injury risk. This load parameter will be shown on a dashboard that is used by coaches and medical staff, so that they can anticipate when the risk for injuries is high.

In short, two types of wearable sensor systems were developed in this research. First, we presented a patch that enables reliable sweat collection and continuous measurement of sweat composition during exercise. And second, we presented a smart sensor garment for movement tracking of the lower limbs in football and hockey. Results from physiological validation experiments proved that both systems acquire new information of an athlete in action, to learn more about an athlete's physical status during exercise.

.....

Bibliography

- 3M. (2013). Technical Information Sheet Product Number #1522 3MTM Double Coated Medical Tape Retrieved from <https://multimedia.3m.com/mws/media/7920490/3m-1522-dc-polyethylene-tape-tis-jul13.pdf>
- Ahmad, N., Ghazilla, R. A. R., Khairi, N. M., & Kasi, V. (2013). Reviews on various inertial measurement unit (IMU) sensor applications. *International Journal of Signal Processing Systems*, 1(2), 256-262.
- Ahsmann, L.L., Steijlen, A.S.M., Wilmes, E., Jansen, K.M.B., Huysmans, T., (2019) Location optimisation for IMUs in the design of motion tracking soccer tights based on comfort and Soft Tissue Artefact analysis
- Alam, F., Jalal, A. H., Forouzanfar, S., Karabiyik, M., Baboukani, A. R., & Pala, N. (2020). Flexible and Linker-Free Enzymatic Sensors Based on Zinc Oxide Nanoflakes for Noninvasive L-Lactate Sensing in Sweat. *IEEE Sensors Journal*, 20(10), 5102-5109. doi:10.1109/JSEN.2020.2968278
- Al-Amri, M., Nicholas, K., Button, K., Sparkes, V., Sheeran, L., & Davies, J. L. (2018). Inertial Measurement Units for Clinical Movement Analysis: Reliability and Concurrent Validity. *Sensors (Basel)*, 18(3). doi:10.3390/s18030719
- Alvear-Ordenes, I., Garcia-Lopez, D., De Paz, J. A., & Gonzalez-Gallego, J. (2005). Sweat lactate, ammonia, and urea in rugby players. *Int J Sports Med*, 26(8), 632-637. doi:10.1055/s-2004-830380
- Anastasova, S., Crewther, B., Bembnowicz, P., Curto, V., Ip, H. M. D., Rosa, B., & Yang, G.-Z. (2017). A wearable multisensing patch for continuous sweat monitoring. *Biosensors and Bioelectronics*, 93, 139-145. doi:10.1016/j.bios.2016.09.038
- Anwary, A. R., Yu, H., & Vassallo, M. (2018). Optimal Foot Location for Placing Wearable IMU Sensors and Automatic Feature Extraction for Gait Analysis. *IEEE Sensors Journal*, 18(6), 2555-2567. doi:10.1109/JSEN.2017.2786587
- Appenzeller, B. M., Schummer, C., Rodrigues, S. B., & Wennig, R. (2007). Determination of the volume of sweat accumulated in a sweat-patch using sodium and potassium as internal reference. *Journal of Chromatography B*, 852(1-2), 333-337.
- Arnason, A., Sigurdsson, S. B., Gudmundsson, A., Holme, I., Engebretsen, L., & Bahr, R. (2004). Risk Factors for Injuries in Football. *The American Journal of Sports Medicine*, 32(1_suppl), 5-16. doi:10.1177/0363546503258912
- Arpinar-Avsar, P., & Soylu, A. R. (2010). Consistency in acceleration patterns of football players with different skill levels. *Journal of Sports Science & Medicine*, 9(3), 382-387.
- Astrand, P. O., & Rodahl, K. (1970). *Textbook of work physiology*. New York: McGraw-Hill.
- Atanasovska, T., Petersen, A. C., Rouffet, D. M., Billaut, F., Ng, I., & McKenna, M. J. (2014). Plasma K⁺ dynamics and implications during and following intense rowing exercise. *Journal of Applied Physiology*, 117(1), 60-68. doi:10.1152/jappphysiol.01027.2013
- Baggish, A. L., & Wood, M. J. (2011). Athlete's Heart and Cardiovascular Care of the Athlete. *Circulation*, 123(23), 2723-2735. doi:10.1161/CIRCULATIONAHA.110.981571
- Baker, L. B. (2017). Sweating Rate and Sweat Sodium Concentration in Athletes: A Review of Methodology and Intra/Interindividual Variability. *Sports Medicine*, 47(1), 111-128. doi:10.1007/s40279-017-0691-5
- Baker, L. B. (2019). Physiology of sweat gland function: The roles of sweating and sweat composition in human health. *Temperature*, 6(3), 211-259. doi:10.1080/23328940.2019.1632145
- Baker, L. B., & Wolfe, A. S. (2020). Physiological mechanisms determining eccrine sweat composition. *European Journal of Applied Physiology*, 120, 719-752. doi:10.1007/s00421-020-04323-7

- Baker, L. B., Stofan, J.R., Hamilton, A. A., Horswill, C. A. (2009). Comparison of regional patch collection vs. whole body washdown for measuring sweat sodium and potassium loss during exercise. *J Appl Physiol* (1985), 107, 887-895. doi: 10.1152/jappphysiol.00197.2009
- Bakker, T. (2019). Real-time monitoring of sweat of Cystic Fibrosis patients. Retrieved from <https://repository.tudelft.nl/islandora/object/uuid:c483a44c-5414-441b-9cb2-599ceac2373c>
- Bandodkar, A. J., Molinnus, D., Mirza, O., Guinovart, T., Windmiller, J. R., Valdés-Ramírez, G., . . . Wang, J. (2014). Epidermal tattoo potentiometric sodium sensors with wireless signal transduction for continuous non-invasive sweat monitoring. *Biosensors and Bioelectronics*, 54, 603-609. doi:10.1016/j.bios.2013.11.039
- Bariya, M., Nyein, H. Y. Y., & Javey, A. (2018). Wearable sweat sensors. *Nature Electronics*, 1(3), 160-171. doi:10.1038/s41928-018-0043-y
- Barnes, C., Archer, D. T., Hogg, B., Bush, M., & Bradley, P. S. (2014). The Evolution of Physical and Technical Performance Parameters in the English Premier League. *Int J Sports Med*, 35(13), 1095-1100. doi:10.1055/s-0034-1375695
- Barré, A., Jolles, B. M., Theumann, N., & Aminian, K. (2015). Soft tissue artifact distribution on lower limbs during treadmill gait: Influence of skin markers' location on cluster design. *J Biomech*, 48(10), 1965-1971. doi:10.1016/j.jbiomech.2015.04.007
- Barrett, S., Midgley, A., & Lovell, R. (2014). PlayerLoad™: Reliability, Convergent Validity, and Influence of Unit Position during Treadmill Running. 9(6), 945. doi:10.1123/ijssp.2013-0418
- Berthier, J. (2013). Chapter 2 - Theory of Wetting**This chapter was written with the collaboration of Kenneth A. Brakke (Mathematics Department, Susquehanna University, Selinsgrove, PA). In J. Berthier (Ed.), *Micro-Drops and Digital Microfluidics (Second Edition)* (pp. 7-73): William Andrew Publishing.
- Bhagavan, N. V., & Ha, C.-E. (2011). Contractile Systems. In *Essentials of Medical Biochemistry* (pp. 241-259).
- Bull, F. C., Al-Ansari, S. S., Biddle, S., Borodulin, K., Buman, M. P., Cardon, G., . . . Willumsen, J. F. (2020). World Health Organization 2020 guidelines on physical activity and sedentary behaviour. *British Journal of Sports Medicine*, 54(24), 1451-1462. doi:10.1136/bjsports-2020-102955
- Buono, M. J., Claros, R., Deboer, T., & Wong, J. (2008). Na⁺ secretion rate increases proportionally more than the Na⁺ reabsorption rate with increases in sweat rate. *J Appl Physiol* (1985), 105(4), 1044-1048. doi:10.1152/jappphysiol.90503.2008
- Burton, D. A., Stokes, K., & Hall, G. M. (2004). Physiological effects of exercise. *Continuing Education in Anaesthesia Critical Care & Pain*, 4(6), 185-188. doi:10.1093/bjaceaccp/mkh050
- Chang, R., & Thoman, J. W., Jr. 7.1.1.3 Conductance (C). In *Physical Chemistry for the Chemical Sciences* (pp. 261-269): University Science Books.
- Chen, Y.-P., Lin, C.-Y., Tsai, M., Jr., Chuang, T.-Y., & Lee, O. K.-S. (2020). Wearable Motion Sensor Device to Facilitate Rehabilitation in Patients With Shoulder Adhesive Capsulitis: Pilot Study to Assess Feasibility. *J Med Internet Res*, 22(7), e17032. doi:10.2196/17032
- Cheuvront, S. N., Kenefick, R. W., Charkoudian, N., & Sawka, M. N. (2013). Physiologic basis for understanding quantitative dehydration assessment. *The American Journal of Clinical Nutrition*, 97(3), 455-462. doi:10.3945/ajcn.112.044172
- Chiasson, D., Xu, J., & Shull, P. (2020). Lossless Compression of Human Movement IMU Signals. *Sensors*, 20(20), 5926. Retrieved from <https://www.mdpi.com/1424-8220/20/20/5926>
- Chlif, M., Keochkerian, D., Temfemo, A., Choquet, D., & Ahmaidi, S. (2018). Relationship Between Electromyogram Spectrum Parameters and the Tension-Time Index During Incremental Exercise in Trained Subjects. *Journal of Sports Science & Medicine*, 17(3), 509-514. Retrieved from <http://www.ncbi.nlm.nih.gov/pmc/articles/PMC6090392/>

Bibliography

- Choi, D.-H., Li, Y., Cutting, G. R., & Searson, P. C. (2017). A wearable potentiometric sensor with integrated salt bridge for sweat chloride measurement. *Sensors and Actuators B: Chemical*, 250, 673-678. doi:10.1016/j.snb.2017.04.129
- Comsol Inc. (n.d.). Capillary Filling - Level Set Method. Retrieved from <https://www.comsol.com/model/capillary-filling-8212-phase-field-method-1878>
- Cross, R. (1999). Standing, walking, running, and jumping on a force plate. *American Journal of Physics*, 67(4), 304-309. doi:10.1119/1.19253
- Cuesta-Vargas, A. I., Galán-Mercant, A., & Williams, J. M. (2010). The use of inertial sensors system for human motion analysis. *Physical Therapy Reviews*, 15(6), 462-473. doi:10.1179/1743288X11Y.0000000006
- Cuperman, R., Jansen, K. M. B., & Ciszewski, M. G. (2022). An End-to-End Deep Learning Pipeline for Football Activity Recognition Based on Wearable Acceleration Sensors. *Sensors*, 22(4), 1347. Retrieved from <https://www.mdpi.com/1424-8220/22/4/1347>
- Datson, N., Drust, B., Weston, M., Jarman, I. H., Lisboa, P. J., & Gregson, W. (2017). Match Physical Performance of Elite Female Soccer Players During International Competition. *The Journal of Strength & Conditioning Research*, 31(9), 2379-2387. doi:10.1519/jsc.0000000000001575
- de Mulatier, S., Nasreldin, M., Delattre, R., Ramuz, M., & Djenizian, T. (2018). Electronic Circuits Integration in Textiles for Data Processing in Wearable Technologies. *Advanced Materials Technologies*, 3(10), 1700320. doi:10.1002/admt.201700320
- del Río García, L. (2021). Ionic sweat analysis for health monitoring in real-time exercise. Retrieved from <https://repository.tudelft.nl/islandora/object/uuid:96578f1d-d7de-42db-a89f-7a7a1258989b>
- Dell'Era, C., & Landoni, P. (2014). Living Lab: A Methodology between User-Centred Design and Participatory Design. *Creativity and Innovation Management*, 23(2), 137-154. doi:10.1111/caim.12061
- Derbyshire, P. J., Barr, H., Davis, F., & Higson, S. P. J. (2012). Lactate in human sweat: a critical review of research to the present day. *The Journal of Physiological Sciences*, 62(6), 429-440. doi:10.1007/s12576-012-0213-z
- Dey, A. (2018). Semiconductor metal oxide gas sensors: A review. *Materials Science and Engineering: B*, 229, 206-217. doi:10.1016/j.mseb.2017.12.036
- Di Paolo, S., Zaffagnini, S., Pizza, N., Grassi, A., & Bragonzoni, L. (2021). Poor Motor Coordination Elicits Altered Lower Limb Biomechanics in Young Football (Soccer) Players: Implications for Injury Prevention through Wearable Sensors. *Sensors*, 21(13), 4371. Retrieved from <https://www.mdpi.com/1424-8220/21/13/4371>
- Dinmohamed, A. G., Visser, O., Verhoeven, R. H. A., Louwman, M. W. J., van Nederveen, F. H., Willems, S. M., . . . Siesling, S. (2020). Fewer cancer diagnoses during the COVID-19 epidemic in the Netherlands. *The Lancet Oncology*, 21(6), 750-751. doi:10.1016/S1470-2045(20)30265-5
- Dobson, R. L., & Sato, K. (1972). The Secretion of Salt and Water by the Eccrine Sweat Gland. *Archives of Dermatology*, 105(3), 366-370. doi:10.1001/archderm.1972.01620060008002
- Doorn, J., Storteboom, T., Mulder, A., de Jong, W., Rottier, B., & Kema, I. (2015). Ion chromatography for the precise analysis of chloride and sodium in sweat for the diagnosis of cystic fibrosis. *Ann Clin Biochem*, 52(4), 421-427. doi:10.1177/0004563214549642
- Dun, S., Fleisig, G. S., Loftice, J., Kingsley, D., & Andrews, J. R. (2007). The relationship between age and baseball pitching kinematics in professional baseball pitchers. *Journal of Biomechanics*, 40(2), 265-270. doi:10.1016/j.jbiomech.2006.01.008
- Dunn, M., Hart, J., & James, D. (2018). Wearing electronic performance and tracking system devices in association football: Potential injury scenarios and associated impact energies. Paper presented at the Multidisciplinary Digital Publishing Institute Proceedings.

- Ekstrand, J., Hägglund, M., & Waldén, M. (2011). Epidemiology of Muscle Injuries in Professional Football (Soccer). *The American Journal of Sports Medicine*, 39(6), 1226-1232. doi:10.1177/0363546510395879
- Ekstrand, J., Waldén, M., Ueblacker, P., Karlsson, J., Hölmich, P., Hänsel, L., & Müller-Wohlfahrt, H. W. (2017). *Encyclopedia of Football Medicine: Injury diagnosis and treatment / Jan Ekstrand, Markus Waldén, Peter Ueblacker, Jón Karlsson, Per Hölmich, Lutz Hänsel, Hans-Wilhelm Müller-Wohlfahrt. Volume 2: Thieme.*
- Fédération Internationale de Football Association. (2007). FIFA Big Count 2006: 270 million people active in football. Retrieved from https://www.fifa.com/mm/document/fifafacts/bcoffsurv/emaga_9384_10704.pdf
- Freckleton, G., & Pizzari, T. (2013). Risk factors for hamstring muscle strain injury in sport: a systematic review and meta-analysis. *British Journal of Sports Medicine*, 47(6), 351-358. doi:10.1136/bjsports-2011-090664
- Gaidhani, A., Moon, K. S., Ozturk, Y., Lee, S. Q., & Youm, W. (2017). Extraction and analysis of respiratory motion using wearable inertial sensor system during trunk motion. *Sensors*, 17(12), 2932.
- Gao, W., Brooks, G. A., & Klonoff, D. C. (2017). Wearable physiological systems and technologies for metabolic monitoring. *Journal of Applied Physiology*, 124(3), 548-556. doi:10.1152/jappphysiol.00407.2017
- Gao, W., Emaminejad, S., Nyein, H. Y. Y., Challa, S., Chen, K., Peck, A., . . . Javey, A. (2016). Fully integrated wearable sensor arrays for multiplexed in situ perspiration analysis. *Nature*, 529, 509. doi:10.1038/nature16521
- Ghaffari, R., Yang, D. S., Kim, J., Mansour, A., Wright, J. A., Model, J. B., . . . Ray, T. R. (2021). State of Sweat: Emerging Wearable Systems for Real-Time, Noninvasive Sweat Sensing and Analytics. *ACS Sensors*, 6(8), 2787-2801. doi:10.1021/acssensors.1c01133
- Geriginov, V., Moore, P., Olsen, N., Godfrey, T., & Cooke, F. (2020). Wearable technology-stimulated social interaction for promoting physical activity: A systematic review. *Cogent Social Sciences*, 6(1), 1742517. doi:10.1080/23311886.2020.1742517
- Gonzalez, M., Axisa, F., Bulcke, M. V., Brosteaux, D., Vandeveld, B., & Vanfleteren, J. (2007, 16-18 April 2007). Design of Metal Interconnects for Stretchable Electronic Circuits using Finite Element Analysis. Paper presented at the 2007 International Conference on Thermal, Mechanical and Multi-Physics Simulation Experiments in Microelectronics and Micro-Systems. EuroSime 2007.
- Grassi, B., Quaresima, V., Marconi, C., Ferrari, M., & Cerretelli, P. (1999). Blood lactate accumulation and muscle deoxygenation during incremental exercise. *Journal of Applied Physiology*, 87(1), 348-355. doi:10.1152/jappl.1999.87.1.348
- Gualtieri, L., Rosenbluth, S., & Phillips, J. (2016). Can a free wearable activity tracker change behavior? The impact of trackers on adults in a physician-led wellness group. *JMIR research protocols*, 5(4), e237.
- Guan, F., Peng, L., Perneel, L., & Timmerman, M. (2016). Open source FreeRTOS as a case study in real-time operating system evolution. *Journal of Systems and Software*, 118, 19-35. doi:https://doi.org/10.1016/j.jss.2016.04.063
- Guinovart, T., Bandodkar, A. J., Windmiller, J. R., Andrade, F. J., & Wang, J. (2013). A potentiometric tattoo sensor for monitoring ammonium in sweat. *Analyst*, 138(22), 7031-7038. doi:10.1039/C3AN01672B
- Guthold, R., Stevens, G. A., Riley, L. M., & Bull, F. C. (2018). Worldwide trends in insufficient physical activity from 2001 to 2016: a pooled analysis of 358 population-based surveys with 1.9 million participants. *The Lancet Global Health*, 6(10), e1077-e1086. doi:10.1016/S2214-109X(18)30357-7
- Halson, S. L. (2014). Monitoring Training Load to Understand Fatigue in Athletes. *Sports Medicine (Auckland, N.z.)*, 44(Suppl 2), 139-147. doi:10.1007/s40279-014-0253-z
- Hammond, K. B., Turcios, N. L., & Gibson, L. E. (1994). Clinical evaluation of the macroduct sweat collection system and conductivity analyzer in the diagnosis of cystic fibrosis. *The Journal of Pediatrics*, 124(2), 255-260. doi:10.1016/S0022-3476(94)70314-0

Bibliography

- Harvey, C. J., LeBouf, R. F., & Stefaniak, A. B. (2010). Formulation and stability of a novel artificial human sweat under conditions of storage and use. *Toxicology in Vitro*, 24(6), 1790-1796. doi:10.1016/j.tiv.2010.06.016
- Heikenfeld, J. (2016). Non-invasive Analyte Access and Sensing through Eccrine Sweat: Challenges and Outlook circa 2016. *Electroanalysis*, 28(6), 1242-1249. doi:10.1002/elan.201600018
- Heikenfeld, J., Jajack, A., Rogers, J., Gutruf, P., Tian, L., Pan, T., . . . Kim, J. (2018). Wearable sensors: modalities, challenges, and prospects. *Lab on a Chip*, 18(2), 217-248. doi:10.1039/C7LC00914C
- Hollander, K., Rahlf, A. L., Wilke, J., Edler, C., Steib, S., Junge, A., & Zech, A. (2021). Sex-Specific Differences in Running Injuries: A Systematic Review with Meta-Analysis and Meta-Regression. *Sports Medicine*, 51(5), 1011-1039. doi:10.1007/s40279-020-01412-7
- Holmes, N., Bates, G., Zhao, Y., Sherriff, J., Miller, V. (2016). The Effect of Exercise Intensity on Sweat Rate and Sweat Sodium and Potassium Losses in Trained Endurance Athletes. *Ann Sports Med Res* 3(2): 1063.[1, 2], 3(2), 1063.
- Hong, Y., & Bartlett, R. (2008). *Routledge Handbook of Biomechanics and Human Movement Science*. London, UNITED KINGDOM: Routledge.
- Hu, B., Ding, T., Peng, Y., Liu, L., & Wen, X. (2020). Flexible and attachable inertial measurement unit (IMU)-based motion capture instrumentation for the characterization of hand kinematics: A pilot study. *Instrumentation Science & Technology*, 1-21. doi:10.1080/10739149.2020.1789657
- Hussain, J. N., Mantri, N., & Cohen, M. M. (2017). Working Up a Good Sweat - The Challenges of Standardising Sweat Collection for Metabolomics Analysis. *The Clinical biochemist. Reviews*, 38(1), 13-34.
- International Organization for Standardization. (2017). Corrosion tests in artificial atmospheres - Salt spray tests (ISO 9227). In (Vol. ISO 9227).
- Januszkiewicz, Ł. (2018). Analysis of Human Body Shadowing Effect on Wireless Sensor Networks Operating in the 2.4 GHz Band. *Sensors*, 18(10), 3412. Retrieved from <https://www.mdpi.com/1424-8220/18/10/3412>
- Johnson, A. T. (2007). *Biomechanics and Exercise Physiology: Quantitative Modeling*. Boca Raton: CRC Press.
- Jones, A. M., Grassi, B., Christensen, P. M., Krstrup, P., Bangsbo, J., & Poole, D. C. (2011). Slow component of VO₂ kinetics: mechanistic bases and practical applications. *Medicine and science in sports and exercise*, 43(11), 2046-2062. doi:10.1249/MSS.0b013e31821f1fc1
- Katchman, B. A., Zhu, M., Blain Christen, J., & Anderson, K. S. (2018). Eccrine Sweat as a Biofluid for Profiling Immune Biomarkers. *PROTEOMICS – Clinical Applications*, 12(6), 1800010. doi:10.1002/prca.201800010
- Kaya, T., Liu, G., Ho, J., Yelamarthi, K., Miller, K., Edwards, J., & Stannard, A. (2019). Wearable Sweat Sensors: Background and Current Trends. *Electroanalysis*, 31(3), 411-421. doi:10.1002/elan.201800677
- Kelly, D. M., Gregson, W., Reilly, T., & Drust, B. (2013). The Development of a Soccer-Specific Training Drill for Elite-Level Players. *The Journal of Strength & Conditioning Research*, 27(4), 938-943. doi:10.1519/JSC.0b013e3182610b7d
- Kinnamon, D., Ghanta, R., Lin, K.-C., Muthukumar, S., & Prasad, S. (2017). Portable biosensor for monitoring cortisol in low-volume perspired human sweat. *Scientific Reports*, 7(1), 13312. doi:10.1038/s41598-017-13684-7
- Kleissen, R. F. M., Buurke, J. H., Harlaar, J., & Zilvold, G. (1998). Electromyography in the biomechanical analysis of human movement and its clinical application. *Gait & Posture*, 8(2), 143-158. doi:10.1016/S0966-6362(98)00025-3
- Klous, L., de Ruyter, C. J., Scherrer, S., Gerrett, N., & Daanen, H. A. M. (2020). The (in)dependency of blood and sweat sodium, chloride, potassium, ammonia, lactate and glucose concentrations during submaximal exercise. *European Journal of Applied Physiology*, 121, 803-816. doi:10.1007/s00421-020-04562-8

- Koh, A., Kang, D., Xue, Y., Lee, S., Pielak, R. M., Kim, J., . . . Rogers, J. A. (2016). A soft, wearable microfluidic device for the capture, storage, and colorimetric sensing of sweat. *Science Translational Medicine*, 8(366), 366ra165. doi:10.1126/scitranslmed.aaf2593
- Kolo, J. G., Shanmugam, S. A., Lim, D. W. G., & Ang, L.-M. (2015). Fast and efficient lossless adaptive compression scheme for wireless sensor networks. *Computers & Electrical Engineering*, 41, 275-287. doi:10.1016/j.compeleceng.2014.06.008
- Komolafe, A., Torah, R., Wei, Y., Nunes-Matos, H., Li, M., Hardy, D., . . . Beeby, S. (2019). Integrating Flexible Filament Circuits for E-Textile Applications. *Advanced Materials Technologies*, 4(7), 1900176. doi:10.1002/admt.201900176
- Kos, A., Milutinović, V., & Umek, A. (2019). Challenges in wireless communication for connected sensors and wearable devices used in sport biofeedback applications. *Future Generation Computer Systems*, 92, 582-592. doi:10.1016/j.future.2018.03.032
- Krivec, M., Gunnigle, G. M., Abram, A., Maier, D., Waldner, R., Gostner, J. M., . . . Leitner, R. (2015). Quantitative Ethylene Measurements with MOx Chemiresistive Sensors at Different Relative Air Humidities. *Sensors*, 15(11), 28088-28098.
- Kurusingal, A., Dhamdhere, A., & Sivaraman, V. (2010, 10-14 Oct. 2010). Modeling signal strength of body-worn devices. Paper presented at the IEEE Local Computer Network Conference.
- La Casse, R. G., & Creasy, W. S. (1999) U.S. patent. 5877254A
- Lantronix. (2021). xPico 200 Series User Guide. Retrieved from <https://docs.lantronix.com/products/xpico-200/ug/4.9/>
- Lee, E. C., Fragala, M. S., Kavouras, S. A., Queen, R. M., Pryor, J. L., & Casa, D. J. (2017). Biomarkers in Sports and Exercise: Tracking Health, Performance, and Recovery in Athletes. *Journal of Strength and Conditioning Research*, 31(10), 2920-2937. doi:10.1519/JSC.0000000000002122
- Lemon, P. W., & Mullin, J. P. (1980). Effect of initial muscle glycogen levels on protein catabolism during exercise. *Journal of Applied Physiology*, 48(4), 624-629. doi:10.1152/jappl.1980.48.4.624
- Li, Q., & Tao, X. (2011). A stretchable knitted interconnect for three-dimensional curvilinear surfaces. *Textile Research Journal*, 81(11), 1171-1182. doi:10.1177/0040517511399965
- Lin, Y., Bariya, M., Nyein, H. Y. Y., Kivimäki, L., Uusitalo, S., Jansson, E., . . . Javey, A. (2019). Porous Enzymatic Membrane for Nanotextured Glucose Sweat Sensors with High Stability toward Reliable Noninvasive Health Monitoring. *Advanced Functional Materials*, 29(33), 1902521. doi:10.1002/adfm.201902521
- Liu, C., Xu, T., Wang, D., & Zhang, X. (2020). The role of sampling in wearable sweat sensors. *Talanta*, 212, 120801. doi:10.1016/j.talanta.2020.120801
- Liu, G., Ho, C., Slappey, N., Zhou, Z., Snelgrove, S. E., Brown, M., . . . Kaya, T. (2016). A wearable conductivity sensor for wireless real-time sweat monitoring. *Sensors and Actuators B: Chemical*, 227, 35-42. doi:10.1016/j.snb.2015.12.034
- Liu, X., Zhang, W., Lin, Z., Meng, Z., Shi, C., Xu, Z., . . . Liu, X. Y. (2021). Coupling of Silk Fibroin Nanofibrils Enzymatic Membrane with Ultra-Thin PtNPs/Graphene Film to Acquire Long and Stable On-Skin Sweat Glucose and Lactate Sensing. *Small Methods*, 5(3), 2000926. doi:10.1002/smt.202000926
- Locher, I., & Tröster, G. (2008). Enabling Technologies for Electrical Circuits on a Woven Monofilament Hybrid Fabric. *Textile Research Journal*, 78(7), 583-594. doi:10.1177/0040517507081314
- López-Valenciano, A., Ruiz-Pérez, I., García-Gómez, A., Vera-García, F. J., De Ste Croix, M., Myer, G. D., & Ayala, F. (2020). Epidemiology of injuries in professional football: a systematic review and meta-analysis. *British Journal of Sports Medicine*, 54(12), 711. doi:10.1136/bjsports-2018-099577
- Luinge, H. J., Veltink, P. H., & Baten, C. T. M. (2007). Ambulatory measurement of arm orientation. *Journal of Biomechanics*, 40(1), 78-85. doi:10.1016/j.jbiomech.2005.11.011

Bibliography

- Ma, B., Chi, J., Xu, C., Ni, Y., Zhao, C., & Liu, H. (2020). Wearable capillary microfluidics for continuous perspiration sensing. *Talanta*, 120786. doi:10.1016/j.talanta.2020.120786
- Madgwick, S. O. H., Harrison, A. J. L., & Vaidyanathan, R. (2011, 29 June-1 July 2011). Estimation of IMU and MARG orientation using a gradient descent algorithm. Paper presented at the 2011 IEEE International Conference on Rehabilitation Robotics.
- Malfait, B., Dingenen, B., Smeets, A., Staes, F., Pataky, T., Robinson, M. A., . . . Verschueren, S. (2016). Knee and hip joint kinematics predict quadriceps and hamstrings neuromuscular activation patterns in drop jump landings. *PLoS ONE*, 11(4), e0153737.
- Mankins, J. C. (1995). Technology readiness levels. White Paper, April, 6(1995), 1995.
- Mazzaracchio, V., Serani, A., Fiore, L., Moscone, D., & Arduini, F. (2021). All-solid state ion-selective carbon black-modified printed electrode for sodium detection in sweat. *Electrochimica Acta*, 394, 139050. doi:10.1016/j.electacta.2021.139050
- McArdle, W. D., Katch, F. I., & Katch, V. L. (2010). *Exercise Physiology: Nutrition, Energy, and Human Performance*: Lippincott Williams & Wilkins.
- Miller, I. F., Becker, A. D., Grenfell, B. T., & Metcalf, C. J. E. (2020). Disease and healthcare burden of COVID-19 in the United States. *Nature Medicine*, 26(8), 1212-1217. doi:10.1038/s41591-020-0952-y
- Mohan, A. M. V., Rajendran, V., Mishra, R. K., & Jayaraman, M. (2020). Recent advances and perspectives in sweat based wearable electrochemical sensors. *TrAC Trends in Analytical Chemistry*, 131, 116024. doi:10.1016/j.trac.2020.116024
- Moonen, E. J. M., Haakma, J. R., Peri, E., Pelssers, E., Mischi, M., & den Toonder, J. M. J. (2020). Wearable sweat sensing for prolonged, semicontinuous, and nonobtrusive health monitoring. *View*, 1(4), 20200077. doi:10.1002/VIW.20200077
- Morgan, R. M., Patterson, M. J., & Nimmo, M. A. (2004). Acute effects of dehydration on sweat composition in men during prolonged exercise in the heat. *Acta Physiol Scand*, 182(1), 37-43. doi:10.1111/j.1365-201X.2004.01305.x
- Morris, N. B., Cramer, M. N., Hodder, S. G., Havenith, G., & Jay, O. (2013). A comparison between the technical absorbent and ventilated capsule methods for measuring local sweat rate. *J Appl Physiol* (1985), 114(6), 816-823. doi:10.1152/jappphysiol.01088.2012
- Mugo, S. M., & Alberkant, J. (2020). Flexible molecularly imprinted electrochemical sensor for cortisol monitoring in sweat. *Analytical and Bioanalytical Chemistry*, 412(8), 1825-1833. doi:10.1007/s00216-020-02430-0
- National Institute for Public Health and the Environment. (2018). Public Health Foresight Study 2018 - A healthy prospect. Retrieved from <https://www.rivm.nl/en/news/public-health-foresight-study-2018-now-available-in-english>:
- Nüesch, C., Roos, E., Pagenstert, G., & Mündermann, A. (2017). Measuring joint kinematics of treadmill walking and running: Comparison between an inertial sensor based system and a camera-based system. *Journal of Biomechanics*, 57, 32-38. doi:10.1016/j.jbiomech.2017.03.015
- Nyein, H. Y. Y., Tai, L.-C., Ngo, Q. P., Chao, M., Zhang, G. B., Gao, W., . . . Javey, A. (2018). A Wearable Microfluidic Sensing Patch for Dynamic Sweat Secretion Analysis. *ACS Sensors*, 3(5), 944-952. doi:10.1021/acssensors.7b00961
- O'Connor, F. G., Kunar, M. T., & Deuster, P. A. (2009). *Exercise Physiology for Graded Exercise Testing: A Primer for the Primary Care Clinician*. In C. H. Evans & R. D. White (Eds.), *Exercise Stress Testing for Primary Care and Sports Medicine* (pp. 3-22). New York, NY: Springer New York.
- Oh, S. Y., Hong, S. Y., Jeong, Y. R., Yun, J., Park, H., Jin, S. W., . . . Ha, J. S. (2018). Skin-Attachable, Stretchable Electrochemical Sweat Sensor for Glucose and pH Detection. *ACS Applied Materials & Interfaces*, 10(16), 13729-13740. doi:10.1021/acsaami.8b03342

- Owoeye, O. B. A., VanderWey, M. J., & Pike, I. (2020). Reducing Injuries in Soccer (Football): an Umbrella Review of Best Evidence Across the Epidemiological Framework for Prevention. *Sports Medicine - Open*, 6(1), 46. doi:10.1186/s40798-020-00274-7
- Özyener, F., Rossiter, H. B., Ward, S. A., & Whipp, B. J. (2001). Influence of exercise intensity on the on- and off-transient kinetics of pulmonary oxygen uptake in humans. *The Journal of Physiology*, 533(3), 891-902. doi:10.1111/j.1469-7793.2001.t01-1-00891.x
- Palmer, B. F. (2015). Regulation of Potassium Homeostasis. *Clin J Am Soc Nephrol*, 10(6), 1050-1060. doi:10.2215/cjn.08580813
- Park, M., Im, J., Shin, M., Min, Y., Park, J., Cho, H., . . . Kim, K. (2012). Highly stretchable electric circuits from a composite material of silver nanoparticles and elastomeric fibres. *Nature Nanotechnology*, 7, 803. doi:10.1038/nnano.2012.206
- Parrilla, M. (2016). New Electrochemical Sensors for Decentralized Analysis. Retrieved from <http://hdl.handle.net/10803/396297>
- Parrilla, M., Cuartero, M., & Crespo, G. A. (2019). Wearable potentiometric ion sensors. *TrAC Trends in Analytical Chemistry*, 110, 303-320. doi:10.1016/j.trac.2018.11.024
- Parrilla, M., Ortiz-Gómez, I., Cánovas, R., Salinas-Castillo, A., Cuartero, M., & Crespo, G. A. (2019). Wearable Potentiometric Ion Patch for On-Body Electrolyte Monitoring in Sweat: Toward a Validation Strategy to Ensure Physiological Relevance. *Analytical Chemistry*, 91(13), 8644-8651. doi:10.1021/acs.analchem.9b02126
- Patterson, M. J., Galloway, S. D. R., & Nimmo, M. A. (2000). Variations in Regional Sweat Composition in Normal Human Males. *Exp Physiol*, 85(6), 869-875. doi:10.1111/j.1469-445X.2000.02058.x
- Payton, C. J., & Bartlett, R. M. (2008). Biomechanical Evaluation of Movement in Sport and Exercise: The British Association of Sport and Exercise Sciences Guide. *Journal of Sports Science & Medicine*, 7(1), 194-194. Retrieved from <http://www.ncbi.nlm.nih.gov/pmc/articles/PMC3763347/>
- Pirovano, P., Dorrián, M., Shinde, A., Donohoe, A., Brady, A. J., Moyna, N. M., . . . McCaul, M. (2020). A wearable sensor for the detection of sodium and potassium in human sweat during exercise. *Talanta*, 219, 121145. doi:10.1016/j.talanta.2020.121145
- Pless, I. B. (2006). A brief history of injury and accident prevention publications. *Injury Prevention*, 12(2), 65-66. doi:10.1136/ip.2006.011817
- Promphet, N., Rattanawaleedirojn, P., Siralertmukul, K., Soatthiyanon, N., Potiyaraj, P., Thanawattano, C., . . . Rodthongkum, N. (2019). Non-invasive textile based colorimetric sensor for the simultaneous detection of sweat pH and lactate. *Talanta*, 192, 424-430. doi:10.1016/j.talanta.2018.09.086
- Rawashdeh, S. A., Rafeldt, D. A., & Uhl, T. L. (2016). Wearable IMU for shoulder injury prevention in overhead sports. *Sensors*, 16(11), 1847.
- Robinson, R. A., & Stokes, R. H. References. In *Electrolyte Solutions (2nd Revised Edition)* (pp. 87-117): Dover Publications.
- Robinson, S., Maletich, R. T., Robinson, W. S., Rohrer, B. B., & Kunz, A. L. (1956). Output of NaCl by Sweat Glands and Kidneys in Relation to Dehydration and to Salt Depletion. *Journal of Applied Physiology*, 8(6), 615-620. doi:10.1152/jappl.1956.8.6.615
- Rodbard, D. (2017). Continuous Glucose Monitoring: A Review of Recent Studies Demonstrating Improved Glycemic Outcomes. *Diabetes Technology & Therapeutics*, 19(S3), S-25-S-37. doi:10.1089/dia.2017.0035
- Roetenberg, D., Slycke, P. J., & Veltink, P. H. (2007). Ambulatory Position and Orientation Tracking Fusing Magnetic and Inertial Sensing. *IEEE Transactions on Biomedical Engineering*, 54(5), 883-890. doi:10.1109/TBME.2006.889184

Bibliography

- Rose, D. P., Ratterman, M. E., Griffin, D. K., Hou, L., Kelley-Loughnane, N., Naik, R. R., . . . Heikenfeld, J. C. (2015). Adhesive RFID Sensor Patch for Monitoring of Sweat Electrolytes. *IEEE Transactions on Biomedical Engineering*, 62(6), 1457-1465. doi:10.1109/TBME.2014.2369991
- Rosero, S. Z., Kutiyafa, V., Olshansky, B., & Zareba, W. (2013). Ambulatory ECG Monitoring in Atrial Fibrillation Management. *Progress in Cardiovascular Diseases*, 56(2), 143-152. doi:10.1016/j.pcad.2013.10.001
- Rutherford, M. M., Akerman, A. P., Notley, S. R., Meade, R. D., Schmidt, M. D., & Kenny, G. P. (2021). Regional variation in the reliability of sweat rate measured via the ventilated capsule technique during passive heating. *Exp Physiol*, 106(3), 615-633. doi:10.1113/EP089074
- Sales, M. M., Sousa, C. V., da Silva Aguiar, S., Knechtle, B., Nikolaidis, P. T., Alves, P. M., & Simões, H. G. (2019). An integrative perspective of the anaerobic threshold. *Physiology & Behavior*, 205, 29-32. doi:10.1016/j.physbeh.2017.12.015
- Sato, K., Kang, W. H., Saga, K., & Sato, K. T. (1989). Biology of sweat glands and their disorders. I. Normal sweat gland function. *J Am Acad Dermatol*, 20(4), 537-563.
- Savitzky, A., & Golay, M. J. E. (1964). Smoothing and Differentiation of Data by Simplified Least Squares Procedures. *Analytical Chemistry*, 36(8), 1627-1639. doi:10.1021/ac60214a047
- Schache, A. G., Dorn, T. W., Blanch, P. D., Brown, N. A., & Pandy, M. G. (2012). Mechanics of the human hamstring muscles during sprinting. *Medicine & science in sports & exercise*, 44(4), 647-658.
- Seki, Y., Nakashima, D., Shiraiishi, Y., Ryuzaki, T., Ikura, H., Miura, K., . . . Katsumata, Y. (2021). A novel device for detecting anaerobic threshold using sweat lactate during exercise. *Scientific Reports*, 11(1), 4929. doi:10.1038/s41598-021-84381-9
- Sekitani, T., Noguchi, Y., Hata, K., Fukushima, T., Aida, T., & Someya, T. (2008). A rubberlike stretchable active matrix using elastic conductors. *Science*, 321(5895), 1468-1472.
- SGXSensortech. (2014). SGX Metal Oxide Gas Sensors. Retrieved from <https://nl.mouser.com/pdfdocs/AN-0172-SGX-Metal-Oxide-Gas-Sensors-V1.pdf>
- Simões, H. G., Campbell, C. S. G., Kushnick, M. R., Nakamura, A., Katsanos, C. S., Baldissera, V., & Moffatt, R. J. (2003). Blood glucose threshold and the metabolic responses to incremental exercise tests with and without prior lactic acidosis induction. *European Journal of Applied Physiology*, 89(6), 603-611. doi:10.1007/s00421-003-0851-1
- Simões, R. P., Mendes, R. G., Castello, V., Machado, H. G., Almeida, L. B., Baldissera, V., . . . Borghi-Silva, A. (2010). Heart-Rate Variability and Blood-Lactate Threshold Interaction During Progressive Resistance Exercise in Healthy Older Men. *The Journal of Strength & Conditioning Research*, 24(5). Retrieved from https://journals.lww.com/nsca-jscr/Fulltext/2010/05000/Heart_Rate_Variability_and_Blood_Lactate_Threshold.22.aspx
- Sivaraman, V., Grover, S., Kurusingal, A., Dhamdhare, A., & Burdett, A. (2010, 11-13 Oct. 2010). Experimental study of mobility in the soccer field with application to real-time athlete monitoring. Paper presented at the 2010 IEEE 6th International Conference on Wireless and Mobile Computing, Networking and Communications.
- Skinner, J. S., & McLellan, T. H. (1980). The Transition from Aerobic to Anaerobic Metabolism. *Research Quarterly for Exercise and Sport*, 51(1), 234-248. doi:10.1080/02701367.1980.10609285
- Smith, C. J., & Havenith, G. (2011). Body mapping of sweating patterns in male athletes in mild exercise-induced hyperthermia. *European Journal of Applied Physiology*, 111(7), 1391-1404. doi:10.1007/s00421-010-1744-8
- Someya, T., Kato, Y., Sekitani, T., Iba, S., Noguchi, Y., Murase, Y., . . . Sakurai, T. (2005). Conformable, flexible, large-area networks of pressure and thermal sensors with organic transistor active matrixes. *Proceedings of the National Academy of Sciences of the United States of America*, 102(35), 12321-12325. doi:10.1073/pnas.0502392102

- Someya, T., Sekitani, T., Iba, S., Kato, Y., Kawaguchi, H., & Sakurai, T. (2004). A large-area, flexible pressure sensor matrix with organic field-effect transistors for artificial skin applications. *Proceedings of the National Academy of Sciences of the United States of America*, 101(27), 9966-9970. doi:10.1073/pnas.0401918101
- Sonner, Z., Wilder, E., Heikenfeld, J., Kasting, G., Beyette, F., Swaile, D., . . . Naik, R. (2015). The microfluidics of the eccrine sweat gland, including biomarker partitioning, transport, and biosensing implications. *Biomicrofluidics*, 9(3). doi:10.1063/1.4921039
- Steijlen, A. S. M., Bastemeijer, J., Groen, P., Jansen, K. M. B., French, P. J., & Bossche, A. (2020a). A wearable fluidic collection patch and ion chromatography method for sweat electrolyte monitoring during exercise. *Analytical Methods*. doi:10.1039/D0AY02014A
- Steijlen, A. S. M., Bastemeijer, J., Groen, W. A., Jansen, K. M. B., French, P. J., & Bossche, A. (2020b, 20-24 July 2020). Development of a microfluidic collection system to measure electrolyte variations in sweat during exercise. Paper presented at the 2020 42st Annual International Conference of the IEEE Engineering in Medicine and Biology Society (EMBC).
- Steijlen, A. S. M., Bastemeijer, J., Plaude, L., French, P. J., Bossche, A., & Jansen, K. M. B. (2020). Development of Sensor Tights with Integrated Inertial Measurement Units for Injury Prevention in Football. Paper presented at the Proceedings of the 6th International Conference on Design4Health, Amsterdam.
- Stewart, I. B., & Pickering, R. L. (2007). Effect of prolonged exercise on arterial oxygen saturation in athletes susceptible to exercise-induced hypoxemia. *Scandinavian journal of medicine & science in sports*, 17(4), 445-451. doi:10.1111/j.1600-0838.2006.00563.x
- Stiefmeier, T., Roggen, D., Ogris, G., Lukowicz, P., & Tröster, G. (2008). Wearable Activity Tracking in Car Manufacturing. *IEEE Pervasive Computing*, 7(2), 42-50. doi:10.1109/MPRV.2008.40
- Stølen, T., Chamari, K., Castagna, C., & Wisløff, U. (2005). Physiology of Soccer. *Sports Medicine*, 35(6), 501-536. doi:10.2165/00007256-200535060-00004
- Tadano, S., Takeda, R., & Miyagawa, H. (2013). Three Dimensional Gait Analysis Using Wearable Acceleration and Gyro Sensors Based on Quaternion Calculations. *Sensors*, 13(7), 9321-9343. Retrieved from <https://www.mdpi.com/1424-8220/13/7/9321>
- Tanskanen, M. M., Kyröläinen, H., Uusitalo, A. L., Huovinen, J., Nissilä, J., Kinnunen, H., . . . Häkkinen, K. (2011). Serum Sex Hormone-Binding Globulin and Cortisol Concentrations are Associated With Overreaching During Strenuous Military Training. *The Journal of Strength & Conditioning Research*, 25(3). Retrieved from https://journals.lww.com/nsca-jscr/Fulltext/2011/03000/Serum_Sex_Hormone_Binding_Globulin_and_Cortisol.28.aspx
- Taylor, K., Chapman, D., Cronin, J., Newton, M. J., & Gill, N. (2012). Fatigue monitoring in high performance sport: a survey of current trends. *J Aust Strength Cond*, 20(1), 12-23.
- Taylor, N. A., & Machado-Moreira, C. A. (2013). Regional variations in transepidermal water loss, eccrine sweat gland density, sweat secretion rates and electrolyte composition in resting and exercising humans. *Extreme physiology & medicine*, 2(1), 4-4. doi:10.1186/2046-7648-2-4
- Teague, C. N., Heller, J. A., Nevius, B. N., Carek, A. M., Mabrouk, S., Garcia-Vicente, F., . . . Etemadi, M. (2020). A Wearable, Multimodal Sensing System to Monitor Knee Joint Health. *IEEE Sensors Journal*, 20(18), 10323-10334. doi:10.1109/JSEN.2020.2994552
- Teng, C., Lu, X., Zhu, Y., Wan, M., & Jiang, L. (2013). Polymer in situ embedding for highly flexible, stretchable and water stable PEDOT:PSS composite conductors. *RSC Advances*, 3(20), 7219-7223. doi:10.1039/C3RA41124A
- Tesla, N. (1920). U.S. patent. 1329559A.

Bibliography

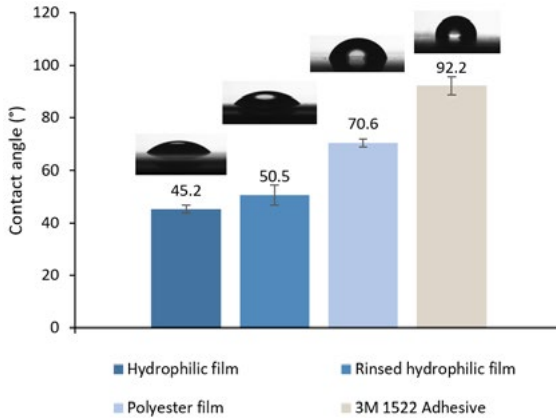
- van der Zwaard, S., Jaspers, R. T., Blokland, I. J., Achterberg, C., Visser, J. M., den Uil, A. R., . . . de Ruiter, C. J. (2016). Oxygenation Threshold Derived from Near-Infrared Spectroscopy: Reliability and Its Relationship with the First Ventilatory Threshold. *PLoS ONE*, 11(9), e0162914. doi:10.1371/journal.pone.0162914
- Van Hoovels, K., Xuan, X., Cuartero, M., Gijssels, M., Swarén, M., & Crespo, G. A. (2021). Can Wearable Sweat Lactate Sensors Contribute to Sports Physiology? *ACS Sensors*, 6(10), 3496-3508. doi:10.1021/acssensors.1c01403
- Varga, M. (2017). Electronics Integration. In S. Schneeegg & O. Amft (Eds.), *Smart Textiles: Fundamentals, Design, and Interaction* (pp. 161-184): Springer International Publishing.
- Veicsteinas, A., Feroldi, P., & Dotti, A. (1985). Ventilatory response during incremental exercise tests in weight lifters and endurance cyclists. *European Journal of Applied Physiology and Occupational Physiology*, 53(4), 322-329. doi:10.1007/bf00422847
- Verplancke, R., Bossuyt, F., Cuypers, D., & Vanfleteren, J. (2012). Thin-film stretchable electronics technology based on meandering interconnections: fabrication and mechanical performance. *Journal of Micromechanics and Microengineering*, 22(1), 015002. Retrieved from <http://stacks.iop.org/0960-1317/22/i=1/a=015002>
- Wallace, J. L., & Norton, K. I. (2014). Evolution of World Cup soccer final games 1966-2010: game structure, speed and play patterns. *J Sci Med Sport*, 17(2), 223-228. doi:10.1016/j.jsams.2013.03.016
- Wallace, L. K., Slattery, K. M., & Coutts, A. J. (2009). The ecological validity and application of the session-RPE method for quantifying training loads in swimming. *J Strength Cond Res*, 23(1), 33-38. doi:10.1519/JSC.0b013e3181874512
- Wang, Q., Chen, W., Timmermans, A. A. A., Karachristos, C., Martens, J. B., & Markopoulos, P. (2015, 25-29 Aug. 2015). Smart Rehabilitation Garment for posture monitoring. Paper presented at the 2015 37th Annual International Conference of the IEEE Engineering in Medicine and Biology Society (EMBC).
- Wang, Y. (2002). Ameer GA, Sheppard BJ, and Langer R. A tough biodegradable elastomer. *Nat Biotechnol*, 20, 602-606.
- Wasserman, K., Whipp, B. J., Koyle, S. N., & Beaver, W. L. (1973). Anaerobic threshold and respiratory gas exchange during exercise. *Journal of Applied Physiology*, 35(2), 236-243. doi:10.1152/jappl.1973.35.2.236
- Wicaksono, I., Tucker, C. I., Sun, T., Guerrero, C. A., Liu, C., Woo, W. M., . . . Dagdeviren, C. (2020). A tailored, electronic textile conformable suit for large-scale spatiotemporal physiological sensing in vivo. *npj Flexible Electronics*, 4(1), 5. doi:10.1038/s41528-020-0068-y
- William, C. J. (1974). Diversity Techniques. In *Microwave Mobile Communications* (pp. 389-544): IEEE.
- Wilmes, E., de Ruiter, C. J., Bastiaansen, B. J. C., Zon, J. F. J. A. v., Vegter, R. J. K., Brink, M. S., . . . Savelsbergh, G. J. P. (2020). Inertial Sensor-Based Motion Tracking in Football with Movement Intensity Quantification. *Sensors*, 20(9), 2527. Retrieved from <https://www.mdpi.com/1424-8220/20/9/2527>
- Wolfe, S., Cage, G., Epstein, M., Tice, L., Miller, H., & Gordon, R. S., Jr. (1970). Metabolic studies of isolated human eccrine sweat glands. *The Journal of clinical investigation*, 49(10), 1880-1884. doi:10.1172/JCI106407
- Woods, C., Hawkins, R. D., Maltby, S., Hulse, M., Thomas, A., & Hodson, A. (2004). The Football Association Medical Research Programme: an audit of injuries in professional football—analysis of hamstring injuries. *British Journal of Sports Medicine*, 38(1), 36-41. doi:10.1136/bjsm.2002.002352
- World Health Organization. (2020). WHO guidelines on physical activity and sedentary behaviour: at a glance.
- Wu, Z., Huang, Y., Chen, X., & Zhang, X. (2018). Capillary-driven flows along curved interior corners. *International Journal of Multiphase Flow*, 109, 14-25. doi:10.1016/j.ijmultiphaseflow.2018.04.004
- Xu, F., Wang, X., Zhu, Y., & Zhu, Y. (2012). Wavy Ribbons of Carbon Nanotubes for Stretchable Conductors. *Advanced Functional Materials*, 22(6), 1279-1283. doi:10.1002/adfm.201102032

- Yan, X., Li, H., Li, A. R., & Zhang, H. (2017). Wearable IMU-based real-time motion warning system for construction workers' musculoskeletal disorders prevention. *Automation in Construction*, 74, 2-11. doi:10.1016/j.autcon.2016.11.007
- Yuan, Z., Hou, L., Bariya, M., Nyein, H. Y. Y., Tai, L.-C., Ji, W., . . . Javey, A. (2019). A multi-modal sweat sensing patch for cross-verification of sweat rate, total ionic charge, and Na⁺ concentration. *Lab on a Chip*, 19(19), 3179-3189. doi:10.1039/C9LC00598F
- Zeng, W., Shu, L., Li, Q., Chen, S., Wang, F., & Tao, X.-M. (2014). Fiber-Based Wearable Electronics: A Review of Materials, Fabrication, Devices, and Applications. *Advanced Materials*, 26(31), 5310-5336. doi:10.1002/adma.201400633
- Zhou, Y., Han, H., Naw, H. P. P., Lammy, A. V., Goh, C. H., Boujday, S., & Steele, T. W. J. (2016). Real-time colorimetric hydration sensor for sport activities. *Materials & Design*, 90, 1181-1185. doi:10.1016/j.matdes.2015.06.078
- Zoerner, A., Oertel, S., Jank, M. P. M., Frey, L., Langenstein, B., & Bertsch, T. (2018). Human Sweat Analysis Using a Portable Device Based on a Screen-printed Electrolyte Sensor. *Electroanalysis*, 30(4), 665-671. doi:10.1002/elan.201700672

A

Appendices: Chapter 4

Figure A1. Contact angle measurements.



134

Figure A2: Measured power output (moving average) and heart rhythm over time during the final cycling experiment.

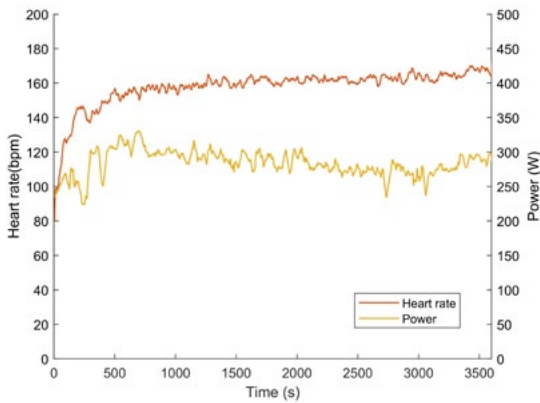
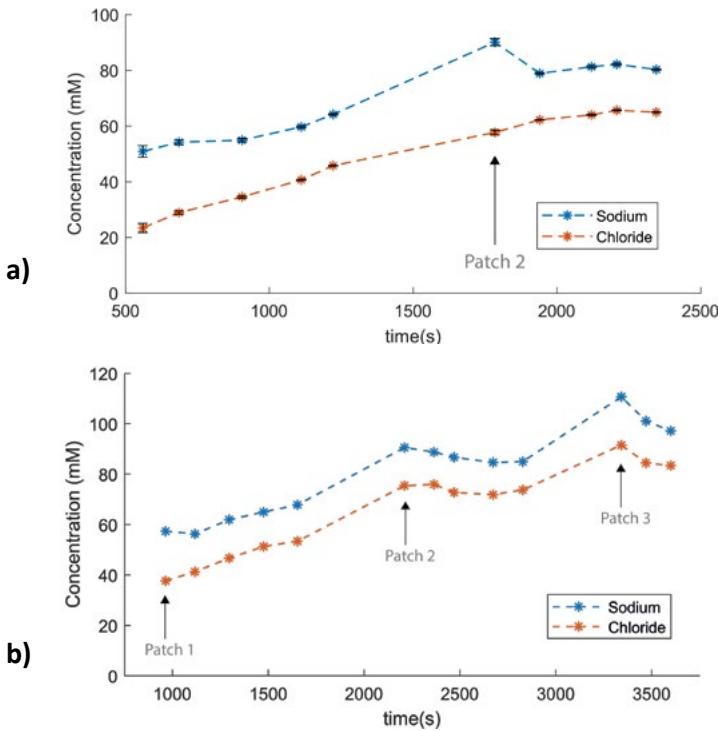


Figure A3: Results from the 1st tests: (a) Experiment 1: Na⁺ and Cl⁻ measurements show an elevation in Na⁺ concentration in the first reservoir of a new patch (arrow). (b) Experiment 2: Na⁺ and Cl⁻ measurements both are elevated when a new patch starts to be filled.



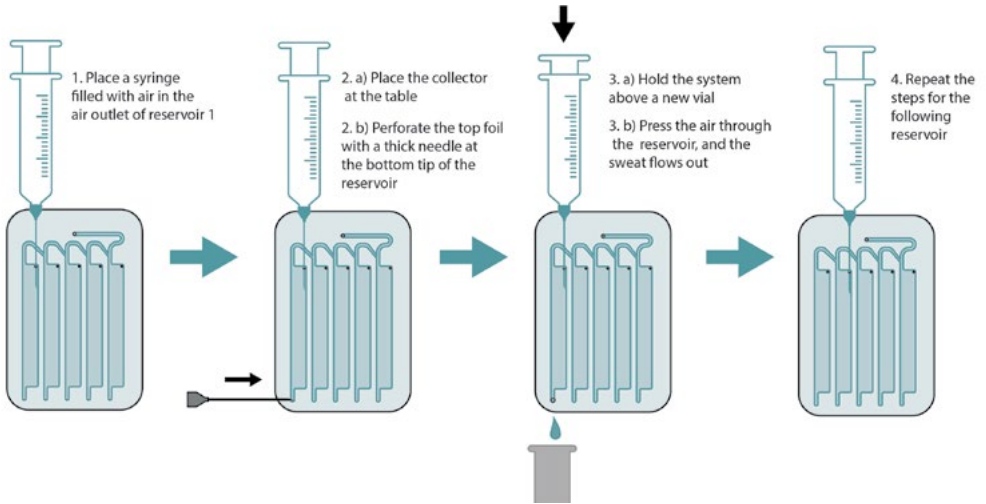
To illustrate the importance of a strict and optimized protocol for sweat collection and analysis two graphs of these first two tests area shown in the figure. Graph a) in figure A3 shows very sudden peaks in Na⁺ concentrations when a new patch was placed, but Cl⁻ concentrations are not elevated. It was expected that this Na⁺ elevation is the result of a surfactant that was placed on the foil to make it more hydrophilic.

In the next experiments, the foils were rinsed with demineralized water to eliminate this source of contamination. To ensure that the contaminants were eliminated, new foil and cleaned foil were placed in vials with 3 ml of water for 24 h. In the new foil 10 ppm of Na⁺ was found and in the cleaned foil the Na⁺ was hardly present. Graph b) in figure A3 is from a consecutive experiment when the surfactants were removed. In this graph is seen that both, Na⁺ and Cl⁻ levels are still increased in the first reservoirs of a patch. In this experiment the skin was wiped with a dry gauze pad, before placing patch 2 and 3. It is expected that this resulted in accumulation of salts at the skin.



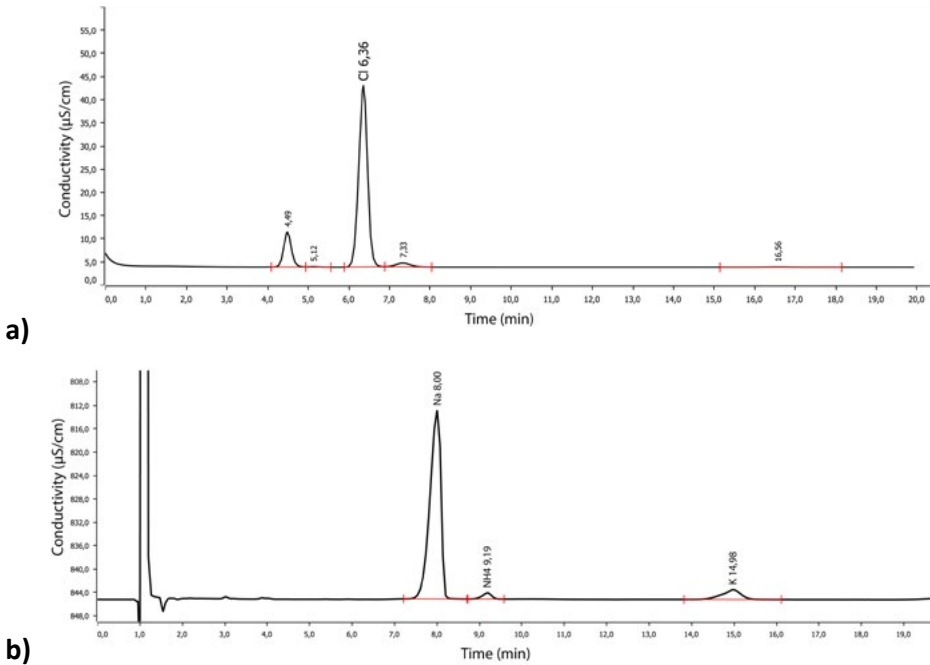
As an improvement, the skin was cleaned with a sterile gauze pad with demineralized water two times before placing a new patch. After this improvement, the peaks were gone. Results of the final experiment are shown in the paper.

Figure A4. Visualization of the steps to transfer the samples to vial



136

Figure A5. Chromatographs of the anions (a) and the cations (b)



B

Appendices: Chapter 5

B1. Performance of the ventilated capsule measurement system

Method:

Lab measurements were performed to characterize the VC system. To find out if we can measure near real-time, it is important to study the response time and recovery time of the system. Absorption of moisture in the system may lower the response time. To quantify the response and recovery time, the cup was placed upside down and an accurately weighed amount of water (90 till 100 μl) was placed in the cup. The bottom of the cup was covered with a hydrophilic membrane (Merck-Millipore, USA) to ensure that the water maintains distributed over the entire surface. The capsule was sealed quickly and attached to the tubing. The capsule was attached to an aluminium U-profile, that was placed in water of 36 °C. Furthermore, it was verified if the total amount of water that was measured by the VC system corresponded to the amount of weighed water that was placed in the capsule. The total amount of sweat was calculated by numerical integration of the sweat rate curve.

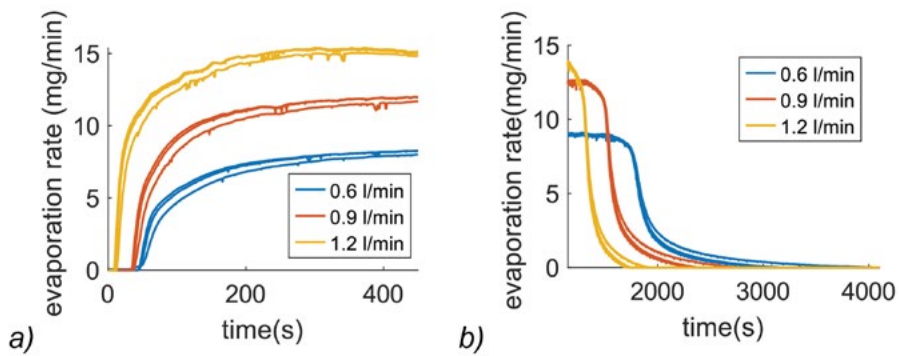
137

Results:

A defined amount of water ($\sim 300 \mu\text{l}$) was placed in the capsule, the capsule was covered and a measurement was performed till all water was evaporated. From the relative humidity readings, the evaporation rate was calculated and by numerical integration the total detected amount of water can be derived. The deviation from the initial amount of water was between 1% and 5%. A small deviation will always be present, because during weighing and during placement of the capsule in the setup, the water can evaporate for a short period of time (60-120 seconds). Figure B1.a shows the response time and Figure B1.b shows the recovery time of the ventilated capsule system at different flow rates. The numbers are shown in the table in Figure B1.c. At a flow rate of 0.6 l/min, the response time (which is defined as the time that it takes to reach 90% of the maximum pump rate) is 332 s and the recovery time is 685 s. At a flow rate of 0.6 l/min, a maximum evaporation rate of 8 mg/min can be reached. For the current capsule with a diameter of 2.6 cm, this means that the maximum sweat rate that can be measured is 1.7 mg/cm²/min. When the flow rate is set at 1.2 l/min the response time and recovery time are 118 seconds and 353 seconds respectively and the maximum sweat rate that can be measured is 2.75 mg/cm²/min. In the

climate chamber, sweat rates at the back of the athlete can be larger than 2 mg/cm²/min and it is important that all sweat is evaporated and measured. Therefore, the ventilated capsule measurement system will be set at a flow rate of 1.2 l/min. So, the response time will be less than 2 minutes. Since sweating is a reaction to increasing body temperature, sweat rates will always increase gradually, which means that the sensor will measure the right humidity value faster than the response time. In short, it can be concluded that the system can be used for continuous sweat rate monitoring.

Figure B1. Response time of the ventilated capsule: the evaporation rate calculated from the relative humidity measurements plotted over time at different flow rates of the dry air (measurements with 3 humidity sensors are plotted) in a) the response time is shown and in b) Recovery time is shown. c) Table with response time and recovery time data.



138

Air flowrate (l/min)	Response time 63 % - 90 % (resp. in sec)	Recovery time 63 % - 90 % (resp. in sec)
0.6 l/min	62-332	355-685
0.9 l/min	43-220	271-499
c) 1.2 l/min	21-118	231-353

Figure B2. Continuous heart rate measurement of participant 1 (top) and continuous measurement of rectal temperature of participant 1 (bottom).

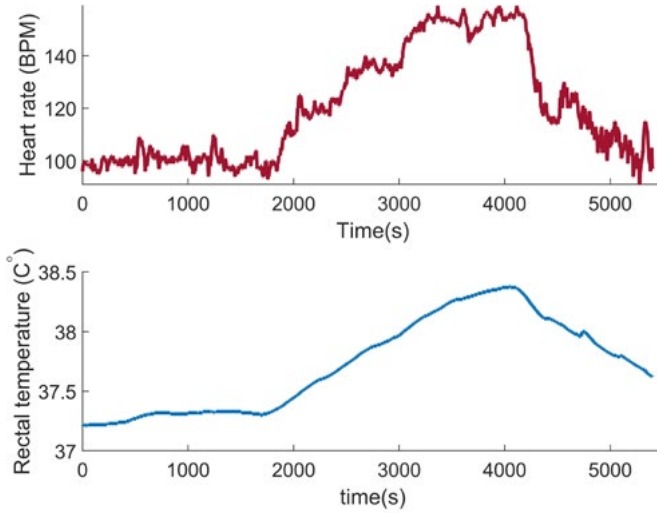


Figure B3. Participant during a physiological test. Patches are placed at the left and the blue capsules are placed at the right.



Figure B4. Raw sweat conductivity data over time for two participants.

The blue, yellow and orange lines show the raw data of the conductance measurements at the 3 locations. The black lines are the filtered data. First, conductances below 0.5×10^3 S were removed, because this indicates that there is air in the chamber. Thereafter, the data were filtered using a Savitsky-Golay sliding window filter (window size = 50 samples and a second order polynomial was chosen). The black dots are the data points that are used in the comparison with the measurements from the ion chromatograph.

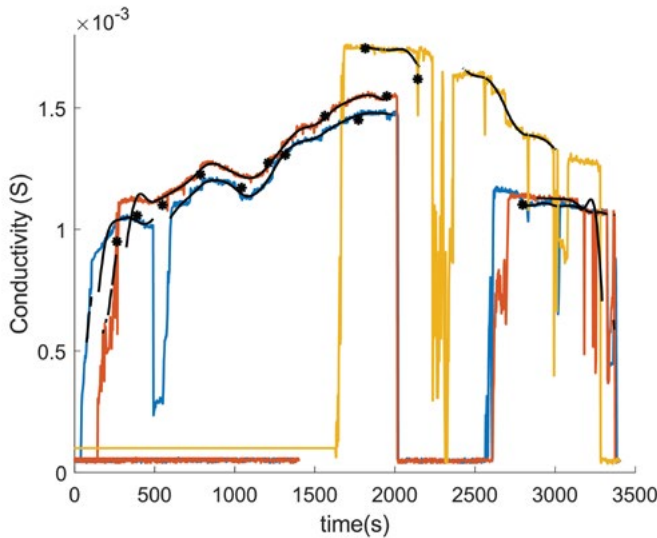
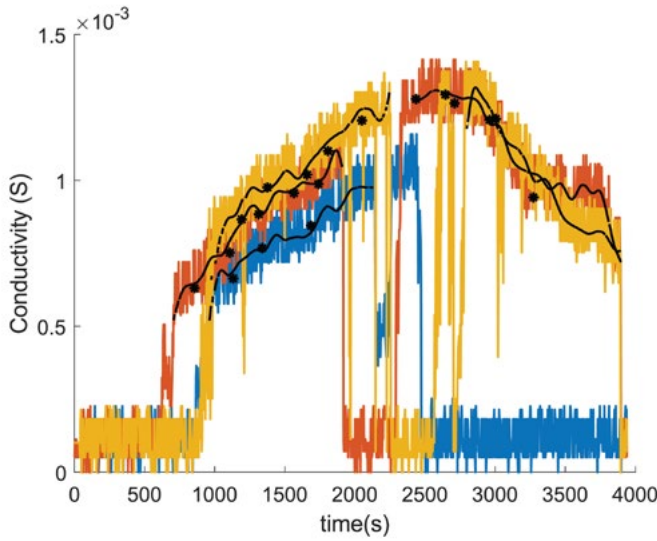


Figure B5. Relationship between $[Na^+]$ and sweat conductivity (left) and $[Cl^-]$ and sweat conductivity (right) at all three locations for each participant. For participant 7, less than two samples per location were collected, because of exceptionally low sweat rates. These results were not shown here. Error bars show the mean root mean square errors between the filtered conductance data and the raw data.

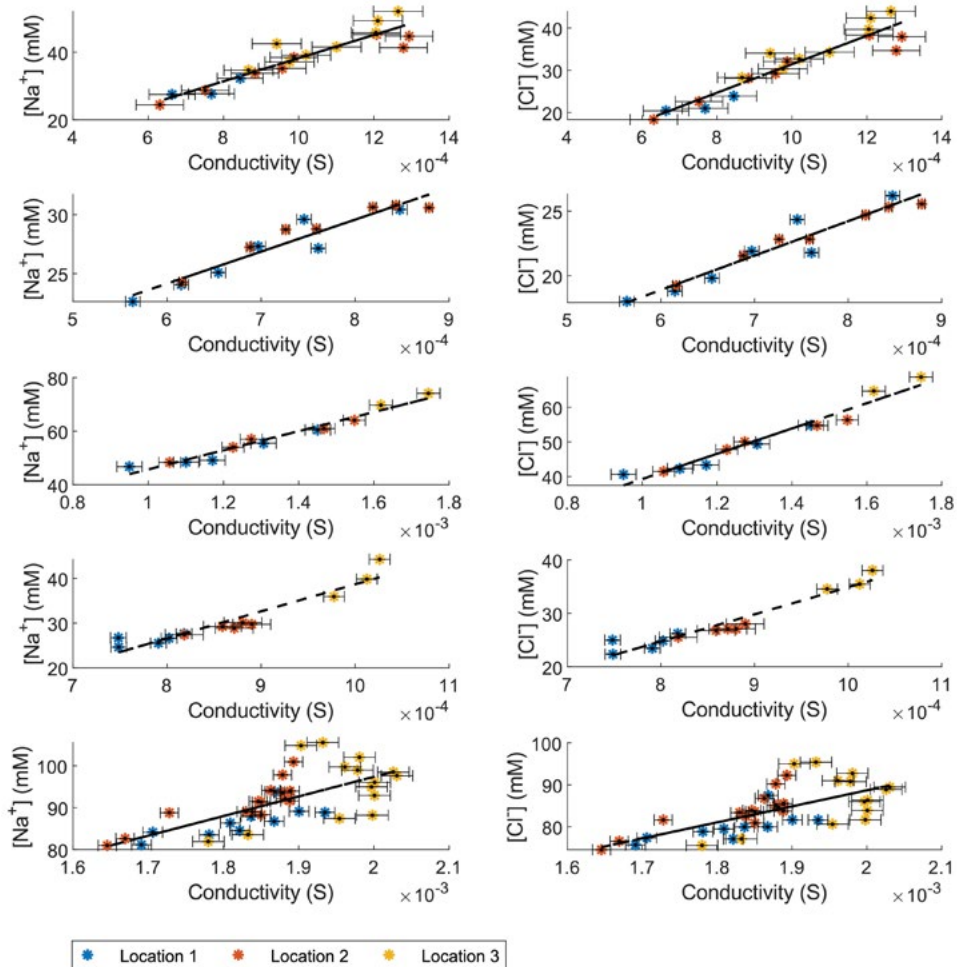


Figure B6. Data processing to find the patch filling rates: an example with two collectors of participant 4.

a) The conductance change for each electrode pair. b) Cumulative conductance change after removal of the conductances below 0.5×10^{-3} S c) Calculated filling rate including the linear fit that was used to derive the average filling rate. The abrupt changes in conductance originate from droplets that are formed and drop down into the reservoir. Sweat rates that are calculated for location 1 (blue) and location 2 (orange) are 1.19 and 1.62 $\text{mg}/\text{cm}^2/\text{min}$.

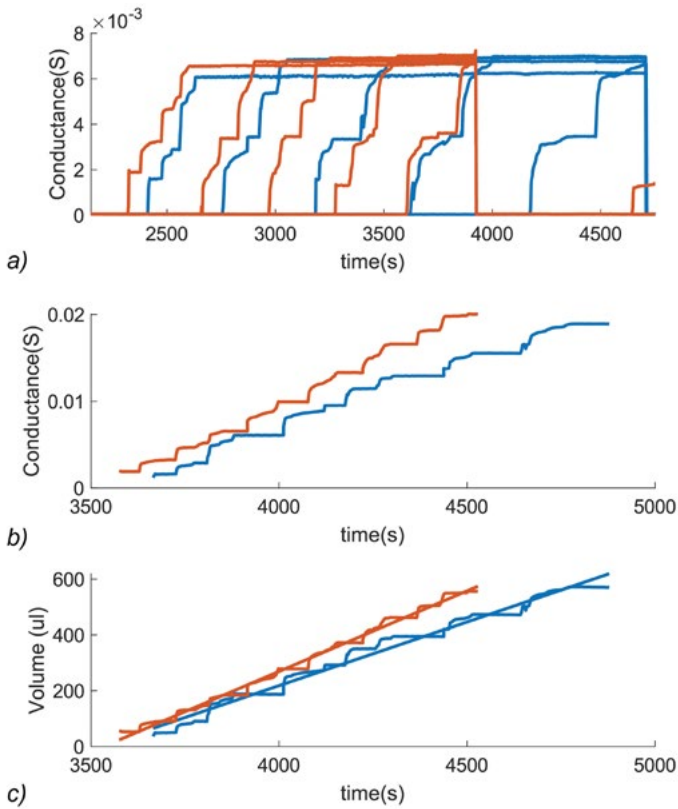


Figure B7. An example of how a novel sweat sensor can be integrated in the patch for validation experiments in a physiological setting. A screen-printed potentiometric sensor is placed between the PCB layer and the spacer tape. The PCB layout is adapted, so that a specific connector, such as an FFC/FPC connector, can be used. Signals can be read out via similar header pins as used for the conductivity readout.

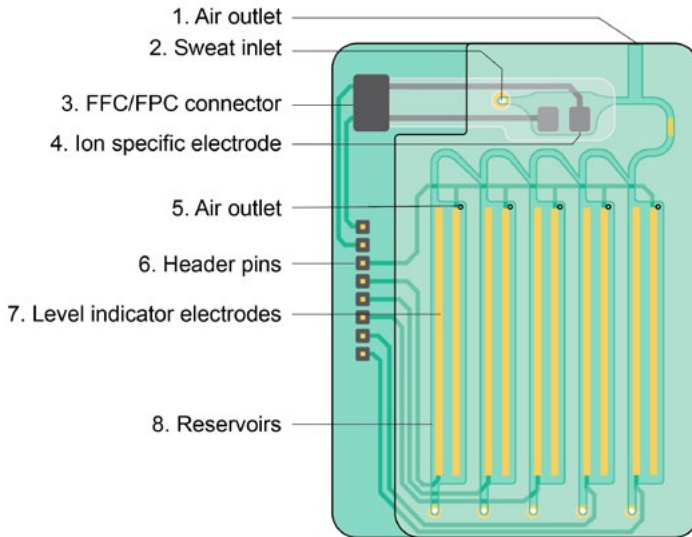
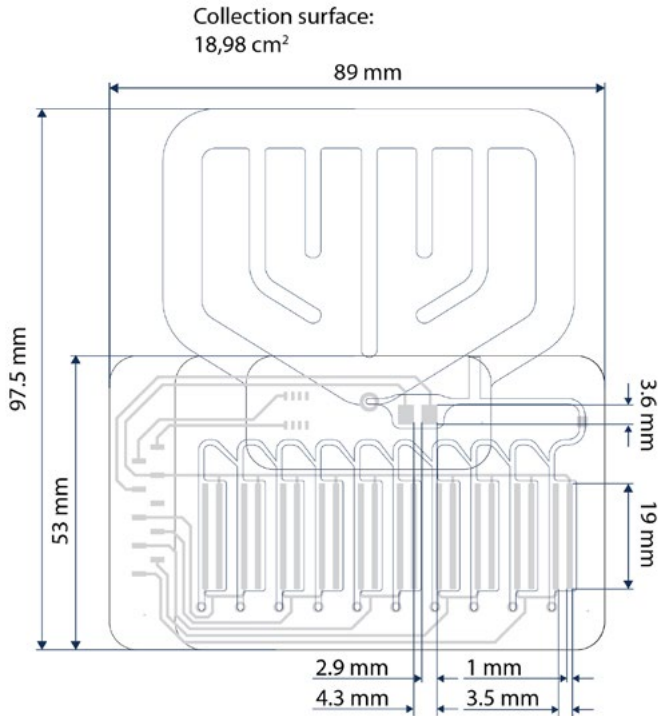
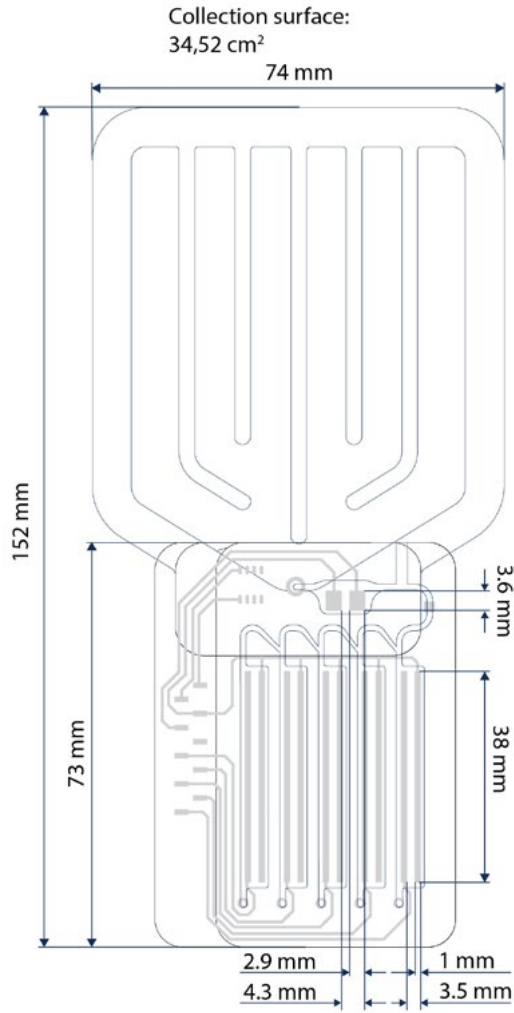


Figure B8. Technical drawings of the sweat patches used in the experiments. The patch with 10 reservoirs (left) and the patch with 5 reservoirs (right). The spacer tape consists of 4 layers of adhesive tape that are laminated to obtain the desired reservoir width (0.64 mm).



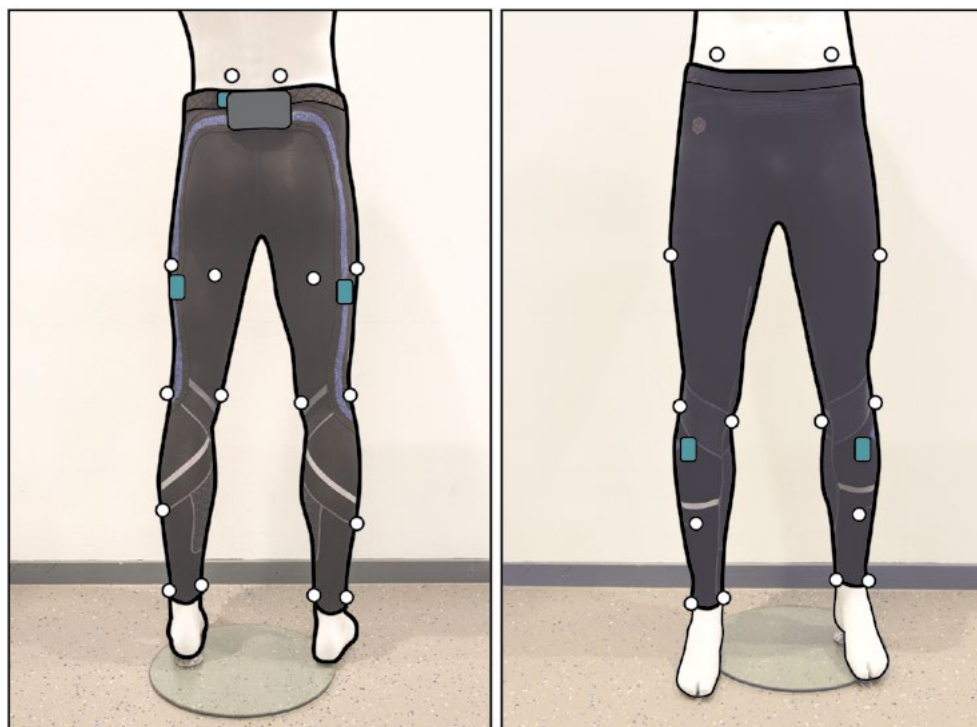


C

Appendices: Chapter 9

Figure C1. The setup for the validation experiment from posterior (left) and anterior (right) view: the IMUs are highlighted in blue. the Vicon markers (white dots) are placed at the following anatomical locations: At the posterior and anterior superior iliac spines, Halfway the length of hip and knee on the lateral and posterior sides of the thighs, at the medial and lateral femoral epicondyles, halfway the length of knee and ankle on the lateral and anterior sides of the shanks, and at the medial and lateral malleoli.

146



C2. Results of the lab validation study.

Root mean square differences between the optoelectronic measurement system and the prototype for the different movement types at different intensity levels.

Movement:	Left Hip Angle (°)	Right Hip Angle (°)	Left Knee Angle (°)	Right Knee Angle (°)	Left Hip Angular Velocity (°/s)	Right Hip Angular Velocity (°/s)	Left Knee Angular Velocity (°/s)	Right Knee Angular Velocity (°/s)
Run 70%	8.88	10.55	7.47	4.12	87.79	75.85	68.71	81.73
Run 85%	7.63	11.14	7.03	5.49	99.05	91.10	80.76	90.08
Run 100%	10.71	8.72	2.98	8.88	168.24	161.05	80.19	141.24
Turn 70%	16.80	7.07	6.76	13.27	65.91	62.22	77.04	70.56
Turn 85%	14.83	7.77	6.46	14.11	64.49	68.48	73.90	77.29
Turn 100%	17.08	9.52	8.07	13.33	61.48	87.62	58.13	91.83
Cut 70%	12.09	12.75	6.14	6.79	138.33	98.78	65.68	58.56
Cut 85%	11.77	12.93	5.68	6.64	84.21	89.51	81.20	53.10
Cut 100%	11.33	10.71	6.18	9.86	95.03	80.18	80.33	52.40
Jump 70%	14.23	10.05	4.61	8.54	65.85	59.08	37.69	45.27
Jump 85%	14.20	9.39	4.88	8.55	61.89	66.90	57.32	73.84
Jump 100%	15.35	13.62	4.58	7.38	61.08	71.65	78.29	64.81
Kick 70%	12.75	10.70	3.91	7.34	61.24	81.63	68.66	68.10
Kick 85%	14.43	9.51	6.05	8.05	76.87	87.80	84.97	77.71
Kick 100%	18.46	8.08	11.63	11.20	93.01	103.10	79.26	96.25
Mean	13.37	10.17	6.16	8.90	85.63	85.66	71.48	76.18



Coefficients of multiple correlation between the optoelectronic measurement system and the prototype for the different movement types at different intensity levels.

Movement:	Left Hip Angle	Right Hip Angle	Left Knee Angle	Right Knee Angle	Left Hip Angular Velocity	Right Hip Angular Velocity	Left Knee Angular Velocity	Right Knee Angular Velocity
Run 70%	0.952	0.952	0.990	0.996	0.948	0.969	0.993	0.989
Run 85%	0.972	0.957	0.992	0.995	0.947	0.968	0.993	0.990
Run 100%	0.966	0.983	0.997	0.989	0.913	0.946	0.994	0.989
Turn 70%	0.853	0.956	0.982	0.930	0.933	0.965	0.978	0.989
Turn 85%	0.872	0.957	0.986	0.911	0.916	0.963	0.983	0.984
Turn 100%	0.855	0.948	0.977	0.936	0.945	0.953	0.988	0.982
Cut 70%	0.855	0.892	0.983	0.979	0.809	0.936	0.989	0.990
Cut 85%	0.788	0.780	0.979	0.978	0.907	0.945	0.983	0.994
Cut 100%	0.757	0.868	0.979	0.951	0.906	0.962	0.983	0.992
Jump 70%	0.940	0.971	0.996	0.987	0.955	0.964	0.992	0.989
Jump 85%	0.932	0.968	0.994	0.981	0.956	0.955	0.985	0.979
Jump 100%	0.920	0.942	0.995	0.986	0.961	0.953	0.979	0.983
Kick 70%	0.628	0.896	0.992	0.952	0.927	0.946	0.987	0.979
Kick 85%	0.830	0.944	0.985	0.972	0.938	0.938	0.982	0.987
Kick 100%	0.839	0.977	0.948	0.966	0.945	0.949	0.984	0.987
Mean	0.864	0.933	0.985	0.967	0.927	0.954	0.986	0.987

Acknowledgements

In April 2018, I entered ‘the EWI tower’ as a PhD researcher for the first time. It was only a few steps away from the IDE faculty, but it felt like I entered a completely different world. I had never heard about ‘tape-outs’, ‘Cadence’ and ‘180-nm CMOS technology’. It seemed that I needed to learn an entirely new language. You designers pick the resistors because they have a nice colour right? This was one of the questions that was asked to me in my first week.

Yet, I was starting a PhD in the Microelectronics department.

And I can recommend it. Never before, I learned so fast.

I would like to use this chapter to express my gratitude to the people that supported me during this journey. Andre Bossche, thank you very much for giving me a crash course in Electronic Instrumentation. I have learned so much from you about microsystems and electronics. I think you were the ideal supervisor for me. I can be very ‘striving’ and when something is not working, I will keep on going till I am burnt out. The tranquillity and pragmatism that you bring, helped me a lot in keeping both feet on the ground and not falling over.

Kaspar Jansen, met jou kan ik schrijven! Opdat we nog veel artikelen samen mogen publiceren. I really enjoyed writing the papers together, it worked really well. Your critical attitude to make it clearer, your pragmatic view in addressing reviewers’ comments, and your ‘bliksemsnelle’ replies brought my academic writing skills to a higher level. I also want to thank you for your faith in my research potential. You motivated me to start a PhD and introduced me to the EWI team. Thank you for creating this great opportunity.

Paddy French, I would like to express my appreciation for the freedom that you gave me. We started with a project proposal to design an optical lactate sensor. There are a lot of results, but we did not work on a lactate sensor. I am very grateful that you gave me the freedom to identify my own design direction to bring sweat sensing to the next level.

Jeroen Bastemeijer, every time when we are supervising practicals in the Tellegen Hall, I see your enormous commitment to learn students the basics of electronics and your love for this profession. I admire your knowledge and expertise in the field of electronics and sensor development very much. And I learned so much from you as well. Without you, we would never have achieved this. We are a perfect team and I hope that we will do more great projects together in the future!

Linda Plaude, I loved working together in designing and prototyping the sensor tights. You played a crucial role in this project as well. It was so impressive to see how you managed to create a textile studio from scratch.

.....

In the project, we worked closely together with NOVAM at Aerospace Engineering. Pim Groen, our project leader, passed away during my PhD project and this was an incredible loss. Pim, I enjoyed working with you very much. Thank you for your enthusiasm and commitment during my project, even though you weren't my promotor. I wish that our collaboration would have lasted much longer. Sybrand van der Zwaag, thank you for the advice and the commitment during our weekly meetings. You excite my ambition to have a career in research. I enjoyed our conversations very much and it helped a lot in planning the next steps of my career.

I would also like to thank my other colleagues: Dimosthenis, I enjoyed the time that you worked in Delft. The trips to Papendal and Nürnberg were really nice, also thank you for your hospitality at NOVAM. Douwe, thank you very much for explaining me 'how things are done' at EI, teaching me how to make my first PCB and thank you for all the sensor tights pictures that you made for this thesis! It was also really nice to organize the SAFE and ProRISC conference with you and Gerd. Weihan, thank you for the nice inspiring lunches and dinners with discussions about cultural differences but also about a great variety in music and films. Erik and Bram, thank you for your patience when the sensor shorts were not finished yet, but also for the sparse but very nice 'borrels' that we had. Lorenzo, Amir, Eren, Thijs, Roger, Jaekyum, Sining, Teruki, thanks for being my roommates and sharing your "never use LabVIEW" and tape-out vibes with me.

150

Several people from other labs and organizations contributed to this research and I would like to thank them as well. The TU Delft Sports Engineering Institute: Dijana and Carlijn among others, for organizing inspiring events and symposia and for the nice opportunities of presenting our research on the Dutch television and radio. Armand Middeldorp, for facilitating the ion chromatography experiments in the WaterLab at CiTG. The Human Performance lab at the VU: Nicola, Lisa, Nienke and Heleen, for facilitating the physiological experiments in the climate chamber. The KNVB Sports Medical Centre, for facilitating motion tracking experiments and hosting our students. Holst Centre, for the nice collaboration on screen printing potentiometric sweat sensors. And lastly, the members of our consortium, Citius Altius Sanius, and especially our partners Adidas and Nedcard/Linxens, for sharing insights from a user's perspective and for supporting this research.

Furthermore, I would like to thank all master students that did their graduation projects with us: Suman, Miguel, Thomas, Wencong, Bastiaan, Robbert, Luis, Adam, Zakaria, Thomas, Pim and Tom. Thank you for your contributions and bringing so much ambition and energy. You were the ones that fuelled this research.

Ruben, jij ook bedankt. Je zei dat ik het bij deze zin kon laten, maar ik wil toch iets meer schrijven. Jij hebt werkelijk alle emoties die bij dit proefschrift horen meegekregen, en de helft zijn we alweer vergeten, want het is gewoon ingeleverd in vier jaar. Wat wel in het boek zit zijn stellingen die er zonder jou niet waren. Er zijn heel wat momenten; wandelingen,

.....

lunches, en avonden in het café voorbijgegaan, waarbij we eindeloze discussies voerden over de verschillende onderwerpen en de formulering ervan. Op een dag begon ik er weer over, en toen zei je, “nu zijn ze wel goed”, en dat was zo.

Ruben, ik hou van jou, evenveel als jij van mij.

List of publications

Journal Papers

- Steijlen, A. S. M., Jansen, K. M. B., Bastemeijer, J., French, P. J., Bossche, A. (2022) A low-cost wearable fluidic sweat collection patch for continuous analyte monitoring and offline analysis. *Analytical Chemistry*. 94(18), 6893-6901. doi:10.1021/acs.analchem.2c01052
- Steijlen, A., Burgers, B., Wilmes, E., Bastemeijer, J., Bastiaansen, B., French, P., . . . Jansen, K. (2021). Smart sensor tights: Movement tracking of the lower limbs in football. *Wearable Technologies*, 2, e17. doi:10.1017/wtc.2021.16
- Steijlen, A. S. M., Bastemeijer, J., Groen, P., Jansen, K. M. B., French, P. J., & Bossche, A. (2020a). A wearable fluidic collection patch and ion chromatography method for sweat electrolyte monitoring during exercise. *Analytical Methods*. doi:10.1039/D0AY02014A
- Bastiaansen, B. J. C., Wilmes, E., Brink, M. S., de Ruiter, C. J., Savelsbergh, G. J. P., Steijlen, A., . . . Lemmink, K. A. P. M. (2020). An Inertial Measurement Unit Based Method to Estimate Hip and Knee Joint Kinematics in Team Sport Athletes on the Field. *JoVE*(159), e60857. doi:10.3791/60857
- Steijlen, A. S., Jansen, K. M., Albayrak, A., Verschure, D. O., & Van Wijk, D. F. (2018). A Novel 12-Lead Electrocardiographic System for Home Use: Development and Usability Testing. *JMIR mHealth and uHealth*, 6(7), e10126-e10126. doi:10.2196/10126

Conference papers

- Steijlen, A., Bastemeijer, J., Nederhoff, R., Jansen, K., French, P., & Bossche, A. (2021). A New Approach for Monitoring Sweat Ammonia Levels Using a Ventilated Capsule. *Engineering Proceedings*, 10(1), 38. Retrieved from <https://www.mdpi.com/2673-4591/10/1/38>
- Steijlen, A. S. M., Bastemeijer, J., Jansen, K. M. B., French, P. J., & Bossche, A. (2020, 25-28 Oct. 2020). A novel sweat rate and conductivity sensor patch made with low-cost fabrication techniques. Paper presented at the 2020 IEEE SENSORS.
- Steijlen, A. S. M., Bastemeijer, J., Plaude, L., French, P. J., Bossche, A., & Jansen, K. M. B. (2020). Development of Sensor Tights with Integrated Inertial Measurement Units for Injury Prevention in Football. Paper presented at the Proceedings of the 6th International Conference on Design4Health, Amsterdam.
- Steijlen, A. S. M., Bastemeijer, J., Groen, W. A., Jansen, K. M. B., French, P. J., & Bossche, A. (2020b, 20-24 July 2020). Development of a microfluidic collection system to measure electrolyte variations in sweat during exercise. Paper presented at the 2020 42st Annual International Conference of the IEEE Engineering in Medicine and Biology Society (EMBC).

About the author

Annemarijn Sebastinie Marie Steijlen

April, 28, 1993

born in Nijmegen, The Netherlands

Experience

April 2018 - Present

PhD Candidate - Wearable Sensor Systems
Electronic Instrumentation
Delft University of Technology

August 2017 - April 2018

Teacher Technical Courses for Designers
Faculty of Industrial Design Engineering TU Delft

May 2017 - August 2017

Junior Product Developer
Pezy Group

2015
3 months, full-time

Internship
Philips Design Shanghai

2013
5 months, full-time

Product Design Internship
Fabrique Public Design

Education

2014 - 2017

Master of Science, Integrated Product Design,
Cum Laude & Honours Programme
Delft University of Technology

2011-2014

Bachelor of Science, Industrieel Ontwerpen,
Cum Laude & Honours Programme
Delft University of Technology

2005-2011

Gymnasium, Cum Laude
Sophianum College Gulpen